TURUN
YLIOPISTO
UNIVERSITY
OF TURKU

# NOVEL IMAGING APPROACHES FOR THE DETECTION OF HEMODYNAMICALLY SIGNIFICANT CORONARY ARTERY DISEASE

## Quantitative Flow Ratio and Artificial Intelligence-Based Ischemia Algorithm

Sarah Bär

TURUN YLIOPISTON JULKAISUJA – ANNALES UNIVERSITATIS TURKUENSIS
SARJA – SER. D OSA – TOM. 1796 | MEDICA – ODONTOLOGICA | TURKU 2024

TURUN
YLIOPISTO
UNIVERSITY
OF TURKU

# NOVEL IMAGING APPROACHES FOR THE DETECTION OF HEMODYNAMICALLY SIGNIFICANT CORONARY ARTERY DISEASE

## Quantitative Flow Ratio and Artificial Intelligence-Based Ischemia Algorithm

Sarah Bär

TURUN YLIOPISTON JULKAISUJA – ANNALES UNIVERSITATIS TURKUENSIS
SARJA – SER. D OSA – TOM. 1796 | MEDICA – ODONTOLOGICA | TURKU 2024

## University of Turku

Faculty of Medicine
Department of Cardiology and Cardiovascular Medicine
Doctoral Programme in Clinical Research
Heart Center and Turku PET Centre, Turku University Hospital

## Supervised by

Professor Juhani Knuuti, MD, PhD
Turku PET Centre
University of Turku and
Turku University Hospital
Turku, Finland

Doctor Teemu Maaniitty, MD, PhD
Turku PET Centre
University of Turku and
Turku University Hospital
Turku, Finland

## Reviewed by

Professor Oliver Gaemperli, MD
University of Zurich and
Zurich Heart Clinic
Zürich, Switzerland

Doctor Helena Rajala, MD, PhD
Heart and Lung Center
University of Helsinki and
Helsinki University Hospital
Helsinki, Finland

## Opponent

Professor Göran Bergström, MD, PhD
Department of Molecular and
Clinical Medicine
University of Gothenburg
Gothenburg, Sweden



ISBN 978-951-29-9709-1 (PRINT)
ISBN 978-951-29-9710-7 (PDF)
ISSN 0355-9483 (Print)
ISSN 2343-3213 (Online)
Painosalama, Turku, Finland 2024

*To Christian, Jari & Ella,*
*and our vaari Matthias*
*- for invaluable support in Turku*

UNIVERSITY OF TURKU
Faculty of Medicine
Department of Cardiology and Cardiovascular Medicine
Heart Center and Turku PET Centre, Turku University Hospital
SARAH BÄR: Novel Imaging Approaches for the Detection of Hemodynamically Significant Coronary Artery Disease: Quantitative Flow Ratio and Artificial Intelligence-Based Ischemia Algorithm
Doctoral Dissertation, 189 pp.
Doctoral Programme in Clinical Research
April 2024

## ABSTRACT

In coronary artery disease (CAD), the decision on revascularization is based on the hemodynamic significance of stenoses. However, this cannot directly be determined from the first-line anatomical imaging methods coronary computed tomography angiography (CCTA) in chronic coronary syndrome (CCS) or invasive coronary angiography (ICA) in acute coronary syndrome (ACS). The aim of this thesis was to investigate the prognostic value of two novel approaches to determine functionally significant CAD according to impaired invasive fractional flow reserve (FFR) directly from CCTA in CCS and ICA in ACS.

Quantitative flow ratio (QFR) is a novel computational fluid dynamic-based technique to estimate the presence of impaired FFR from biplane ICA. In this study, QFR from untreated non-culprit lesions showed incremental 5-year prognostic value for major adverse cardiac events among ST-elevation myocardial infarction patients undergoing angiography-guided complete revascularization. However, non-culprit QFR did not independently predict non-target-vessel related events prior to planned staged percutaneous coronary intervention (PCI) in ACS patients, and the study does not provide conceptual evidence that QFR could be useful to refine the timing of staged PCI on top of clinical judgement.

AI-QCT$_{ischemia}$ is an artificial intelligence-based method to predict the probability of an impaired invasive FFR using 37 morphological features from CCTA. Among symptomatic patients with suspected CAD undergoing CCTA, AI-QCT$_{ischemia}$ showed incremental prognostic value for the composite of death, myocardial infarction, or unstable angina pectoris throughout a median of 7 years follow-up. This risk stratification pertained especially to patients with no/non-obstructive disease. Patients with obstructive disease on CCTA were referred for downstream myocardial perfusion imaging with positron emission tomography (PET), and among those, AI-QCT$_{ischemia}$ showed incremental risk stratification among patients with normal PET perfusion, but not among those with abnormal PET perfusion.

KEYWORDS: coronary artery disease, quantitative flow ratio, coronary computed tomography angiography, artificial intelligence, prognosis

TURUN YLIOPISTO
Lääketieteellinen tiedekunta
Kardiologia ja kardiovaskulaarilääketiede
Sydänkeskus ja Turun PET-keskus, Turun yliopistollinen keskussairaala
SARAH BÄR: Uusia kuvantamismenetelmiä hemodyaamisesti merkittävän sepelvaltimotaudin diagnosointiin: kvantitatiivinen virtaussuhde ja tekoälyyn perustuva iskemia-algoritmi
Väitöskirja, 189 s.
Turun kliininen tohtoriohjelma
Huhtikuu 2024

## TIIVISTELMÄ

Sepelvaltimotaudissa revaskularisaatiopäätös perustuu hemodynaamisesti merkittävän ahtauman osoitukseen. Tätä ei voida kuitenkaan suoraan määrittää kaikilla kuvantamismenetelmillä, kuten sepelvaltimoiden tietokonetomografialla (TT) kroonisessa sepelvaltimo-oireyhtymässä tai kajoavalla angiografialla akuutissa sepelvaltimotautikohtauksessa. Tämän väitöskirjan tavoitteena oli tutkia kahden uuden sepelvaltimoahtauman hemodynaamisen merkityksen arvioimiseen käytettävän menetelmän ennusteellista arvoa: kajoavaan angiografiaan pohjautuva menetelmä akuutissa sepelvaltimotautikohtauksessa ja TT:aan pohjautuva menetelmä kroonisessa sepelvaltimo-oireyhtymässä.

Kvantitatiivinen virtaussuhde (KVS) on uusi laskennalliseen virtausdynamiikkaan perustuva menetelmä, jolla kajoavaan painevaijerimittaukseen perustuvaa sydänlihasiskemiaa pyritään arvioimaan suoraan tavanomaisista angiografiakuvista. Ei-revaskularisoidun non-culprit-ahtauman KVS:n määrityksellä osoitettiin ennusteellista lisäarvoa 5 vuoden sydän- ja verisuonitautitapahtumien suhteen ST-nousuinfarktipotilailla, joille oli tehty angiografiaohjattu täydellinen revaskularisaatio. Non-culprit-ahtauman KVS ei kuitenkaan ennustanut kyseiseen suoneen liittyviä tapahtumia ennen suunniteltua viivästettyä non-culprit-ahtauman perkutaanista sepelvaltimotoimenpidettä, joten tämän tutkimuksen perusteella KVS ei vaikuta hyödylliseltä menetelmältä viivästetyn sepelvaltimotoimenpiteen ajoituksen optimoimiseksi.

AI-QCT$_{ischemia}$ on tekoälyyn perustuva menetelmä, jolla arvioidaan kajoavaan painevaijerimittaukseen perustuvan sydänlihasiskemian todennäköisyyttä käyttäen 37 morfologista sepelvaltimoiden TT:aan pohjautuvaa muuttujaa. Oireisilla potilailla, joille tehtiin TT-tutkimus sepelvaltimotaudin epäilyn vuoksi, AI-QCT$_{ischemia}$ tarjosi ennusteellista lisäarvoa yhdistelmätapahtumalle (kuolema, sydäninfarkti tai epävakaa angina pectoris) 7 vuoden seurannan aikana. Tämä riskiluokittelu koski erityisesti potilaita, joilla ei todettu ahtauttavaa sepelvaltimotautia TT:ssa. Potilaat, joilla todettiin TT:n perusteella ahtauttava sepelvaltimotauti, ohjattiin sydänlihasperfuusion kuvantamiseen positroniemissiotomografialla (PET). Tässä joukossa AI-QCT$_{ischemia}$ antoi ennusteellista lisätietoa potilailla, joilla oli normaali sydänlihasperfuusio, mutta ei niillä, joilla perfuusio oli alentunut.

AVAINSANAT: sepelvaltimotauti, kvantitatiivinen virtaussuhde, tietokonetomografia, tekoäly, ennuste

# Table of Contents

# Abbreviations

| | |
|---|---|
| ACE | Angiotensin-converting enzyme |
| ACS | Acute coronary syndrome |
| AI | Artificial intelligence |
| AI-QCT | Artificial intelligence-based quantitative computed tomography |
| AI-QCT$_{ischemia}$ | Artificial intelligence-based quantitative computed tomography ischemia algorithm |
| ATII | Angiotensin-receptor-2 |
| CABG | Coronary artery bypass grafting |
| CAD | Coronary artery disease |
| CCS | Chronic coronary syndrome |
| CCTA | Coronary computed tomography angiography |
| CFD | Computational fluid dynamics |
| CFV | Contrast flow velocity |
| CI | Confidence interval |
| CMR | Cardiac magnetic resonance |
| CNN | Convolutional neuronal network |
| COMFORTABLE AMI | Comparison of biolimus eluted from an erodible stent coating with bare metal stents in acute ST-elevation myocardial infarction |
| COMPARE-ACUTE | Comparison Between FFR Guided Revascularization Versus Conventional Strategy in Acute STEMI Patients With MVD |
| CONSERVE | Coronary Computed Tomographic Angiography for Selective Cardiac Catheterization |
| CPV | Calcified plaque volume |
| CREDENCE | Computed tomogRaphic Evaluation of atherosclerotic DEtermiNants of myocardial isChEmia |
| CT | Computed tomography |
| CT-FFR | Computed tomography-based fractional flow reserve |
| CTP | Computed tomography perfusion |

| | |
|---|---|
| DANAMI-3-PRIMULTI | Primary PCI in Patients With ST-elevation Myocardial Infarction and Multivessel Disease: Treatment of Culprit Lesion Only or Complete Revascularization |
| DAPT | Dual antiplatelet therapy |
| DEFER | Deferral Versus Performance Of PTCA In Patients Without Documented Ischemia |
| DISCHARGE | Diagnostic Imaging Strategies for Patients with Stable Chest Pain and Intermediate Risk of Coronary Artery Disease |
| DL | Deep learning |
| DS | Diameter stenosis |
| ECG | Electrocardiogram |
| FAME | Fractional Flow Reserve Versus Angiography For Multivessel Evaluation |
| FAVOR III | The Comparison of Quantitative Flow Ratio Guided and Angiography Guided Percutaneous Intervention in Patients with Coronary Artery Disease |
| FDA | Food and Drug Administration |
| FFR | Fractional flow reserve |
| FFR-CT | Fractional flow reserve from computed tomography |
| FLOWER-MI | Flow Evaluation to Guide Revascularization in Multivessel ST-Elevation Myocardial Infarction |
| FRAME-AMI | Fractional Flow Reserve vs. Angiography-Guided Strategy for Management of Non-Infarction Related Artery Stenosis in Patients with Acute Myocardial Infarction |
| HFV | Hyperemic flow velocity |
| HR | Hazard ratio |
| ICA | Invasive coronary angiography |
| iFR | Instantaneous wave-free ratio |
| IQR | Interquartile range |
| ISCHEMIA | International Study of Comparative Health Effectiveness with Medical and Invasive Approaches |
| LAD | Left anterior descending artery |
| LCX | Left circumflex artery |
| LM | Left main artery |
| MBF | Myocardial blood flow |
| MI | Myocardial infarction |
| ML | Machine learning |
| MLD | Minimum lumen diameter |

| | |
|---|---|
| MPI | Myocardial perfusion imaging |
| MVD | Multivessel disease |
| NCPV | Non-calcified plaque volume |
| Non-TV-MI | Non-target vessel myocardial infaction |
| Non-TV-PCI | Non-target vessel percutaneous coronary intervention |
| Non-TVR | Non-target vessel revacularization |
| NPV | Negative predictive value |
| NSTE-ACS | Non-ST-elevation acute coronary syndrome |
| NSTEMI | Non-ST-elevation myocardial infarction |
| ORBITA-2 | Objective Randomized Blinded Investigation with Optimal Medical Therapy of Angioplasty in Stable Angina |
| PACIFIC | Prospective Comparison of Cardiac PET/CT, SPECT/CT Perfusion Imaging and CT Coronary Angiography With Invasive Coronary Angiography |
| PAV | Percent atheroma volume |
| PCI | Percutaneous coronary intervention |
| PET | Positron emission tomography |
| PPV | Positive predictive value |
| PROMISE | Prospective Multicenter Imaging Study for Evaluation of Chest Pain |
| QFR | Quantitative flow ratio |
| RCA | Right coronary artery |
| RCT | Randomized-controlled trial |
| ROC | Reciever-operating curve |
| SCOT-HEART | Scottish Computed Tomography of the Heart |
| SD | Standard deviation |
| SPECT | Single-photon emission computed tomography |
| STEMI | ST-elevation myocardial infarction |
| SYNTAX | Synergy Between PCI With Taxus and CABG |
| TIMI | Thrombolysis in Myocardial Infarction |
| uAP | Unstable angina pectoris |
| VIF | Variance inflation factors |
| 2D | Two-dimensional |
| 2D-QCA | Three-dimensional quantitative coronary angiography |
| 3D | Three-dimensional |
| 3D-QCA | Three-dimensional quantitative coronary angiography |

# List of Original Publications

This dissertation is based on the following original publications, which are referred to in the text by their Roman numerals:

I **Bär S**, Kavaliauskaite R, Ueki Y, Otsuka T, Kelbæk H, Engstrøm T, Baumbach A, Roffi M, von Birgelen C, Ostojic M, Pedrazzini G, Kornowski R, Tüller D, Vukcevic V, Magro M, Losdat S, Windecker S, Räber L. Quantitative Flow Ratio to Predict Non-Target-Vessel Related Events at 5 Years in STEMI Patients Undergoing Angiography-Guided Revascularization (COMFORTABLE QFR). *J Am Heart Assoc* 2021;10:e019052.

II **Bär S**, Kavaliauskaite R, Otsuka T, Ueki Y, Häner J, Lanz J, Fürholz M, Praz F, Hunziker L, Siontis GC, Pilgrim T, Stortecky S, Losdat S, Windecker S, Räber L. Quantitative Flow Ratio to Predict Non-Target-Vessel Events Prior to Planned Staged PCI in ACS Patients. *J Am Heart Assoc* 2024;2:e031847.

III **Bär S**, Nabeta T, Maaniitty T, Saraste A, Bax JJ, Earls JP, Min JK, Knuuti J. Prognostic Value of a Novel Artificial Intelligence-Based Coronary Computed Tomography Angiography-Derived Ischemia Algorithm for Patients with Suspected Coronary Artery Disease. *Eur Heart J Cardiovasc Imaging* 2024;25:657-667.

IV **Bär S**, Maaniitty T, Nabeta T, Saraste A, Bax JJ, Earls JP, Min JK, Knuuti J. Prognostic Value Of A Novel Artificial Intelligence-Based CCTA-Derived Ischemia Algorithm Among Patients With Normal or Reduced Myocardial Perfusion. *J Cardiovasc Comput Tomogr* 2024 Apr 24:S1934-5925(24)00075-3; [ePub ahead of print], doi:10.1016/j.jcct.2024.04.001.

# 1 Introduction

Coronary artery disease (CAD) has an incidence of 5.8 million new cases per year and remains a leading cause of mortality and morbidity world-wide (Timmis et al. 2022). CAD can manifest as stable disease, i.e. chronic coronary syndrome (CCS), which may progress to an acute plaque event causing acute coronary syndrome (ACS) (Libby and Theroux 2005). In CAD, the decision on revascularization generally mandates the presence of functionally significant disease (Knuuti et al. 2020). And, since there is disagreement between the anatomical and hemodynamic significance of coronary stenoses in approximately 40% of the cases (Meijboom et al. 2008; Tonino et al. 2010), the appropriate detection of hemodynamically significant stenoses is paramount for patient management. However, the functional significance of CAD cannot directly be identified by the first-line anatomical imaging modalities used in ACS, i.e. invasive coronary angiography (ICA) or CCS, i.e. coronary computed tomography angiography (CCTA). Therefore, downstream assessment of the hemodynamic significance of coronary stenoses is generally required. During ICA, this is usually performed with fractional flow reserve (FFR) an invasive pressure-wire based method to assess the pressure drop across a stenosis. And after CCTA, hemodynamic assessment can be performed with several non-invasive functional imaging tests, e.g. with positron emission tomography (PET) perfusion imaging.

This thesis focusses on two novel approaches to determine hemodynamically significant CAD directly from the first-line anatomical imaging methods ICA in ACS and CCTA in CCS. Quantitative flow ratio (QFR) is novel method to assess the hemodynamic significance of coronary stenoses from biplane ICA. From two standard angiographic projections, it generates a three-dimensional (3D) vessel model and estimates the flow based on computational fluid dynamics (CFD) (Tu et al. 2016). Owing to its non-invasive and hyperemia-free nature, QFR may be specifically beneficial in ACS patients, where a time-efficient and safe procedure is required.

AI-QCT$_{ischemia}$ is novel artificial intelligence (AI)-guided algorithm that aims to determine the presence of hemodynamically significant CAD directly from CCTA images. It incorporates 37 morphological CCTA features into a machine-learned

random forest algorithm and estimates the probability of an abnormal invasive FFR (Nurmohamed et al. 2024a). With the adoption of this algorithm, information on the anatomical and functional extent of CAD can be gained from one single CCTA session.

This thesis aims at validating the prognostic value of QFR in ACS populations and of AI-QCT$_{ischemia}$ in a CCS population, where these novel methods could potentially find their clinical adoption.

# 2 Review of the Literature

## 2.1 Coronary artery disease

### 2.1.1 Epidemiology and pathophysiology

CAD affects ~50 million people across 57 countries in and in proximity to Europe. Despite substantial improvements in diagnostic modalities, medical therapy, as well as interventional and surgical techniques over the last decades, CAD remains a leading cause of mortality and morbidity world-wide (Timmis et al. 2022).

CAD is a pathological process characterized by atherosclerotic plaque accumulation in the coronary arteries. The risk of developing CAD is dependent on the prevalence, extent, and combination of various risk factors, traditionally consisting of age, male sex, smoking, diabetes mellitus, hypertension, dyslipidemia, obesity, and family history of CAD. More recent research also indicates that sedentary lifestyle per se (Fiuza-Luces et al. 2013), psychosocial stressors (Kivimäki and Steptoe 2018), chronic comorbidities such as inflammatory processes (Peters et al. 2010) or malignancies (Darby et al. 2003), also contribute to the risk of developing CAD. The combination of these conditions leads to macrophage infiltration into the coronary intima, foam cell generation and accumulation of intracellular lipid streaks, inflammation, progressive intra- and extracellular lipid accumulation, followed by fibrosis and calcification – all of it together building up the coronary plaque (Libby et al. 2002; Libby and Theroux 2005).

### 2.1.2 Clinical manifestations of coronary artery disease

CAD represents a disease continuum, usually starting as long-standing clinically silent process of plaque accumulation. When enough obstruction of one or more coronary arteries is achieved, usually at least 40-50% stenosis (Klopp and Gott 1975), the disease may become clinically manifest in terms of exertional chest pain, dyspnea, fatigue, or less typical symptoms (Knuuti et al. 2020). CAD in this form, whether symptomatic or asymptomatic, is called chronic coronary syndrome (CCS).

This stable disease state may progress to an acute plaque event, triggering thrombus formation, vessel obstruction and downstream myocardial ischemia,

causing acute coronary syndrome (ACS) and myocardial infraction (MI) (Libby 2013) (**Figure 1**). In approximately 70% of the cases, this is related to plaque rupture, in 20-25% to plaque erosion, and rarely (~5%) to other entities such as eruptive calcified nodule (Virmani et al. 2006; Arbab-Zadeh et al. 2012; Libby 2013).

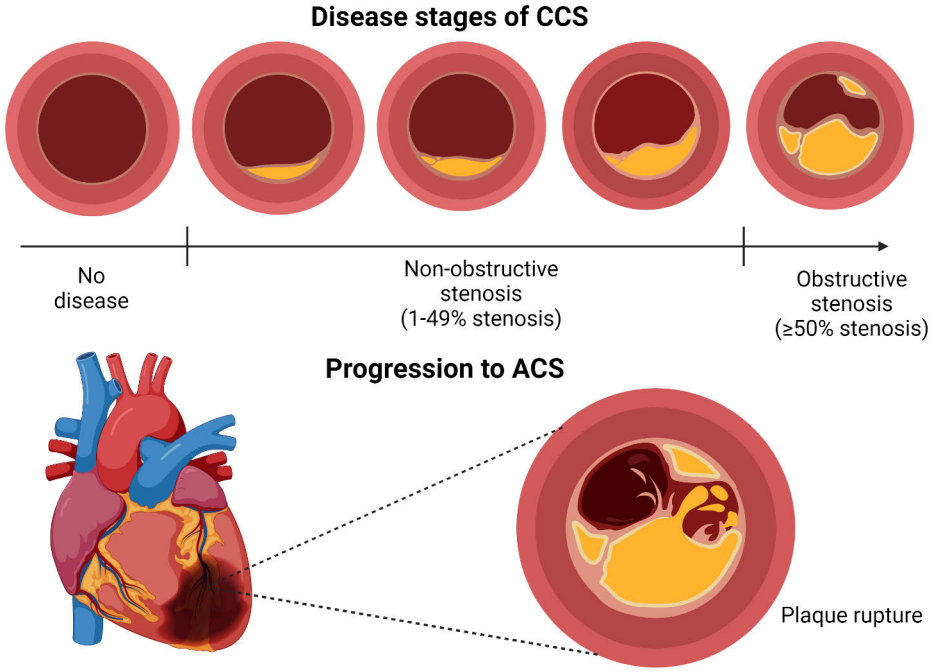


**Figure 1.** Chronic coronary syndrome (CCS) and acute coronary syndrome (ACS). Plaque rupture is shown as most frequent atherosclerotic cause of ACS. Author's own drawing with BioRender.com.

Importantly, only approximately half of the plaques causing future ACS are found to be obstructive at their initial evaluation (Stone et al. 2011). The other half of events is related to non-obstructive plaques with vulnerable morphological features such as thin fibrous cap, high plaque burden, large lipid core, presence of inflammatory cells, and spotty calcification (Stone et al. 2011; Libby 2013). A plaque with an event responsible for ACS is called "culprit-lesion" and the affected vessel "target-vessel". Vice versa, a bystander lesion not directly responsible for the ACS is called "non-culprit lesion" and the vessel "non-target vessel"

After ACS, the disease may return to its stable form CCS, but subsequent risk for future cardiovascular events is increased thereafter, and depends on the adoption of the risk modifiers, such as lifestyle adjustment, medical therapy, and completeness of revascularization (Neumann et al. 2019; Knuuti et al. 2020; Byrne et al. 2023).

### 2.1.3 Anatomy vs. physiology in coronary stenoses

From historical flow models it is known, that coronary blood flow starts to be significantly impaired at approximately 40-50% luminal stenosis (Klopp and Gott 1975). However, in approximately 40% of the cases, there is disagreement between the anatomical and hemodynamic severity of CAD (Meijboom et al. 2008; Tonino et al. 2010), highlighting the need of a combined anatomical and functional diagnostic approach to CAD.

The extent of myocardial ischemia in CAD has been shown to be continuously related to worse outcome (Hachamovitch et al. 2003). And if the amount of ischemia exceeds ~10-15% of the myocardium, observational studies suggested a survival benefit from revascularization as compared to medical therapy alone (Hachamovitch et al. 2003, 2011). Also for invasive FFR, a continuously increasing event risk with lower FFR has been observed (Johnson et al. 2014; Barbato et al. 2016). The FAME 2 (Fractional Flow Reserve Versus Angiography For Multivessel Evaluation 2) trial demonstrated that patients with significantly impaired invasive FFR ≤0.80 randomized to percutaneous coronary intervention (PCI) underwent less frequently urgent revascularization throughout 5 years as compared to patients randomized to medical therapy alone. Of note, the rate of death or MI did not differ between the groups. And further, patients in the FFR ≤0.80 group who underwent PCI, had a similar outcome throughout 5 years as patients with FFR >0.80 managed medically. (De Bruyne et al. 2012; Xaplanteris et al. 2018). Therefore, current guidelines recommend to base decisions on revascularization on the presence of the hemodynamic significance of coronary stenoses, unless a very high degree of stenosis (>90%) is present (Neumann et al. 2019; Knuuti et al. 2020).

New information to this topic was provided by the ISCHEMIA (International Study of Comparative Health Effectiveness with Medical and Invasive Approaches) trial, which was released after the latest version of the ESC guidelines. This international randomized-controlled trial (RCT) randomized CAD patients with moderate to severe ischemia to an invasive strategy with revascularization on top of optimal medical therapy vs. optimal medical therapy alone. Over a median follow-up of 3.2 years, there was no difference in the risk of ischemic cardiovascular events or all-cause death between the treatment groups (Maron et al. 2020). However, angina burden was more effectively improved with the invasive strategy as compared to the conservative strategy (Spertus et al. 2020). The results of the ISCHEMIA trial should be interpreted in the light of several important aspects: 1) The study was not tailored to investigate the clinical value of ischemia itself, but whether revascularization is superior to optimal medical therapy with respect to outcome. 2) Due to slow recruitment, the initial primary endpoint was changed from all-cause death or MI to include also resuscitated cardiac arrest and hospitalization for unstable angina (uAP) or heart failure, which may have diluted hard ischemic outcomes. 3)

Whereas there was no difference in the overall rate of MI between the treatment strategies, spontaneous MI was reduced with the invasive strategy. This was counterbalanced by an increased rate of periprocedural MI, however, periprocedural MI has generally smaller impact on overall prognosis (Ueki and Kuwahara 2023). Also, spontaneous MI was more frequently associated with cardiovascular death than periprocedural MI in the ISCHEMIA population (Chaitman et al. 2021). 4) 1/7 patients had only mild or no ischemia according to Corelab reading of the non-invasive stress test, and after a protocol amendment due to slow recruitment, even exercise treadmill testing without imaging was allowed for the assessment of ischemia. 5) The extent of ischemia did not generally identify patients who benefit from revascularization, but there was trend towards a signal of reduced MI for patients with the highest extent of ischemia (Reynolds et al. 2021). 6) Patients with the anatomically most severe CAD were identified to benefit from the invasive strategy with respect to cardiovascular death or MI (Reynolds et al. 2021). 7) Significant left main (LM) disease was excluded by CCTA in all patients. 8) The results from the extended follow-up of ISCHEMIA to a median of 5.7 years showed continued reduction in cardiovascular death with the invasive strategy. The overall benefit on mortality however was zeroed by an increased rate of non-cardiovascular mortality in the invasive group, which is biologically currently unexplained (Hochman et al. 2023). These findings were confirmed in a meta-analysis on 25 RCTs including ISCHEMIA, where the cardiac survival benefit with revascularization improved with longer follow-up and was associated with fewer spontaneous MI (Navarese et al. 2021).

Even more recently, the ORBITA-2 (Objective Randomized Blinded Investigation with Optimal Medical Therapy of Angioplasty in Stable Angina) trial has provided new insights on the effect of revascularization on angina burden in ischemic CAD (Rajkumar et al. 2023). In ORBITA-2, patients with stable angina and non-invasively or invasively proven ischemia were randomized to either PCI or a sham procedure to investigate the effect on angina burden after 12 weeks. Importantly, patients underwent a washout phase of anti-anginal medication prior to trial enrolment and only patients with actual angina symptoms in a 2-weeks assessment phase were included. The initiation of anti-anginal medication in the 12-weeks follow-up phase in both groups was triggered by patient symptoms. At the end of the trial, patients assigned to the PCI group had a lower angina symptom score, indicating better health status with respect to angina, and assignment to PCI was associated with a three times higher odds of becoming free from angina as compared to assignment to the sham procedure, while the mean daily anti-anginal medication use during follow-up was comparable between both treatment groups. The ORBITA-2 trial strengthens the role of revascularization for symptom control in CAD in agreement with previous investigations (Boden et al. 2007; Spertus et al.

2020). However, ORBITA-2 represents a landmark trial, as it used a sham-procedure in the medical therapy group to mitigate the placebo effect of invasive procedures on angina burden. Despite this, patients in the PCI group continued to have angina in 60% of the cases, although they had near-normalization of ischemia. This phenomenon needs future dedicated investigation.

These aspects may need consideration when tailoring therapy to a specific patient, and future evidence with more mechanistic insights and systematically collected non-fatal ischemic outcomes over the longterm are required to allow for definite conclusions.

## 2.2 Acute coronary syndrome

### 2.2.1 General approach to diagnosis and treatment

The most frequent clinical manifestation of ACS is presentation with acute chest pain, being present in more than 80% of the patients. The diagnosis of ACS is established based on the combination of the clinical presentation, ischemic electrocardiogram (ECG) changes, and cardiac biomarkers. According to the ECG changes, ACS can further be divided into ST-segment elevation myocardial infarction (STEMI), where elevation of the ST-segment is indicative of transmural ischemia and vessel occlusion, or non-ST-segment elevation ACS (NSTE-ACS) without persistent ST-segment elevation on the ECG, indicating non-transmural ischemia and vessel obstruction. NSTE-ACS is then subdivided into non-ST-segment elevation myocardial infarction (NSTEMI), where cardiac biomarkers indicate myocardial necrosis, and uAP without biomarker release (Byrne et al. 2023).

The first line imaging method in case of high likelihood of ACS is ICA. For ICA, the radial (or femoral) artery is punctuated to insert via a guidewire a small-lumen catheter into the coronary ostia. Iodine-based contrast medium is injected into the coronary tree to visualize the anatomy. Revascularization can then be performed immediately with PCI.

Presentation with STEMI requires immediate ICA and culprit-lesion PCI, latest within 2 hours of symptom onset. For NSTE-ACS, ICA and revascularization should be performed within 24 hours for NSTEMI, or elective in case of uAP (Byrne et al. 2023). After effective culprit-lesion revascularization, medical therapy consisting of the antiplatelet agents aspirin and a P2Y12-inhibitor, potent lipid-lowering therapy, angiotensin-converting-enzyme (ACE) inhibitors / angiotensin receptor II (ATII) antagonists, betablockers, other heart failure medication as needed, lifestyle adjustments (e.g. smoking cessation, mediterranean diet, physical activity), and cardiac rehabilitation represent cornerstones of ACS treatment (Byrne et al. 2023).

### 2.2.2 Multivessel disease in ACS

Among ACS patients, approximately 50% of patients have multivessel disease (MVD), i.e. at least one other significant stenosis besides the culprit-lesion (Byrne et al. 2023). These patients have impaired prognosis as compared to those with single-vessel disease (Sorajja et al. 2007; Park et al. 2014). In MVD, complete revascularization results in improved clinical outcomes compared to culprit-lesion only revascularization in STEMI (Wald et al. 2013; Gershlick et al. 2015; Engstrøm et al. 2015; Smits et al. 2017; Mehta et al. 2019) and indirect evidence supports the same for NSTE-ACS (Rathod et al. 2018; Siebert et al. 2019). Accordingly, complete revascularization obtains a Class I ("is recommended") (level of evidence A) recommendation for STEMI and a Class IIa ("should be considered) (level of evidence C) for NSTE-ACS in the current ESC treatment guidelines on ACS (Byrne et al. 2023).

Hemodynamic assessment for lesions considered for PCI is recommended in CCS (Neumann et al. 2019; Knuuti et al. 2020). However, for non-culprit lesions of NSTE-ACS patients, such benefits are less established (Ntalianis et al. 2010; Layland et al. 2015; Lee et al. 2023), and the use of physiology is currently recommended with a Class IIB ("may be considered") (level of evidence B) recommendation. For STEMI, the current recommendation is to base the decision on non-culprit revascularization on the angiographic severity (Class I, level of evidence A), due to favourable outcomes of an angiography-based full revascularization strategy (Wald et al. 2013; Gershlick et al. 2015; Mehta et al. 2019), concerns about the reliability of a physiologic assessment in the acute setting of STEMI (van der Hoeven et al. 2019), and inconclusive results from randomized-controlled outcome trials (Puymirat et al. 2021; Lee et al. 2023).

### 2.2.3 Fractional flow reserve

#### 2.2.3.1 Concept of FFR

On the basis of a linear realationship between pressure and flow under conditions of constant and minimized intracoronary resistance (Gould et al. 1990), the concept of FFR has been developed (Pijls et al. 1993, 1995). FFR represents the current invasive gold standard of the hemodynamic assessment of coronary stenoses (Neumann et al. 2019; Knuuti et al. 2020). FFR is defined as the maximal blood flow to the myocardium in the presence of a stenosis in the supplying coronary artery, divided by the theoretical normal maximal flow in this territory. Thus, FFR represents the fraction of the normal maximal myocardial flow that can be achieved despite the coronary stenosis (Pijls et al. 1996). FFR is independent of changes in systemic blood

pressure and heart rate and takes into account the contribution of collateral blood supply (De Bruyne et al. 1994).

FFR is measured during ICA by advancing a pressure wire distal to a coronary stenosis. The pressure distal to this stenosis (Pd) is measured under maximum steady-state hyperemia with vasodilators such as adenosine and then divided by the mean aortic pressure (Pa) (Pijls et al. 1995, 1996) (**Figure 2**). FFR is a highly reproducible index with almost no variability (Pijls et al. 1995; Berry et al. 2013). The normal value is 1.0 and the clinically used threshold for functionally significant CAD is ≤0.80 (Tonino et al. 2009; De Bruyne et al. 2012).

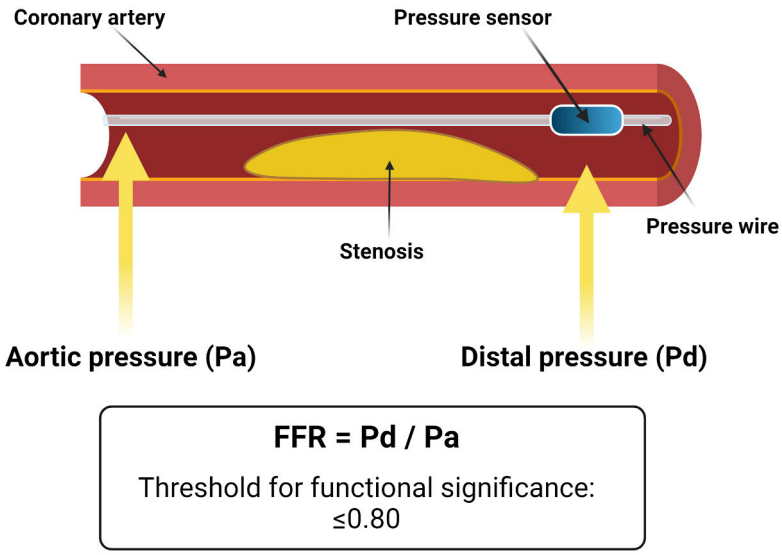


**Figure 2.** Illustration of the concept of fractional flow reserve (FFR). A pressure wire is advanced distally to a coronary stenosis. FFR is defined as the pressure distal (Pd) to this stenosis divided by the aortic pressure (Pa). The threshold for functionally significant CAD is ≤0.80. Author's own drawing with BioRender.com.

Importantly, since FFR measures the pressure drop across a stenosis in an epicardial main vessel, while myocardial ischemia is also determined by other factors such as the disease in smaller side branches not well suitable for FFR interrogation, the microcirculation, oxygen demand, and wall stress, some disagreement in the classification of hemodynamically significant CAD between FFR and imaging methods assessing myocardial perfusion (see section 2.3.2) is expected and also observed in practice (Knuuti et al. 2018). Therefore, strictly speaking, the terms "impaired FFR" and "myocardial ischemia" may not be used

interchangeably, although such jargon is common in the dedicated literature (Tonino et al. 2009; De Bruyne et al. 2012).

#### 2.2.3.2 Clinical evidence on FFR

Among CCS patients, FFR-guided treatment decisions have shown to be associated with favourable prognosis in the DEFER (Deferral Versus Performance Of PTCA In Patients Without Documented Ischemia), FAME, and FAME 2 trials (van Nunen et al. 2015; Zimmermann et al. 2015; Xaplanteris et al. 2018), as well as a patient-level meta-analysis (Zimmermann et al. 2019). These favourable outcomes were generally achieved with a lower rate of revascularization and fewer number of stents as for angiography-guided PCI, and therefore, FFR-guided revascularization is recommended by current guidelines (Neumann et al. 2019; Knuuti et al. 2020).

Among STEMI patients, two RCTs, the COMPARE-ACUTE (Comparison Between FFR Guided Revascularization Versus Conventional Strategy in Acute STEMI Patients With MVD) and DANAMI-3-PRIMULTI (Primary PCI in Patients With ST-elevation Myocardial Infarction and Multivessel Disease: Treatment of Culprit Lesion Only or Complete Revascularization) trials, have compared FFR-guided complete revascularization to culprit-lesion only PCI. Both trials have shown improved outcomes for the FFR-guided complete revascularization arm (Engstrøm et al. 2015; Smits et al. 2017). However, the control-arm underwent culprit-lesion-only revascularization, a treatment concept that has been rejected (Byrne et al. 2023) in the view of consistent randomized-controlled evidence indicating harm of such a strategy (Wald et al. 2013; Gershlick et al. 2015; Mehta et al. 2019). For NSTE-ACS, a susbstudy of the FAME trial indicated equal treatment benefit of FFR-guided PCI for NSTE-ACS vs. CCS patients (Sels et al. 2011).

Only recently, two major outcome RCTs comparing angiography-guided vs. FFR-guided complete revascularization in ACS patients have been published (Puymirat et al. 2021; Lee et al. 2023). The FRAME-AMI (Fractional Flow Reserve vs. Angiography-Guided Strategy for Management of Non-Infarction Related Artery Stenosis in Patients with Acute Myocardial Infarction) trial enrolled 52.8% STEMI and 47.2% NSTE-ACS patients. FFR-guided revascularization was superior as compared to angiography-guided revascularization (Lee et al. 2023). In contrast, in the FLOWER-MI (Flow Evaluation to Guide Revascularization in Multivessel ST-Elevation Myocardial Infarction) trial on STEMI patients only, no benefit of FFR-guided over angiography-guided revascularization with a point estimate even indicating harm has been found (Puymirat et al. 2021). It has been hypothesized, that these discordant conclusions could be related to the questionable appropriateness of FFR in STEMI patients. Further reasons may be the timepoint of non-culprit lesion revascularization (FRAME-AMI 40% vs. FLOWER-MI 96.2% staged PCI) as well

as premature termination of the FRAME-AMI trial due to the Covid-19 pandemic (Mehta and McGrath 2023).

FFR carries some important limitations that are specifically disadvantageous in ACS. It is an invasive technique with the need for additional wire manipulation, the administration of adenosine with well-known adverse effects (e.g. chest pain, dyspnoea, headache, hypotension), increased costs, and prolongation of procedural time (Pijls and Tonino 2011). Along these lines, even in international trials, the use of FFR in the acute setting of STEMI has been shown to be inconvenient and was infrequently used (Mehta et al. 2019; Puymirat et al. 2021). Furthermore, there are concerns about the reliability of FFR in STEMI patients. The vasodilatory capacity of the microcirculation in response to adenosine was shown to be blunted in the acute phase of STEMI (van der Hoeven et al. 2019). This can lead to overestimation of FFR, which may leave some non-culprit lesions inappropriately unrevascularized.

### 2.2.4 Hyperemia-free alternative to FFR: iFR

To overcome the limitations of hyperemia induction needed for FFR measurement, instantaneous wave-free ratio (iFR) as another invasive pressure index has been developed (Sen et al. 2012; Petraco et al. 2013). iFR is measured with a coronary pressure wire and is defined as the mean ratio of the instantaneous phasic distal coronary pressure to aortic pressure during a diastolic window free of newly generated wave activity, called the "wave-free period". In this specific period of diastole lasting from 25% into diastole (identified from the dicrotic notch of pressure waveform) to 5 ms before the end of diastole, there are no flow/pressure waves generated from the proximal or distal circulation. The coronary blood flow is intrinsically at its highest and microcirculatory resistance most stable as compared with the whole cardiac cycle (Sen et al. 2012), thereby waiving the need for pharmacologically induced hyperemia. iFR has been validated against FFR (Sen et al. 2012; Petraco et al. 2013) and the clinically used threshold for hemodynamically significant impairment is iFR $\leq$0.89 (Petraco et al. 2013).

The concept of iFR has been questioned by important experts in the field (Pijls et al. 2012; Berry et al. 2013). However, two RCTs have validated the clinical usefulness of iFR by showing similar outcomes for patients treated based on iFR or FFR (Davies et al. 2017; Götberg et al. 2017). This has pathed the way for iFR to be implemented in treatment guidelines (Neumann et al. 2019; Knuuti et al. 2020). Also, the longer-term follow-up data of these trials indicate safe results for iFR (Berntorp et al., 2023; Götberg et al., 2022). However, the data of these outcome trials were derived from mostly simpler lesions from patients with low event risk, and data on higher-risk patients with more complex lesions and higher baseline

cardiovascular risk such as ACS patients with MVD and STEMI patients are missing to date.

## 2.2.5 Quantitative flow ratio

### 2.2.5.1 Concept of QFR

In order to shift the hemodynamic assessment of coronary stenoses further away from its invasive nature, a method to derive virtual FFR from ICA images, quantitative flow ratio (QFR), has been developed (Morris et al. 2013). From two standard angiographic projections, a 3D vessel reconstruction, the 3D-quantitative coronary angiography (3D-QCA) is generated. By applying CFD equations to this 3D anatomic vessel model, the hyperemic blood flow velocity (HFV) is simulated (**Figure 3**). The initial QFR model (Morris et al. 2013) was improved to allow for shorter computational time and expansion to more complex lesions (Tu et al. 2014). Several models for optimal simulation of hypermia have been tested, showing that contrast QFR correlates best with invasive FFR (Tu et al. 2016). Contrast QFR calculates HFV based on the contrast flow velocity (CFV) derived from Thrombolysis in Myocardial Infarction (TIMI) frame counts from the angiographic images using the following equation (Tu et al. 2016):

$$HFV = a0 + a1 \cdot CFV + a2 \cdot CVF^2$$

Where a0, a1, and a2 are parameters that characterize the best fit minimizing the mean distance from all sample points to the fitting curve. The optimal values were obtained from a training dataset (Tu et al. 2014) and were derived at a0 = 0.10; a1 = 1.55, and a2 = -0.93, with an $R^2$ of 0.34 (Tu et al. 2016).

TIMI frame-counting is commonly done manually by the analyst, but more recent software versions also contain an automated tool, which shows high accuracy in comparison with manual frame counting (Devineni et al. 2022).

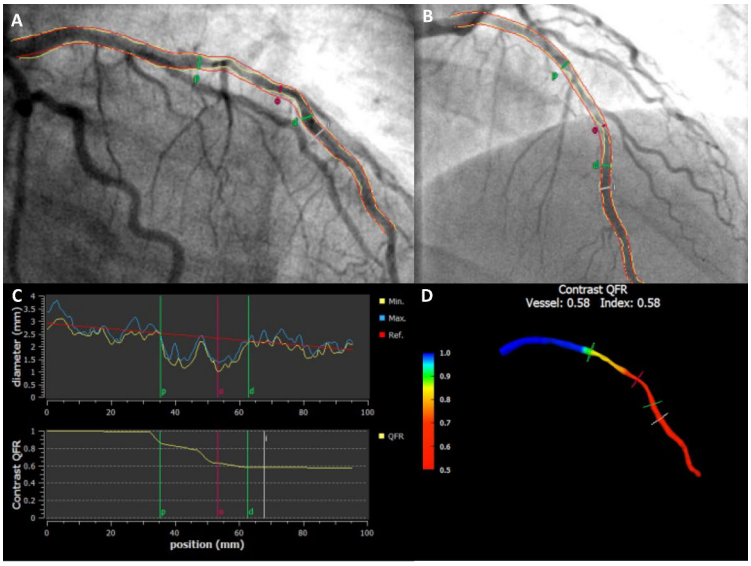


**Figure 3.** Illustration of quantitative flow ratio (QFR). From biplane invasive coronary angiography (A & B), a three-dimensional (3D) vessel model, the 3D-quantitative coronary angiography (3D-QCA) is reconstructed (D). From there, QFR is calculated based on the modelled hyperemic flow velocity from contrast flow velocity using computational fluid dynamics (C). Author's own illustration.

QFR has been broadly validated against FFR and the same cut-off as for FFR, i.e. QFR ≤0.80, to determine hemodynamically significant CAD is used (Tu et al. 2016; Xu et al. 2017; Collet et al. 2018). The pooled AUC across validation studies for the detection of FFR ≤0.80 is 0.94 (Cortés et al. 2021). Reproducibility of QFR is good, but depends on the angiographic quality and the experience of the analysts showing best agreement in those with ≥2000 vessels experience ($r^2$=0.93) (Westra et al. 2022).

Appropriate angiographic angulation is a key quality requirement for QFR, since 3D geometrical assumptions are made from two planar images. The two angiographic views used for the 3D reconstruction must be taken at least 25° apart and should image each specific vessel from its optimal angiographic projections. And beyond this, it should be considered, that more tangential projections can lead to overestimation, and more orthogonal projections to underestimation of stenosis severity. Specific care should also be taken for the image angulation of very eccentric lesions. Since only two projections are sufficient for QFR calculation, radiation and contrast medium amount are not generally increased as compared to a standard diagnostic ICA procedure. Further angiographic quality requirements for QFR calculation are good contrast filling, avoidance of overlap and foreshortening, and the administration of nitroglycerin. Current exclusion criteria for QFR calculation are the presence of ostial LM or ostial right coronary artery (RCA) stenosis, severe

tortuosity, TIMI flow ≤2 (Doucette et al. 1992), tachycardia >100/min, atrial fibrillation or other relevant arrhythmias, bifurcation lesions with a medina 1,1,1 classification (Medina et al., 2006), bypass grafts, bypassed vessels, or vessels with retrograde fillings.

QFR reduces procedural time and radiation dose as compared to FFR (Westra et al. 2018; Ziubryte and Jarusevicius 2021) or iFR (Ziubryte and Jarusevicius 2021; Antoniadis et al. 2022).

#### 2.2.5.2 Clinical evidence on QFR

In the FAVOR III China (The Comparison of Quantitative Flow Ratio Guided and Angiography Guided Percutaneous Intervention in Patients with Coronary Artery Disease) trial, CCS patients were randomized to a QFR-based vs. angiography-based revascularization strategy and improved clinical outcomes throughout 2 years for the QFR-based strategy were found (Xu et al. 2021; Song Lei et al. 2022).

For ACS, no outcome trials of a QFR-guided revascularization strategy are available to date. But, good correlation with FFR with AUCs of 0.91-0.97 (Chu et al. 2022), as well as good agreement between QFR in the acute vs. stable setting have been reported (Spitaleri et al. 2018; Lauri et al. 2019; Chu et al. 2022) in ACS populations. In STEMI, this agreement between acute vs. stable setting has even been reported to be better for QFR than for FFR, possibly related to the inability of the microvasculature to fully dilate under adenosine in the acute setting. This limitation may be overcome with QFR, which mathematically assumes stable conditions (Wang et al. 2023).

QFR respresents a promising novel approach to determine the hemodynamic significance of non-culprit lesions in ACS, owing to its non-invasive, hyperemia-free nature, and the absence of negative effects on procedural safety in the unstable condition of ACS. Data on its prognostic value in the ACS population are needed to further investigate its applicability in this patient population.

### 2.2.6 Timing of non-culprit lesion revascularization

#### 2.2.6.1 Current recommendations

Another aspect in the treatment of non-culprit lesions of ACS patients is the optimal timepoint of non-culprit lesion revascularization. Current ESC guidelines on the management of STEMI provide a Class I (level of evidence A) recommendation for non-culprit-lesion revascularization during the index procedure or staged within 45 days from index PCI (Byrne et al. 2023). This recommendation is based on the treatment strategies of the RCTs which compared culprit-lesion only vs. complete

revascularization (Wald et al. 2013; Gershlick et al. 2015; Engstrøm et al. 2015; Smits et al. 2017; Mehta et al. 2019). In a pivotal subanalysis of one of these trials, the benefit of complete revascularization over culprit-lesion only PCI was independent of whether staged PCI was performed during index hospitalization (median 1 day, IQR 1-3 days) or after hospital discharge within maximum 45 days (median 23 days, IQR 12.5-33.5 days) (Wood et al. 2019).

For NSTE-ACS, a Class IIa (level of evidence C) recommendation is given for immediate complete revascularization (Byrne et al. 2023) based on the RCT SMILE (Impact of Different Treatment in Multivessel Non ST Elevation Myocardial Infarction Patients: One Stage Versus Multistaged Percutaneous Coronary Intervention) (Sardella et al. 2016) and a meta-analysis (Siebert et al. 2019), where immediate complete revascularization was superior as compared to staged PCI.

Two recent RCTs on ACS patients with multivessel disease showed non-inferiority of immediate complete revascularization as compared to staged PCI (within 19-45 days (Stähli et al. 2023) or in-hospital up to 42 days from index PCI (Diletti et al. 2023)). These trials included 100% (Stähli et al. 2023) or 40% (Diletti et al. 2023) STEMI patients. The results from these RCTs indicate, that immediate complete revascularization is safe (in hemodynamically stable patients). And, according to the secondary superiority analyses, immediate complete revascularization may even be protective with respect to early events before planned staged PCI.

However, no evidence on the optimal duration to staged PCI can be derived from these trials. Thus, the optimal timepoint of staged PCI in ACS patients with MVD remains a matter of debate. In clinical practice, the timing of staged PCI is generally based on the operators' judgement and performed either in-hospital or within 2-8 weeks from index PCI (Otsuka et al. 2021). Novel approaches to refine this subjective approach may warrant investigation.

#### 2.2.6.2 A physiology-guided approach to the timing of non-culprit lesion PCI?

An inverse, non-linear relationship between FFR from untreated non-culprit lesions in STEMI patients and non-TV events has been reported (Piróth et al. 2020). Additional evidence exists from retrospective analyses from mixed populations including 29% ACS patients, where FFR was shown to be continuously and inversely related to ischemic event risk (Johnson et al. 2014). These analyses support the concept that the functional significance of non-culprit lesions may represent an ischemic continuum with increasing inverse event risk, rather than a dichotomous state dividing at FFR 0.80.

However, it remains currently unknown, whether such a continuous association also exists for events occurring prior to planned staged PCI, and thus, whether the continuum of hemodynamic impairment could potentially be helpful to optimize the timing of staged PCI. This could ultimately translate to a strategy, where staged PCI would be scheduled earlier in case of a higher degree of flow limitation. Since QFR carries important advantages over FFR in ACS patients, this concept of physiology-based timing of staged PCI may warrant investigation with QFR.

## 2.3 Chronic coronary syndrome

### 2.3.1 General approach to diagnosis and treatment

The diagnostic management of patients with suspected CAD includes the assessment of symptoms, comorbidities and quality of life, a clinical examination, resting ECG, laboratory biochemistry (as appropriate), chest X-ray in selected patients, and resting echocardiography. Based on the integration of these findings as well as the pre-test probability and clinical likelihood of CCS, the appropriate diagnostic modality should be chosen (Knuuti et al. 2020).

The pre-test probability of obstructive CAD can be estimated from age, sex, and the nature of symptoms (Diamond and Forrester 1979; Knuuti et al. 2020). Traditionally, the main symptom of CAD, i.e. chest pain, is divided into typical angina, atypical angina, and non-anginal chest pain. Typical angina is characterized by all of the three following characteristics: 1) constricting discomfort in the front of the chest, in the neck, jaw, shoulder, or arm; 2) precipitated by physical exertion; and 3) relieved by rest or nitrates within 5 min. Atypical angina meets two of these characteristics. And non-anginal chest pain meets only one or none of these characteristics. In the latest version of the guidelines, also dyspnea is considered as symptom (Knuuti et al. 2020). Traditionally, the pre-test probability has been defined as low (<15%), intermediate (15-85%), or high (>85%). Non-invasive diagnostic testing has been recommended in patients with intermediate pre-test probability and invasive testing with high pre-test probability. In the most recent ESC guideline, however, the limits were refined due to reduced prevalence of CAD in contemporary cohorts (Juarez-Orozco et al. 2019).

According to the current guidelines, patients with a pre-test probability <5% can be assumed to have such a low probability of CAD that diagnostic testing should be performed only for compelling reasons. In patients with a pre-test probability >15%, diagnostic testing is generally warranted. The diagnostic testing in patients with a pre-test probability of 5-15% may be considered, particularly if symptoms are limiting and require clarification. In this range of pre-test probability, patient preference, local resources and the availability of tests, clinical judgement, and

appropriate patient information remain important when making a decision to proceed with non-invasive diagnostic testing for an individual patient, and the higher likelihood of a false-positive test must be considered (Knuuti et al. 2020).

Furthermore clinical models that incorporate information on risk factors for cardiovascular disease (e.g. family history of cardiovascular disease, dyslipidaemia, diabetes, hypertension, smoking, and other lifestyle factors), resting and exercise ECG changes, or coronary calcification on CT further improve the identification of patients with obstructive CAD compared with age, sex, and symptoms alone. Therefore, these factors can be used to improve estimations of the pre-test probability of obstructive CAD (Rasmussen et al. 2023).

When diagnostic testing is warranted, CCTA is one of the first-line tests in patients with low to intermediate pre-test probability. CCTA provides information on the anatomical extent of CAD and has high accuracy when used in low clinical likelihood patients (Gueret et al. 2013). For patients with intermediate to high pre-test probability, non-invasive functional testing for ischemia is preferred, since these tests have better rule-in power (Knuuti et al. 2018), and also, revascularization is more likely, which generally mandates the proof of ischemia (Knuuti et al. 2020). Currently available non-invasive functional imaging methods are single-photon emission computed tomography (SPECT), PET, cardiac magnetic resonance (CMR) imaging, and stress echocardiography (Knuuti et al. 2018). When deciding on what test to apply in a specific patient, their specific test characteristics (Knuuti et al. 2018), local availability and expertise, patient characteristics affecting image quality, costs, radiation concerns, and patient preference should be taken into account.

ICA can alternatively be performed upfront among patients with a very high clinical likelihood of CAD, severe symptoms refractory to medical therapy, typical angina at low level of exercise, or clinical evaluation that indicates high event risk. However, also for these patients, functional information of a stenosis should be available for the decision on revascularization, unless a very high grade stenosis (i.e. >90%) is found.

Revascularization is generally performed for two reasons: 1) for prognosis in case of relevant ischemia (Hachamovitch et al. 2003, 2011; Navarese et al. 2021), or 2) for angina control and quality of life (Bangalore et al. 2020; Rajkumar et al. 2023). Besides revascularization of ischemia-causing stenosis, the treatment of CCS consists of medical therapy with antiplatelet agents, lipid-lowering drugs, and anti-anginal medication as needed. Further, lifestyle adaptations with smoking cessation, regular exercise, and weight reduction, as well as optimal therapy of contributing risk factors such as hypertension and diabetes mellitus represent cornerstones of CCS therapy (Knuuti et al. 2020).

## 2.3.2 Non-invasive functional assessment of CAD

### 2.3.2.1 Nuclear myocardial perfusion imaging

SPECT and PET are nuclear myocardial perfusion imaging (MPI) techniques, which use the emissions of radioactive tracers, injected into the blood and taken up by the myocardium to visualize myocardial perfusion. Distribution and accumulation of radioactive perfusion tracers in the myocardium are related to coronary blood flow. During rest, coronary autoregulation may maintain adequate myocardial blood flow (MBF) even in the presence of significant coronary stenosis. However, during stress, MBF increases 3-4 times as compared to rest. This flow increase is impaired in the presence of relevant stenosis. Therefore, tracer accumulation in malperfused areas is reduced as compared with normally perfused myocardium. Accordingly, local abnormalities in myocardial tracer uptake provide information on the location and severity of a functionally significant coronary stenosis. In case of previous myocardial infarction, in the fibrous scar tissue, no tracer accumulation is observed, resulting in a persistent perfusion defect in both rest and stress perfusion images. Therefore, to differentiate between normally perfused, ischemic, and infarcted regions, a combined imaging protocol with acquisitions at rest and during/after stress is required (Veltman et al. 2013).

Physical exercise or pharmacological stress can be used in MPI. Stress imaging with physical exercise allows for concomitant assessment of symptoms, functional capacity, blood pressure and heart rate response, and ECG changes. However, it can only be used with radiotracers with a long half-life and that are trapped into the myocardium, which are most commonly used for SPECT. For pharmacological stress, the vasodilators adenosine, regadenoson, or dipyridamole are in use. Alternatively, dobutamine may be used in patients with contraindications to vasodilatative agents such as severe bronchospastic lung disease, higher grade atrioventricular conduction block, or low blood pressure (Veltman et al. 2013).

#### 2.3.2.1.1 SPECT MPI

SPECT MPI uses gamma ray-emitting tracers, whose photons are being detected by a rotating or surrounding gamma camera. The gamma camera consists of detecting scintillation crystals with separating collimators to allow for localization of the emission. The technetium-99m ($^{99m}$Tc) -labeled tracers sestamibi and tetrofosmin are commonly used. 3D images are reconstructed in a short axis, horizontal long axis, and vertical long axis plane. Additionally, a polar map (bull's eye) is generated (Henzlova et al. 2016). The use of attenuation correction (e.g. using computed

tomography (CT)) (Huang et al. 2016) as well as combined supine and prone positioning (Nishina et al. 2006) increase the diagnostic accuracy of SPECT MPI.

SPECT perfusion images are interpreted visually with the highest tracer uptake assumed to be normal perfusion and other myocardial areas being compared to this reference region. Alternatively, a semiquantitative approach is used, in which the individual myocardial segments based on the 17-segment model (Cerqueira et al. 2002) are numerically graded according to their relative impairment of tracer uptake. The segmental values are then summed up to provide a patient-based summary score. The summed rest score is calculated on rest images and reflects fixed perfusion defects (scars). The summed stress score is calculated on stress images and represents fixed and reversible perfusion defects. The summed difference score is calculated as difference between stress and rest images and represents reversible perfusion defects, i.e. inducible ischemia (Henzlova et al., 2016).

As the analysis is based on relative image reading, in patients with globally reduced perfusion, such as with severe multivessel or LM disease, ischemia may be underestimated or completely missed. This problem may be partly eliminated by detecting stress associated left ventricle dilation or attenuation CT derived coronary calcifications.

More recently, SPECT-based methods for absolute MBF quantification have become available, but they are currently not routinely used (D'Antonio et al. 2023). Radiation exposure from a stress-rest study for $^{99m}$Tc-labelled tracers is 6-7 mSv. A stress-only protocol reduces the radiation dose by 35% (Gimelli et al. 2018).

SPECT has a pooled sensitivity of 73% and specificity of 83% for the detection of FFR ≤0.80 (Knuuti et al. 2018). Also, a perfusion deficit exceeding ~10-15% of the myocardium by SPECT has been shown to be associated with worse prognosis (Hachamovitch et al. 2003, 2011). SPECT is widely available and has relatively low costs, but diagnostic accuracy is generally lower than for PET MPI or CMR, and radiation dose higher than for PET.

#### 2.3.2.1.2 PET MPI

PET MPI uses positron-emitting tracers. The emitted positrons annihilate with free electrons, producing two gamma photons with an energy of 511 keV moving in 180° opposite directions. These coincidental events are recorded with a PET scanner. The detection of conincident photons waives the need for collimators, resulting in higher sensitivity as compared to SPECT. Also, spatial resultion is better as compared to that of SPECT. Attenuation correction (preferably with CT) is routinely used with PET (Driessen et al. 2017).

As for SPECT, PET perfusion images can be interpreted visually based on relative tracer distribution. But PET also allows for quantitative measurement of

absolute MBF. For this, the activity concentration of the radiotracer in the blood and myocardium as a function of time (time-activity curve) is measured, and with mathematical models describing tracer kinetics over time, absolute MBF in ml/g/min can be calculated. This is also useful for the detection of MVD or microvascular dysfunction. An ideal radiotracer for measurement of absolute MBF would be characterized by accumulation in and clearance from the myocardium proportionally linear to the perfusion, irrespective of flow rate or metabolic state. Currently, there are different tracers in use, which have their specific advantages and disadvantages. When interpreting the results of PET MPI studies, the characteristics of the different tracers must be taken into account (Murthy et al. 2018; Sciagrà et al. 2021).

Oxygen-15 ($^{15}$O)-labelled water ($H_2O$) is a metabolically inert and freely diffusible tracer. Myocardial uptake is linear to MBF, which makes it an optimal tracer for absolute MBF quantification. The half-life of oxygen-15 is ~2 minutes, and therefore, the production of this isotope requires an on-site cyclotron. There is almost no retention of the tracer in the myocardium, and consequently, visual analysis of perfusion defects (tracer accumulation) is not feasible with $^{15}$O-$H_2O$ PET (Murthy et al. 2018). $^{15}$O-$H_2O$ PET is currently considered the gold standard for MBF quantification.

Rubidium-82 ($^{82}$Rb) is a widely-used PET perfusion tracer with a half –life of 75 s. It can be produced from Strontium-82 ($^{82}$Sr) with a shelf life of 4-5 weeks, and does not require an on-site cyclotron. The extraction fraction of $^{82}$Rb is low and even more impaired with high MBF, which results in underestimation of myocardial perfusion at high flow rates. These underestimated flow values must be corrected with a mathematical model. In turn, the washout rate for $^{82}$Rb is slow, leading to relatively high retention of the tracer in the myocardium and thus good quality of visual perfusion images (Murthy et al. 2018).

Nitrogen-13 ($^{13}$N) -labelled ammonia also has a high extraction fraction over a wide range of flow values, and is a good tracer for MBF quantification. The half-life of nitrogen-13 isotope is ~10 minutes, and its production also requires an on-site cyclotron. In addition, the retention fraction is relatively high compared to other perfusion tracers, also allowing visual perfusion image analysis (Murthy et al. 2018).

Radiation exposure from a stress-rest study is 0.5–2 mSv for $^{15}$O-$H_2O$, 3–5 mSv for $^{82}$Rb, and 2–4 mSv for $^{13}$N-ammonia. As for SPECT, stress-only protocols are in use to reduce radiation dose (Gimelli et al. 2018).

PET MPI has a pooled sensitivity of 89% and specificity of 85% for the detection of flow-limiting CAD defined as FFR ≤0.80 (Knuuti et al. 2018) and is generally acknowledged as the test with the highest accuracy to determine myocardial perfusion deficits. Also, the prognostic value of PET MPI has been shown in multiple studies (Juárez-Orozco et al. 2018). However, more limited availability and higher costs than SPECT are disadvantages of PET MPI.

#### 2.3.2.2 Cardiac magnetic resonance imaging

CMR is a method based on magnetic resonance imaging and provides information on cardiac morphology, tissue characteristics, flow, and function. In stress CMR, myocardial perfusion and left ventricular wall motion in response to stress with either dobutamine or vasodilators are assessed. In first-pass CMR perfusion, dynamic gadolinium-based contrast medium enhanced images are obtained at rest and after pharmacologic stress with a vasodilator (adenosine, regadenosone, or dipyridamole). The reduced signal increase of the gadolinium contrast agent during first pass is indicative of hemodynamically significant stenosis. Dobutamine stress CMR is based on the visual assessment of low-signal areas with abnormal perfusion. Quantitative perfusion techniques are now also available. This requires two imaging sequences to obtain an arterial input function. The dynamic signal intensity profiles of the left ventricular blood pool and myocardium are converted to gadolinium concentration profiles. Mathematical modelling allows for calculation of absolute MBF. Late gadolinium enhancement analysis 10-15 minutes after gadolinium contrast medium administration demonstrate scar and fibrosis as high-intensity signals due to increased uptake and delayed washout of the contrast medium (Rajiah et al. 2023).

Stress CMR has shown a pooled sensitivity of 89% and specificity of 87% for the detection of FFR ≤0.80 (Knuuti et al. 2018). The prognostic value of reduced stress CMR perfusion (Lipinski et al. 2013; Greenwood et al. 2016) and late gadolinium enhancement (Lipinski et al. 2013) have been shown. Advantages of CMR are lack of radiation and high accuracy, but it is less available, associated with high costs and requires high expertise.

#### 2.3.2.3 Stress echocardiography

In stress echocardiography, transthoracic echocardiography is performed either with exercise or pharmacologic stress. It enables the detection of regional wall motion abnormalities with semiquantitative visual scoring and reduced myocardial wall thickening as surrogates for myocardial ischemia. With respect to exercise stress echocardiography, up to 20% of the patients cannot exercise, 20% exercise submaximally, and 20% have an uniterpretable ECG. Further, chest wall movement and hyperventilation during exercise renders echocardiographic examination difficult (Sicari et al. 2009). Pharmacological stressors in use are either dobutamine (Geleijnse et al. 1997), or less preferably, vasodilators such as adenosine or dipyridamole (Picano 1992). Both, exercise and pharmacological stress echocardiography have similar test characteristics (Picano et al. 2008) with a pooled sensitivity of 85% and specificity of 82% for ≥50% stenosis on ICA across studies

(Knuuti et al. 2018). The prognostic value of stress echocardiography is similar to that of PET MPI and CMR (Metz et al. 2007).

Advantages of stress echocardiography are good availability, lack of radiation, and low cost. However, the technique is highly dependent on operator's experience and patient-specific echo image quality.

#### 2.3.2.4 Exercise ECG

Exercise ECG is no longer recommended as an initial test to diagnose obstructive CAD (Knuuti et al. 2020), due to its low diagnostic performance as compared to non-invasive functional imaging (Knuuti et al. 2018). However, in case functional imaging tests are not available, e.g. in low-income countries, it can still be an alternative, if the risk of false-negative and false-positive results is kept in mind. Also, an exercise ECG is of no diagnostic value in patients with ECG changes at rest that prevent appropriate interpretation of ST-segment deviation during exercise, such as left bundle branch block, paced rhythm, Wolff-Parkinson-White syndrome, ≥0.1 mV ST-segment deviation at rest, or digitalis treatment. However, exercise ECG provides complementary clinical information such as symptom assessment, exercise capacity, blood pressure and heart rate response, and arrhythmias (Knuuti et al. 2020) that can be important to guide clinical management.

### 2.3.3 Coronary computed tomography angiography

#### 2.3.3.1 Concept of CCTA

CCTA is an anatomical non-invasive imaging technique using X-ray computed tomography. Substantial improvements in spatial and temporal resolution over the last two decades have enabled accurate visualization of the epicardial coronary arteries and branches down to 1.5 mm size (Narula et al. 2021; Gaemperli et al. 2022).

Multi-detector computed tomography scanners with 64-320 detector rows are currently used for CCTA. Short-acting nitrates for coronary vasodilation and betablockers to optimize heart rate to ≤60/min are generally given prior to CCTA imaging to improve image quality. The acquisition of the CCTA scan is done with ECG synchronization to the phases with minimal cardiac motion, i.e. either mid- to late diastole (diastasis) or in case of higher heart rate, directly after systole (isovolumetric relaxation). The application of intravenous iodine contrast agent allows for coronary artery lumen visualization and measurement of the degree of stenosis (Pontone et al., 2022a; Abbara et al., 2016). Radiation exposure from a

CCTA scan using contemporary scanners and protocols is 1-6 mSv (Gimelli et al. 2018; Chiong et al. 2023).

In contrast to ICA, which is based on the lumenogram, CCTA also allows for the assessment of atherosclerotic plaque burden. This adds important information to the stage of the atherosclerotic disease, since in the accumulative process of atherosclerosis, before development of obstructive stenosis, vessels undergo positive (i.e. outwards) remodelling for the sake of lumen preservation, a concept called "Glagov phenomenon" (Glagov et al. 1987). As such, visualization of only the lumenogram with ICA, does not visualize the whole burden of disease, carrying important prognostic information, since higher plaque burden in non-obstructive lesions has consistently been related to poorer prognosis (Stone et al. 2011; Thomsen and Abdulla 2016; Williams et al. 2019; Mortensen et al. 2020). Besides positive remodelling, also other features of plaque vulnerability such as low-attenuation (i.e. lipid-rich) plaques, napkin-ring sign (necrotic core) and spotty calcifications can be visualized on CCTA (Pontone et al., 2022a; Abbara et al., 2016).

Several common artifacts still affect image quality in CCTA. Most importantly, high coronary artery calcification can cause blooming and beam-hardening artifacts. Blooming artifacts are related to partial-volume averaging effects and can make a calcified plaque "bloom", i.e. appear larger than it actually is. Beam-hardening artifacts cause dark image areas in proximity to heavy calcifications and can falsely be interpreted as a non-calcified plaque (Abbara et al., 2016). These artifacts can lead to overestimation of stenosis severity (Hecht and Bhatti 2008). Therefore, CCTA may not be performed among patients with abundant calcification, although no united threshold for this has been implemented in the guiding scientific documents (Abbara et al. 2016; Knuuti et al. 2020; Narula et al. 2021; Pontone et al. 2022a). Other CCTA artifacts include motion, misalignment (step artifacts), metal artifacts, reduced signal-to-noise ratio, and low contrast intensity. These artifacts can be reduced by optimal patient selection and preparation (e.g. patient positioning, breath hold training, optimal and regular heart rate, optimizing tube potential and current in obesity) (Pontone et al., 2022a; Abbara et al., 2016).

The sensitivity of CCTA for the detection of obstructive CAD (i.e. >50% stenosis on ICA) is 97%. But, specificity is moderate with ~78% with ICA as a reference standard and 53% with FFR as a reference standard (Knuuti et al. 2018).

CT technology has recently undergone a revolution with the introduction of the first photon-counting CT scanner, which may overcome many of the limitations of conventional CT imaging (Leng et al. 2019; Stein et al. 2023). Although availability of photon-counting CT for clinical routine represents currently a privilege of few centers in the world, widespread use of this technique and replacement of traditional CT technology is expected. Also, for cardiac applications, already promising results have been published (Koons et al. 2022; Decker et al. 2023; Hagar et al. 2023). The

expected wide-spread adoption of photon-counting CT may further strengthen the role of CCTA in the diagnostic path of CAD.

#### 2.3.3.2 Clinical evidence and current role of CCTA

To date, CCTA represents one of the first-line imaging methods for patients with low- to intermediate pre-test probability of CAD (Knuuti et al. 2020) mainly due to its excellent negative predictive value (NPV) of 97% to exclude obstructive CAD (Knuuti et al. 2018). Thus, CCTA can exclude significant CAD with high confidence, which is the main diagnostic aim in this population. The favourable prognosis of patients with excluded CAD on CCTA has consistently been shown (Min et al. 2011; Nielsen et al. 2017). The routine introduction of CCTA has important implications on patient workflow, since only about 1/3 of patients referred for ICA have traditionally been reported to actually need revascularization (Patel et al. 2010). This highlights the importance of CCTA being now established as an effective gatekeeper for ICA referral. The feasibility of CCTA in these low to intermediate risk populations has been shown in several landmark trials.

In the SCOT-HEART (Scottish Computed Tomography of the Heart) trial it was shown that in patients with stable chest pain, CCTA improved the diagnostic certainty and increased the frequency of CAD as compared to standard care. Furthermore, based on the CCTA findings, antiplatelet agents and lipid-lowering drugs were more frequently prescribed than in the standard care group (SCOT-HEART investigators 2015), which plausibly translated to a reduced risk of death from CAD or MI throughout 5 years (The SCOT-HEART Investigators 2018). In the PROMISE (Prospective Multicenter Imaging Study for Evaluation of Chest Pain) trial, the use of CCTA as initial diagnostic modality was associated with similar prognosis as functional testing (Douglas et al. 2015). And in the CONSERVE (Coronary Computed Tomographic Angiography for Selective Cardiac Catheterization) and DISCHARGE (Diagnostic Imaging Strategies for Patients with Stable Chest Pain and Intermediate Risk of Coronary Artery Disease) trials, initial diagnostic testing for suspected CAD with CCTA vs. ICA was associated with similar prognosis (Chang et al. 2019; Maurovich-Horvat et al. 2022), reduced rate of revascularization (Chang et al. 2019), reduced procedural complications from ICA, and similar frequency of angina (Maurovich-Horvat et al. 2022).

Beyond the assessment of the degree of stenosis, vulnerabe plaque characteristics on CCTA were shown to be associated with impaired prognosis in a multitude of studies (Hadamitzky et al. 2013; Chang et al. 2018; Pontone et al. 2022b). In a large meta-analysis, the prevalence of vulnerable features was 9-13% for low-attenuation plaque (<30 Houndsfields units density), 3-4% for the napkin-ring sign, 11-16% for positive remodelling ≥110% (plaque level), and 16-21% for spotty calcification

(patient level). In this analysis, the napkin-ring sign and low-attenuation plaque showed the highest prognostic value, followed by positive remodelling and spotty calcification (Nerlekar et al. 2018). Generally, the positive predictive value (PPV) of vulnerable plaque characteristics is increased with greater magnitude and number of vulnerable features (Pontone et al. 2022b).

However, the main disadvantage of CCTA is its rather low specificity for obstructive disease and rate of false positives (Knuuti et al. 2018), which may trigger further testing. Furthermore, it is an anatomical test only and does not provide the functional information needed to select lesions appropriate for revascularization. To overcome this limitation, several approaches to gain functional information from CCTA are currently being investigated and developed.

#### 2.3.3.3 CT perfusion imaging

CT perfusion imaging (CTP) is a method to detect myocardial perfusion deficits using cardiac CT with specific acquisition protocols. Static and dynamic CTP methods exist.

In static CTP, myocardial attenuation during first-pass perfusion with iodine contrast medium is measured. This provides qualitative measures of low-perfused, i.e. hypo-enhanced, myocardial regions as compared to normal myocardial segments. As for PET, perfusion defects on stress images are evaluated against baseline perfusion to determine reversibility. Subendocardial hypo-enhancement may be seen in severe multivessel disease. However, qualitative assessment with static CTP may miss globally reduced myocardial perfusion, since it highly relies on the presence of a normally perfused area as a reference. Concomitant interpretation of coronary atherosclerosis on CCTA and the clinical information may mitigate this limitation (Danad et al. 2016; Pontone et al. 2022b). The mean radiation dose for static CTP is 6 mSv (Danad et al. 2016).

In dynamic CTP, multiple low-resolution scans during the first-pass of contrast medium are acquired. The time course of myocardial iodine distribution by serial temporal sampling at different time points after injection is used to create time-activity curves. Mathematic modelling of these time-activity curves allows for the quantification of myocardial perfusion in absolute terms (Valdiviezo et al. 2010). Balanced ischemia in case of severe multivessel or LM disease can be detected more reliably than with static CTP. The mean radiation dose of dynamic CTP is 9 mSv (Danad et al. 2016). Further, there is currently no clear threshold to determine normal MBF from dynamic CTP and heterogeneity among various studies exists (Danad et al. 2016; Pontone et al. 2022b).

The addition of CTP to CCTA has shown to decrease the number of false positives, and an overall sensitivity of 81% and a specificity of 86% for the detection

of invasive FFR ≤0.80. Dynamic CTP has shown to have higher sensitivity but lower specificity than static CTP (85% vs. 72% and 81% vs. 90%, respectively) (Celeng et al. 2019). The prognostic value of CTP has been shown for up to 2.9 years (van Assen et al. 2019; Nakamura et al. 2020). However, owing to the high radiation dose and absence of unified threshold for normal MBF, CTP has currently no widely established role in clinical routine.

#### 2.3.3.4 FFR-CT

FFR-CT is a method to estimate FFR from CCTA based on a finite element mesh vessel model and CFD methods to simulate coronary blood flow (Taylor et al. 2013; Min et al. 2015). FFR-CT has been broadly validated against FFR with AUCs for the detection of invasive FFR ≤0.80 of 0.90-0.92 (Driessen et al. 2019; Zhuang et al. 2020). The threshold for hemodynamically significant CAD is ≤0.80, as for FFR. The addition of FFR-CT to CCTA improves the specificity for the detection of invasive FFR ≤0.80 from 61% to 80% (Celeng et al. 2019). Also, the prognostic value of FFR-CT has been shown for up to 5 years (Nørgaard et al. 2018; Ihdayhid et al. 2019; Patel et al. 2020).

CT-FFR is already recommended by some societal guidelines (Gulati et al. 2021; National Institute for Health and Care Excellence 2021) and used in clinical practice in some sites. However, FFR-CT is dependent on optimal CCTA image quality (Taylor et al. 2013), which can lead to at least one unanalyzable vessel in up to 25% of the patients (Driessen et al. 2019). And, if FFR-CT data is analyzed in an intention-to-diagnose approach, i.e. classifying those patients/vessels with unanalyzable result as having hemodynamically significant disease, the AUC for the detection of invasive FFR ≤0.80 deflates to 0.79 per-patient (0.83 per-vessel). This is comparable to that of CCTA alone (0.76 per-patient, 0.80 per-vessel) and markedly lower than that of PET perfusion imaging (0.90 per-patient, 0.86 per-vessel) (Driessen et al. 2019). Furthermore, in recent real-world data, the calculability due to suboptimal image quality was even lower and test characteristics deflated further, questioning the accuracy and applicability of FFR-CT in the broad clinical use (Hamilton et al. 2022; Mittal et al. 2023). Thus, there is room for novel or improved methods to determine the hemodynamic significance from CCTA images.

#### 2.3.3.5 Artificial intelligence

The term artificial intelligence (AI) is used for computational programs able to perform tasks that are characteristics of human intelligence, such as pattern recognition, planning, understanding language, recognizing objects and sounds, and

problem solving. The development of AI dates back to the 1950s, but widespread breakthrough of AI was only possible after the acquisition of large volume data sets, development of computational power to process this "big data", robust computational networks to stratify and weight data, and the emergence of user-friendly software packages (Szolovits, 1988; Russel, 2003).

Machine learning (ML) is an area of AI that can be used to identify patterns and learn rules from large datasets, without being specifically programmed for this or without any prior assumptions (Dey et al. 2019). ML can be performed supervised or unsupervised (Mayr et al. 2014).

In supervised learning, data are assigned labels based on existing classes. With iterative analysis of the data, individual features are selected, processed, and weighted to identify the best combination to fit the outcome of interest. One application of supervised learning with deep learning (DL) mimics human cognition by using multiple layers of convolutional neural networks (CNN). DL informs associations based on previous experience, effectively training the learning process, so that the probability of correct classification increases (Lee et al. 2017). Mathematical models are used to pass on results of a given to a successive layer of the CNN, thereby mathematically modelling the ability of human neurons to process, associate, combine, and classify data.

In unsupervised learning, pattern recognition is allowed to develop freely within the supplied data and the program is not trying to fit data to a defined outcome, but instead is trying to identify consistent patterns in the data (Dey et al. 2019). Various mathematical approaches are used to allow for data clustering, a process of creating homogenous, related groups from hidden patterns in the data without prior knowledge (Mayr et al. 2014). An example of unsupervised learning is identification of novel imaging features from patients with known adverse outcomes.

Validation of any AI algorithm is key. This can be performed in a split sample approach, where the testing dataset used for validation is independent of the initial training dataset (Molinaro et al. 2005). Alternatively, x-fold cross validation techniques are currently used, by using a certain fraction of a dataset (e.g. 90%) for training, and the rest (e.g. 10%) of the data for testing with a given times of iterations (e.g. 10 times) (Dey et al. 2019).

Ensemble learning is an approach in which two or more models are fitted to the same data, and the predictions of each model are combined. One example of ensemble learning is random forest. Random forest is a commonly used ML algorithm, which combines the output of multiple (a "forest" of) decision trees into a single result. It uses bootstrap aggregation, a method in which a random sample of data in a training set is selected with replacement, i.e. individual data points can be chosen more than once. After several data samples are generated, the models are trained on these samples by using a random selection of features in the dataset. This

generates random, uncorrelated decision trees, which are less sensitive to the training data and improve generalizability of the algorithm by reducing overfitting, bias, and overall variance. In classification tasks, the majority of vote of the individual trees is then combined into the final output of the random forest algorithm, for example 1 or 0 (disease present or disease absent) (Dey et al. 2019).

#### 2.3.3.6 Applications of AI in CCTA

AI-based algorithms are expected to revolutionize cardiac imaging in the future, since they have the potential to improve almost all steps of the imaging process. As such, the usefulness of AI-based algorithms in image acquisition and reconstruction, image segmentation, image (co)registration, precision phenotyping, disease classification, and risk stratification have already been shown (Dey et al. 2019; Slart et al. 2021)

In CCTA, cardiac chamber quantification by ML/DL is already an established technique (Baskaran et al. 2020). ML/DL models were also shown to correctly identify coronary calcification (Zeleznik et al. 2021), the presence of previous MI (Mannil et al. 2018), and pericoronary adipose tissue (Commandeur et al. 2019). Furthermore, ML can be used to identify the coronary centreline and vessel surface enabling automated plaque burden quantification (Choi et al. 2021).

However, many AI-applications in cardiac imaging are currently only in use in research settings. For the clinical use, thorough validation is required, for which generally two approaches are applied. The first is transfer learning, where a developed algorithm is distributed to other centers where the algorithm can be trained further and refined to optimize the accuracy for that specific population. In the second approach, instead of algorithm sharing, the data is shared. This becomes increasingly convenient due to growing international collaborations for open source databases (van Assen et al. 2020).

Beyond this, AI applications will need testing and validation in the clinical setting itself. The European Union (EU) has published a white paper on the use of AI (European Commision 2020), where they propose specific regulations for AI applications including requirements of training data, record-keeping of used datasets, transparency, robustness and accuracy, and human oversight. Furthermore, AI applications will need to conform to the medical device and data protection laws. Establishing AI in medicine remains a major task for the medical and regulatory instances of this generation.

#### 2.3.3.7 AI-QCT

Artificial intelligence-enabled quantitative computed tomography (AI-QCT) is an AI-guided cloud-based software algorithm for automated CCTA analysis (Cleerly LABS, Cleerly Inc, Denver, CO, USA) with approval from the U.S. Food and Drug Administration (FDA) since 2021 (Cleerly LABS, 2019). AI-QCT has been used clinically for 3 years with about 40'000 patients in the United States. It utilizes a series of validated CNNs (3D U-Net and VGG network variants) for CCTA image quality assessment, coronary segmentation and labelling, lumen wall evaluation and vessel contour determination, and plaque characterization. The quantitative output of the AI-QCT algorithm consists of presence or absence of features of: 1) stenosis parameters, such as diameter stenosis (DS%) and area stenosis (%), number of severe stenosis >70% and number of moderate stenosis 50-70%, 2) atherosclerosis measurements, such as non-calcified plaque volume (NCPV), total plaque volume, lesion length, 3) vascular morphology features such as total vessel volume, total lumen volume and vessel length and 4) diffuseness that includes a calculation of the sum of volumes and lengths across all involved segments (Choi et al. 2021; Griffin et al. 2023). AI-QCT analysis is available within 10 min.

Stenosis assessment by AI-QCT has shown high agreement with Level 3 (i.e. the most experienced) CCTA readers (Choi et al. 2021) as well as invasive quantitative coronary angiography (QCA) (Lipkin et al. 2022; Griffin et al. 2023). And, plaque quantification with AI-QCT has recently been shown to improve risk stratification for 10-year atherosclerotic events (Nurmohamed et al. 2023). Furthermore, AI-QCT analysis significantly improves physicians' confidence in disease severity assessment and patient management (Nurmohamed et al. 2024b).

#### 2.3.3.8 AI-QCT$_{ischemia}$

There has been growing evidence on a pathophysiological link between plaque burden and type and coronary physiology that goes beyond the degree of luminal stenosis. As such, the traditional stenosis-ischemia model in CAD is about to change to a stenosis-morphology-ischemia model (Ahmadi et al. 2020; Yang et al. 2022).

Low-attenuation plaque volume as a surrogate of lipid-rich plaque as well as positive remodelling were shown to independently predict impaired FFR beyond the degree of luminal stenosis (Driessen et al. 2018; Ahmadi et al. 2018). These factors provide potential and partial explanations to the discrepancy between FFR and obstructive luminal stenosis, which is present in approximately 40% of the cases (Ahmadi et al. 2018, 2020). It is hypothesized, that positive remodelling and high low-attenuation plaque burden impair coronary vasodilatory response to hyperemic stimuli, thereby contributing to low FFR independent of luminal narrowing (Ahmadi et al. 2020; Yang et al. 2022).

Based on these findings, ML methods to improve prediction of ischemic FFR from CCTA with qualitative and quantitative plaque features were tested. Indeed, it was shown that a ML model incorporating features of luminal narrowing, plaque burden, plaque type, remodelling index, and other metrics from semiautomated quantitative computed tomography (QCT) analysis, improves the prediction for lesion specific FFR ≤0.80 (Dey et al. 2018). This model had been improved and validated in a different cohort against FFR and $^{15}O$-$H_2O$ PET perfusion imaging, where it showed similar AUCs as FFR-CT (Lin et al. 2022).

More recently, a ML model to predict invasive FFR ≤0.80 using AI-QCT metrics, has been developed (AI-$QCT_{ischemia}$) (Cleerly ISCHEMIA, Cleerly Inc, Denver, CO, USA). AI-$QCT_{ischemia}$ has received clearance by the FDA in October 2023 (Cleerly ISCHEMIA, 2023) and is in clinical use in the United States since January 2024.

AI-$QCT_{ischemia}$ determines the probability of abnormal invasive FFR with 37 quantitative AI-QCT variables from Cleerly LABS using a random forest ML algorithm (Cleerly ISCHEMIA, 2023) (**Figure 4**). AI-$QCT_{ischemia}$ was trained against invasive FFR (Nurmohamed et al. 2024a) on data from the CREDENCE (Computed tomogRaphic Evaluation of atherosclerotic DEtermiNants of myocardial isChEmia) trial (Stuijfzand et al. 2020). 50% of the data was used for derivation and 50% for internal validation. External validation was performed in the PACIFIC (Prospective Comparison of Cardiac PET/CT, SPECT/CT Perfusion Imaging and CT Coronary Angiography With Invasive Coronary Angiography) trial cohort (Danad et al. 2017).

For AI-$QCT_{ischemia}$ calculation, all coronary arteries with their side branches with diameter ≥1.5 mm are evaluated according to the 18-segment system (Leipsic et al. 2014). AI-$QCT_{ischemia}$ automatically selects the image series per vessel with the best quality. The AI-$QCT_{ischemia}$ cannot be calculated in case of coronary anomalies (except for absent left main), the presence of stents, or if >15% downstream of a vessel cannot be evaluated. The final output is a calculation by a machine learned algorithm to provide non-invasive estimates of FFR, as categorized by professional societal guideline-indicated thresholds of functionally significant disease likely (≤0.80 invasive FFR) vs. functionally significant disease unlikely (>0.80 invasive FFR) (Neumann et al. 2019; Knuuti et al. 2020; Gulati et al. 2021). These results are then presented to the end user in binary fashion (i.e. abnormal AI-$QCT_{ischemia}$ result or normal AI-$QCT_{ischemia}$ result) for ease of understanding for non-specialists and to be in direct accordance with the guideline recommended thresholds to guide coronary revascularization or deferral (Neumann et al. 2019; Knuuti et al. 2020; Gulati et al. 2021). Further, given that hemodynamic impairment is the result of the totality of disease from the ostium to the site of the lesion across the entire vessel, and that the hemodynamic impairment in a proximal portion of a vessel naturally

propagates distally, segments distal to a point along the same vessel tree, where the AI-QCT$_{ischemia}$ result becomes abnormal, are also classified as having an abnormal AI-QCT$_{ischemia}$ result (Nurmohamed et al. 2024a). This enables direct anatomic and physiologic characterization of all coronary lesions across the vascular tree.

AI-QCT$_{ischemia}$ represents a promising novel approach to pair anatomical and functional information from one single CCTA session, which could potentially waive the need for further downstream functional testing after CCTA and simplify the diagnostic path of CAD. Owing to the growing number of patients worldwide with an indication for CCTA (Knuuti et al. 2020; Narula et al. 2021; Pontone et al. 2022a), and growing applications of CCTA across various clinical scenarios (Serruys et al. 2023), AI-QCT$_{ischemia}$ carries the potential to impact patient care at large. However, the performance of AI-QCT$_{ischemia}$ in real-world CCTA data and its prognostic value are unknown to date.

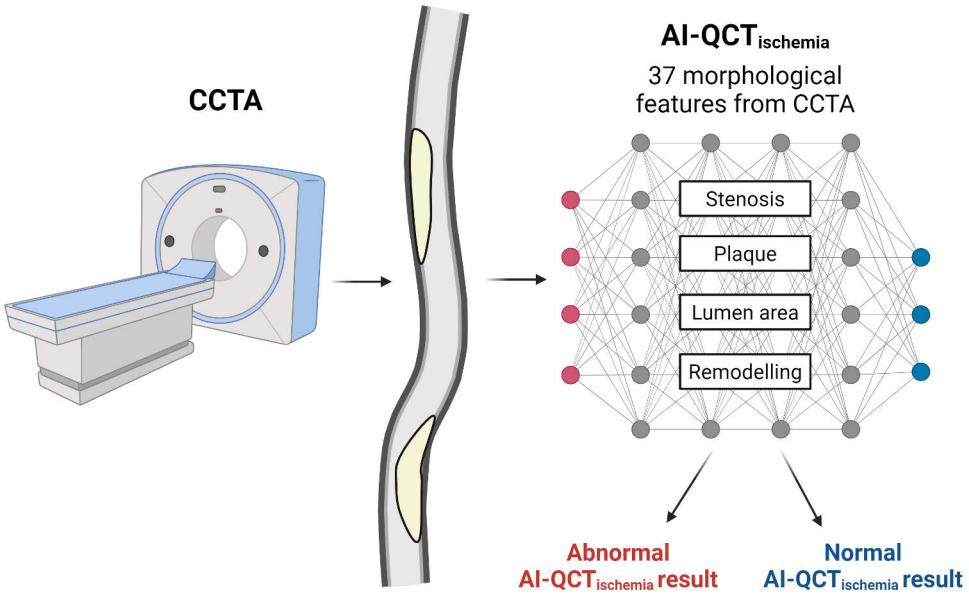


**Figure 4.** Illustration of artificial intelligence-guided quantitative computed tomography ischemia algorithm (AI-QCT$_{ischemia}$). 37 morphological variables from coronary computed tomography angiography (CCTA) are incorporated into a random forest algorithm to determine the probability of invasive fractional flow reserve ≤0.80. The output is binary, i.e. abnormal or normal AI-QCT$_{ischemia}$ result. Author's own illustration with Biorender.com.

# 3 Aims

The aims of this thesis are to 1) evaluate the prognostic value of QFR in ACS patients with MVD undergoing angiography-guided complete revascularization and timing of staged PCI according to operators' judgment, and 2) to assess the prognostic value of AI-QCT$_{ischemia}$ in symptomatic patients with suspected CCS entering diagnostic imaging with CCTA and selective downstream PET perfusion imaging. The aims of the individual articles are as follows:

I. To study the prognostic value of QFR for 5-year non-target vessel events among STEMI patients undergoing angiography-guided complete revascularization.

II. To evaluate the association between QFR from non-target vessel of ACS patients scheduled for staged PCI and non-target vessel events prior to planned staged PCI, to derive first conceptual knowledge, whether QFR could be useful to guide the optimal timepoint of staged PCI.

III. To study the prognostic value of AI-QCT$_{ischemia}$ for long-term clinical events in a population with suspicion of CAD undergoing CCTA, and to assess the risk stratification potential of AI-QCT$_{ischemia}$ separately among patients with no/non-obstructive CAD (i.e. ≤50% stenosis) or those with obstructive CAD (i.e. >50% stenosis) on CCTA.

IV. To investigate the prognostic value of AI-QCT$_{ischemia}$ for long-term clinical events in a population with visual obstructive CAD on CCTA and normal or abnormal myocardial perfusion on downstream PET imaging.

# 4 Materials and Methods

## 4.1 Study I

### 4.1.1 Study design and patient population (Study I)

This was a posthoc analysis on STEMI patients from the prospective COMFORTABLE AMI (Comparison of biolimus eluted from an erodible stent coating with bare metal stents in acute ST-elevation myocardial infarction) trial. COMFORTABLE AMI was an international multicenter RCT on STEMI patients to compare bare metal stents (BMS) with biolimus-eluting stents (BES). The study design as well as 1, 2 and 5 year outcomes have been published previously (Räber et al. 2012a, b; Räber et al. 2014; Moschovitis et al. 2019). Briefly, COMFORTABLE AMI was a single-blinded RCT of 1161 patients with STEMI undergoing primary PCI comparing BMS and BES at 11 sites in Europe and Israel between 2009 and 2011. Main exclusion criteria were MI secondary to stent thrombosis, mechanical complications of acute MI, non-cardiac comorbid conditions with life expectancy <1 year, planned surgery within 6 months of PCI (unless dual antiplatelet therapy was maintained throughout the peri-surgical period), history of bleeding diathesis or known coagulopathy, use of vitamin K antagonists, known intolerance to aspirin, clopidogrel, heparin, stainless steel, biolimus, or contrast material, and (possible) pregnancy. Patients were 1:1 randomly assigned to receive either BMS or BES. Patients underwent angiography-guided complete revascularization for stenoses ≥70% by visual estimate (Räber et al. 2012a). For this QFR study, all untreated non-target vessels at any degree of stenosis, were eligible for QFR measurement. The study complied with the Declaration of Helsinki and was approved by all institutional ethics committees. All patients provided written informed consent.

## 4.1.2 Data acquisition and analysis (Study I)

### 4.1.2.1 ICA and 2D-QCA

All patients underwent diagnostic ICA using standard angiographic projections with at least two orthogonal planes per region of interest at the time of PCI. Administration of nitroglycerin prior to angiography was performed whenever clinically feasible. Complete revascularization based on visual estimation from angiography (i.e. stenosis ≥70% by visual estimate) was recommended with staged PCI to be performed within no longer than 3 months. Treatment of lesions between 50-70% were left to the discretion of the operators. Untreated lesions were categorized in focal ≤20 mm versus diffuse >20 mm (Levine et al. 2011). Two-dimensional (2D)-QCA was assessed with a dedicated software (QAngio XA version 7.3, Medis Medical Imaging Systems, Leiden, the Netherlands).

### 4.1.2.2 QFR and 3D-QCA

QFR and 3D-QCA analysis was performed in the Bern University Hospital Corelab by a certified analyst blinded for patient outcomes using a dedicated software (QAngio XA 3D version 1.2, Medis Medical Imaging Systems, Leiden, the Netherlands). If obtained, optimal angiographic projections for QFR computation as defined by the software manufacturers were used. Contrast QFR using frame-counting (Tu et al. 2016) was measured from the ostium of the index vessel to a distal anatomic landmark visible on both projections at a vessel diameter of ≥2.0 mm. Distal endpoint selection at a minimum vessel diameter of ≥1.5 was chosen in vessels with ≤2.5-2.0 mm proximal reference diameter, which is in line with a previous study (Spitaleri et al. 2018). All analyses were performed according to a previously suggested standard operating procedure (Westra et al. 2018). The conventional cut-off of ≤0.80 for detection of hemodynamically significant CAD was used (Tu et al. 2016; Xu et al. 2017; Westra et al. 2018). For intra- and interobserver reliability testing, repeated QFR analyses by three independent Corelab analysts including 20 randomly assigned vessels were used.

All non-target vessels including major side branches (obtuse marginal, intermediate branch, diagonal branch) without staged PCI and ≥2.0 mm proximal reference diameter were eligible for QFR analysis. QFR-specific exclusion criteria were absence of 2 projections with angle ≥ 25° apart, lack of isocenter calibration, substantial vessel overlap or vessel foreshortening, severe tortuosity, poor contrast, TIMI flow ≤2, tachycardia >100/min, atrial or ventricular arrhythmia, ostial LM or ostial RCA stenosis, bifurcation lesions with 1,1,1 Medina classification (Medina et al. 2006), vessels with retrograde fillings, grafted coronary arteries, and bypass grafts.

#### 4.1.2.3 Primary endpoint and clinical endpoint definitions

The primary endpoint was the composite of cardiac death, spontaneous non-target vessel myocardial infarction (non-TV-MI) and clinically indicated non-target vessel revascularization (non-TVR) throughout 5 years in patients with at least one vessel with QFR ≤0.80 versus patients with all vessels with QFR >0.80. Secondary endpoints included the individual components of the primary endpoint, any spontaneous MI, and any revascularization. We additionally performed multivariable predictor analysis of the primary endpoint and determined the predictive power of QFR ≤0.80 (accuracy, sensitivity, specificity, PPV, NPV) to detect the primary endpoint. Clinical endpoints were adjudicated by an independent clinical events committee. Detailed definitions of all clinical endpoints were reported previously (Räber et al. 2012a).

Cardiac death was defined as any death due to immediate cardiac cause (e.g. MI, low-output failure, fatal arrhythmia), unwitnessed death and death of unknown cause, and all procedure-related deaths, including those related to concomitant treatment. MI was defined according to the extended historical definition (Vranckx et al. 2010). All MIs (TV-MI, non-TV-MI, Q wave MI, non-Q-wave MI) were spontaneous MIs >48 hours after intervention. Periprocedural MIs ≤48 hours after intervention were excluded from the present analysis. TV-MI was defined as MI attributed to a vessel treated at baseline, and non-TV-MI as MI attributed to untreated vessels at baseline, respectively. Non-TVR was clinically indicated using the same definition as for TVR, i.e. lesions with DS% ≥70% (by 2D-QCA) or DS% ≥50% (by 2D-QCA) and one of the following: 1. A positive history of recurrent angina pectoris presumably related to the non-target vessel. 2. Objective signs of ischemia at rest (ECG changes) or during exercise test (or equivalent) presumably related to the non-target vessel. 3. Abnormal results of any invasive functional diagnostic test (e.g. Doppler flow velocity reserve, FFR) (Räber et al. 2012a).

#### 4.1.2.4 Statistical analysis

Continuous variables are presented as mean ± standard deviation (SD) and categorical variables as counts with percentages. Baseline, procedural and 3D-QCA variables were compared using Chi-square test, Fisher's exact test, or t-test, as appropriate. Cumulative incidences of the clinical endpoints through 5 years and from 1-5 years were compared using Cox proportional hazard models and are displayed via Kaplan-Meier curves. Hazard ratios (HR) are provided with 95% confidence intervals (CI). To identify predictors of the 5-year primary endpoint, we ran univariable Cox proportional hazards models for all patient baseline characteristics, QFR ≤0.80, and DS ≥50%, and we subsequently ran a multivariable Cox proportional hazards model including all variables that had a significant

association with the primary endpoint in univariable analysis. We conducted receiver operating characteristic (ROC) analysis to assess the sensitivity, specificity and PPV/NPV value of QFR≤0.80 for the 5-year primary endpoint. To account for changing event risk over time, we additionally performed cumulative case/dynamic control (i.e. time-dependent) ROC analyses at 1, 2, 3, 4, and 5 years using the Kaplan-Meier estimator of the censoring distribution. All analyses were conducted in Stata 15 and RStudio 1.1.463. Significance tests were two-tailed with a significance level set to 0.05.

## 4.2 Study II

### 4.2.1 Study design and patient population (Study II)

This was an observational cohort study on patients enrolled into the Cardiobase Bern PCI registry (NCT02241291) from 2009 to 2017. This is a prospective, single-center observational, registry of all consecutive patients undergoing PCI at Bern University Hospital, Switzerland established in 2009. There are no exclusion criteria other than inability or unwillingness to provide written informed consent. Baseline clinical, procedural and clinical outcomes are assessed at hospital discharge and 1 year after PCI by an independent clinical events committee. The registry complies with the Declaration of Helsinki and is approved by the institutional ethics committee.

Patients are systematically and prospectively followed throughout 1 year to assess clinical outcomes and status of medical treatment. A health questionnaire is sent to all living patients with questions on re-hospitalization and adverse events, followed by telephone contact in case of missing response. General practitioners, referring cardiologists, and patients are contacted as necessary for additional information. For patients who underwent treatment for adverse events at other medical institutions, external medical records, discharge letters, and coronary angiography documentation are systematically collected and reviewed. Clinical events were adjudicated by a clinical event committee consisting of two cardiologists (and a third one in case of disagreement) with use of original source documents.

Specific clinical in- and exclusion criteria for this investigation have been reported previously (Otsuka et al. 2021). In brief, 1432 ACS patients included into the Cardiobase Bern PCI registry scheduled to undergo single staged PCI between 2009 and 2017 were eligible for this analysis. According to the institutional protocol, patients were mostly scheduled for staged PCI between 2-8 weeks from index PCI, however up to 6 months was allowed. Patients with in-hospital staged PCI were excluded, as reported previously, since they usually represent different subsets of patients with either critical lesions requiring urgent intervention or patients who are not willing to return for staged PCI procedures (i.e. advanced age or living far away)

(Otsuka et al. 2021). Patients with cardiogenic shock, multiple staged PCIs, staged cardiac surgery, or missing information on staged PCI were also excluded (Otsuka et al. 2021).

### 4.2.2 Data acquisition and analysis (Study II)

#### 4.2.2.1 QFR and 3D-QCA

QFR and 3D-QCA were assessed using the index procedure angiogram in the non-TV planned for staged PCI by experienced and certified analysts blinded for patient outcomes at the Corelab of Bern University Hospital, Switzerland using a dedicated software (QAngio XA 3D version 1.2, Medis Medical Imaging Systems, Leiden, the Netherlands) as described for Study I. QFR was assessed post-hoc and had no role in patient management. Lesion complexity was assessed according to the American College of Cardiology/American Heart Association (ACC/AHA) criteria (Ryan et al. 1988).

#### 4.2.2.2 Treatment

PCI was performed according to the recommendations and guidelines (Steg et al. 2012; Roffi et al. 2016; Ibanez et al. 2018; Collet et al. 2020) valid at the time of presentation. Briefly, unfractionated heparin (initial bolus of 70-100 I.U. per kg body weight) was administrated during the procedure. Dual antiplatelet therapy (DAPT) consisting of acetylsalicylic acid and a potent P2Y12 inhibitor was initiated before or immediately after the index procedure. The recommended DAPT duration was usually 12 months from index treatment, but modified among patients taking oral anticoagulants or at high bleeding risk. Drug-eluting stents were routinely used. Angiography-guided complete revascularization was performed in non-TV of ACS patients with visual angiographic stenosis ≥50% if deemed technically feasible. Staged procedures were usually performed between 2-8 weeks following index PCI according to institutional practice, but the exact timing was left to the operators' discretion (Otsuka et al. 2021). It cannot be excluded, that patient- or lesion-related factors may have played a role in the scheduling.

#### 4.2.2.3 Primary analysis and clinical endpoint definitions

The primary analysis was an independent predictor analysis of the association between lowest QFR per patient (per 0.1 increase) and the composite of non-target vessel myocardial infarction (non-TV-MI) and urgent unplanned non-target-vessel PCI (non-TV-PCI), occurring before the planned staged PCI.

MI was defined according to a modified historical definition (Vranckx et al. 2010). Non-target-vessel MI (non-TV-MI) was defined as MI attributed to non-culprit-vessels at baseline. Urgent unplanned non-TV-PCI was defined as urgent PCI in non-TVs performed earlier than planned due to ≥1 of the following: 1) recurrent MI (Vranckx et al. 2010), 2) unstable angina (Collet et al. 2020), 3) worsening congestive heart failure, 4) cardiogenic shock, or 5) symptomatic arrhythmia refractory to medication. This event had to be clearly distinguishable from the staged PCI procedure scheduled at index presentation (Otsuka et al. 2021).

QFR was assessed linearly, and, based on previous evidence on inverse, non-linear relationship between FFR and non-TV events plateauing at FFR 0.60 (Piróth et al. 2020), an additional analysis with a non-linear term for QFR was performed. Other covariates were added based on clinical reasoning and consisted of age (per 1 year increase), female sex, renal failure (i.e. glomerular filtration rate (GFR) <60 ml/min), diabetes mellitus, and 3D-QCA DS% (per 5% increase). We also assessed these associations separately for the primary endpoint components, except for non-linear QFR, owing to the limited number of events.

In addition, we planned 2 sensitivity analyses: 1) patient-level, using the same model as described, but with DS% replaced by ACC/AHA lesion complexity, and 2): vessel-level, using the following QFR and angiographic/3D-QCA characteristics: QFR per vessel (per 0.1 increase), 3D-QCA DS% (per 5% increase), minimum lumen diameter (MLD) (per 1mm increase), residual QFR (per 0.1 increase) (i.e. the residual QFR after virtual PCI predicted by an inherent algorithm in the QAngio XA 1.2 software), and ACC/AHA lesion complexity.

#### 4.2.2.4 Statistical analysis

Continuous variables are expressed as mean ± SD and categorical variables are expressed as counts with percentages. For the primary endpoint, we fitted univariable and multivariable Cox proportional hazards regressions including the variables as indicated above. For the vessel-level analysis we used mixed-effects Cox proportional hazards models including patient identity as random factor to correct for multiple vessels per patient. Owing to the model's higher complexity, we did not use a non-linear term for QFR. For all multivariable models, we checked for the presence of multicollinearity by calculating the variance inflation factors (VIF) of all independent variables and confirmed that all VIFs were below 2.

Patients were censored at the time of the primary endpoint event, or at the time of the planned staged PCI, whichever occurred first. For vessel-level analysis, the culprit-vessel of a non-TV-MI was attributed a non-TV-MI event and an urgent unplanned non-TV PCI. If other vessels were treated during this same procedure, these were not adjudicated to have an event, since this treatment is likely to have

been driven by logistical reasons, i.e. if a patient presents for another urgent invasive procedure, all remaining vessels are usually treated, even though they may not be responsible for the acute presentation. For urgent unplanned PCI, if no clear culprit-vessel could be identified from source data, all vessels treated during this procedure were adjudicated as urgent unplanned PCI event. Significance tests were two-tailed with a significance level set to 0.05. All analyses were performed using Stata 16 and R version 4.2.0.

## 4.3 Study III

### 4.3.1 Study design and patient population (Study III)

This was a observational cohort-study on 2271 patients with suspected CAD enrolled into the Turku CCTA registry from 2007 to 2016. This is a single-centre registry of patients undergoing CCTA at Turku University Hospital, Finland. Patients with previous coronary revascularization or documented obstructive CAD (i.e. >50% DS% on ICA) were not considered for inclusion. Data on clinical characteristics, symptoms, and medication were retrospectively collected from electronic medical records. Comprehensive data on all-cause death, MI, and uAP were recorded using the registries of the Finnish National Institute for Health and Welfare and the Centre for Clinical Informatics of the Turku University Hospital. The events identified from the registries were confirmed by investigators using electronic medical records. The follow-up time was median 6.9 [IQR 4.8-9.0] years. The study complied with the Declaration of Helsinki and the Ethics Committee of the Hospital District of Southwest Finland approved the study protocol and waived the need for written informed consent.

### 4.3.2 Data acquisition and analysis (Study III)

#### 4.3.2.1 CCTA

CCTA imaging was performed as described previously (Kajander et al. 2010). In brief, CCTA scans were performed with at least 64-row hybrid PET-CT scanner (GE Discovery VCT or GE D690, General Electric Medical Systems, Waukesha, Wisconsin, United States). Before CCTA image acquisition, intravenous metoprolol (0-30 mg) to achieve a target heart rate of 60 beats/min, as well as isosorbide dinitrate aerosol (1.25 mg) or sublingual nitrate (800 µg) were administered. CCTA was performed using intravenously administered low-osmolal iodine contrast agent. Prospectively triggered acquisition was applied whenever feasible.

CCTA data were initially analyzed visually according to the American Heart Association (AHA) recommendations valid during the enrollment period (Austen et al. 1975) by experienced clinical readers including vessels with diameter ≥1.5 mm.

#### 4.3.2.2 AI-QCT$_{ischemia}$

CCTA scans from the retrospective cohort were uploaded in 2022-2023 to a server and re-analyzed in a blinded manner with the AI-QCT algorithm for automated plaque quantification and characterization (Cleerly LABS, Cleerly Inc, Denver CO) (Choi et al. 2021; Griffin et al. 2023). The AI-QCT results were then fed into the AI-QCT$_{ischemia}$ algorithm (Cleerly ISCHEMIA, Cleerly Inc, Denver CO). The final output is binary, i.e. abnormal AI-QCT$_{ischemia}$ result or normal AI-QCT$_{ischemia}$ result.

Patients were classified as having an abnormal AI-QCT$_{ischemia}$ result in case ≥1 analyzable vessel or side branch was ischemic based on the algorithm. Patients were classified as having a normal AI-QCT$_{ischemia}$ result in case all main vessels (LM, LAD, LCX, RCA) and side branches were analyzable and non-ischemic according to the algorithm. If there was ≥1 non-evaluable vessel in the absence of any ischemic vessels, patients were considered as non-evaluable by AI-QCT$_{ischemia}$ and excluded from the per-protocol analysis. In the full-analysis set, these patients were assessed in an intention-to-diagnose approach, i.e. by classifying those with an inconclusive AI-QCT$_{ischemia}$ result or those excluded due to coronary anomalies as having an abnormal AI-QCT$_{ischemia}$ result.

#### 4.3.2.3 Primary endpoint

The primary endpoint was the composite of all-cause death, MI, or uAP among patients with abnormal vs. normal AI-QCT$_{ischemia}$ result. As a secondary analysis, the primary endpoint was assessed separately among patients with no/non-obstructive CAD (i.e. visual DS ≤50%) and patients with obstructive CAD (visual DS >50%) according to abnormal vs. normal AI-QCT$_{ischemia}$ result in order to evaluate the prognostic value of AI-QCT$_{ischemia}$ among two patient subgroups that are currently managed differently (i.e. non-obstructive disease with medical treatment and obstructive disease with referral for functional testing and/or invasive angiography to assess the need for revascularization). MIs were type 1 MIs (Thygesen et al. 2019) and uAP was defined according to the clinical definition (Collet et al. 2021) and an acute plaque event confirmed by invasive angiography.

#### 4.3.2.4 Statistical analysis

The statistical analyses were performed in an independent academic setting at Turku University Hospital. Continuous variables are shown as mean ±SD or median [IQR]. Categorical variables are shown as numbers with percentages. Mann Whitney U test was used to compare continuous variables and 2-sided Chi-square test was used for categorical variables. Kaplan-Meier curves for clinical events were created and compared with the log-rank test between patients with abnormal vs. normal AI-$QCT_{ischemia}$ result. We report crude HR and adjusted HRs from multivariable Cox proportional hazards models. Adjusting covariates were chosen based on clinical reasoning and consisted of age, sex, hypertension, diabetes mellitus, smoking, dyslipidemia, family history of CAD, and typical angina. Variables with a significant association in univariable models were included into the multivariable models. We also compared three multivariable Cox models for the primary endpoint with the following covariates: Clinical model (1): age, sex, hypertension, diabetes, smoking, typical angina (based on significant univariable associations with the primary endpoint); Clinical+Stenosis model (2): with added visual obstructive stenosis >50%; and Clinical+Stenosis+AI-$QCT_{ischemia}$ model (3): with added AI-$QCT_{ischemia}$. We subsequently ran model 1 and 3 stratified according to the presence of obstructive stenosis and sex. The prognostic performance of the models was compared with Harrel's C. Prognostic modelling with stenosis degree determined by AI-QCT and the result of AI-$QCT_{ischemia}$ combined was not feasible due to multicollinearity (VIF >5). Analyses were two-tailed and a p-value of <0.05 was considered statistically significant. All analyses were performed in Stata version 15.

## 4.4 Study IV

### 4.4.1 Study design and patient population (Study IV)

This was a observational cohort-study from the same population as for Study III, but for Study IV, only 1037 consecutive patients with visual obstructive CAD (adopting the threshold of DS ≥50%) undergoing downstream adenosine stress myocardial PET perfusion imaging after coronary CTA were eligible. 137 patients were excluded due to unavailable CTA data, 97 due to non-adherence to the imaging protocol, 32 due to a non-diagnostic imaging study, and 3 were lost to follow-up. Thus, the final study population consisted of 768 patients eligible for AI-$QCT_{ischemia}$ analysis. Analyses of this subcohort were censored at 10 years due to the low number of patients at risk after 10 years. The follow-up time was median 6.2 [IQR 4.4-8.3] years.

### 4.4.2 Data acquisition and analysis (Study IV)

#### 4.4.2.1 CCTA and AI-QCT$_{ischemia}$

CCTA and AI-QCT$_{ischemia}$ were performed as described for Study III.

#### 4.4.2.2 $^{15}$O-$H_2O$ PET perfusion

According to the institutional imaging protocol, patients with suspected CAD first undergo the CCTA. If there is suspicion of obstructive visual stenosis (adapting the threshold of ≥50%), patients are referred for downstream PET perfusion imaging, while for patients with <50% stenosis, functional imaging is not generally performed (Maaniitty et al. 2017; Stenström et al. 2019). Patients selected based on this protocol underwent dynamic quantitative PET perfusion scan during adenosine stress using a hybrid PET-CT device, as previously described (Kajander et al. 2010). $^{15}$O-$H_2O$ was used as a radiotracer and adenosine infusion (140 µg/kg/min) was used for vasodilator stress (stress-only protocol) (Kajander et al. 2010). The patients were instructed to abstain from caffeine for 24h before PET imaging. PET perfusion scan was usually performed in the same imaging session with CCTA, but for some patients in the following days or weeks due to logistic reasons or caffeine use.

PET data were quantitatively analyzed using Carimas software version 1.0-2.10 (developed at Turku PET Centre, Turku, Finland) to measure stress MBF in standardized 17 segments according to AHA recommendations (Cerqueira et al. 2002; Kajander et al. 2010). Absolute stress MBF ≤2.3 ml/g/min in at least 2 adjacent myocardial segments was considered abnormal based on previous validation against invasive FFR (Danad et al. 2014).

#### 4.4.2.3 Primary endpoint

The primary endpoint was the composite of all-cause death, MI, or uAP among patients with an abnormal vs. a normal AI-QCT$_{ischemia}$ result. This endpoint was assessed separately among patients with normal or abnormal stress MBF in $^{15}$O-$H_2O$-PET. MIs were type 1 MIs (Thygesen et al. 2019) and uAP was defined according to the standard definition (Collet et al. 2021).

#### 4.4.2.4 Statistical analysis

The statistical analyses were performed in an independent academic setting at Turku University Hospital. Continuous variables are shown as mean ± SD or median [IQR]. Categorical variables are shown as numbers with percentages. Student's T test or the

Mann Whitney U test were used to compare continuous variables and 2-sided Chi-square test was used for categorical variables. Kaplan-Meier curves for clinical events were created and compared with the log-rank test between patients with a normal vs. abnormal AI-$QCT_{ischemia}$ result separately among patients with normal or abnormal stress MBF. We report crude HR from univariable and adjusted HR from multivariable Cox proportional hazards models. Analyses were censored at 10 years due to the low number of patients at risk after 10 years. Adjusting covariates were chosen based on clinical reasoning and consisted of age, sex, hypertension, diabetes mellitus, smoking, dyslipidemia, family history of CAD, and typical angina. Variables with a significant association in univariable models were included into the multivariable models. Analyses were two-tailed and a p-value of $<0.05$ was considered statistically significant. All analyses were performed in Stata version 15.

# 5 Results

## 5.1 QFR to predict non-target-vessel-related events at 5-years in STEMI patients (Study I)

### 5.1.1 Baseline patient and procedural characteristics

A total of 1161 STEMI patients were randomized and 1157 patients included in the present analysis (4 patients withdrew consent). At 5 years, clinical follow-up information was available in 1100 patients, out of whom 927 (84.3%) patients were eligible for QFR analysis. After exclusion due to clinical or technical exclusion criteria, a total of 617 (56.1%) patients with 946 vessels were available for the final analysis (**Figure 5**).

Baseline clinical and procedural characteristics were similar for the QFR ≤0.80 and QFR >0.80 group, except for MI SYNTAX (Synergy Between PCI With Taxus and CABG) Score (i.e. post wire-crossing SYNTAX Score) (Magro et al. 2011, 2014) which was significantly higher, and DS% ≥50% by 3D-QCA, which was significantly more frequent in the QFR ≤0.80 group (**Table 1**).

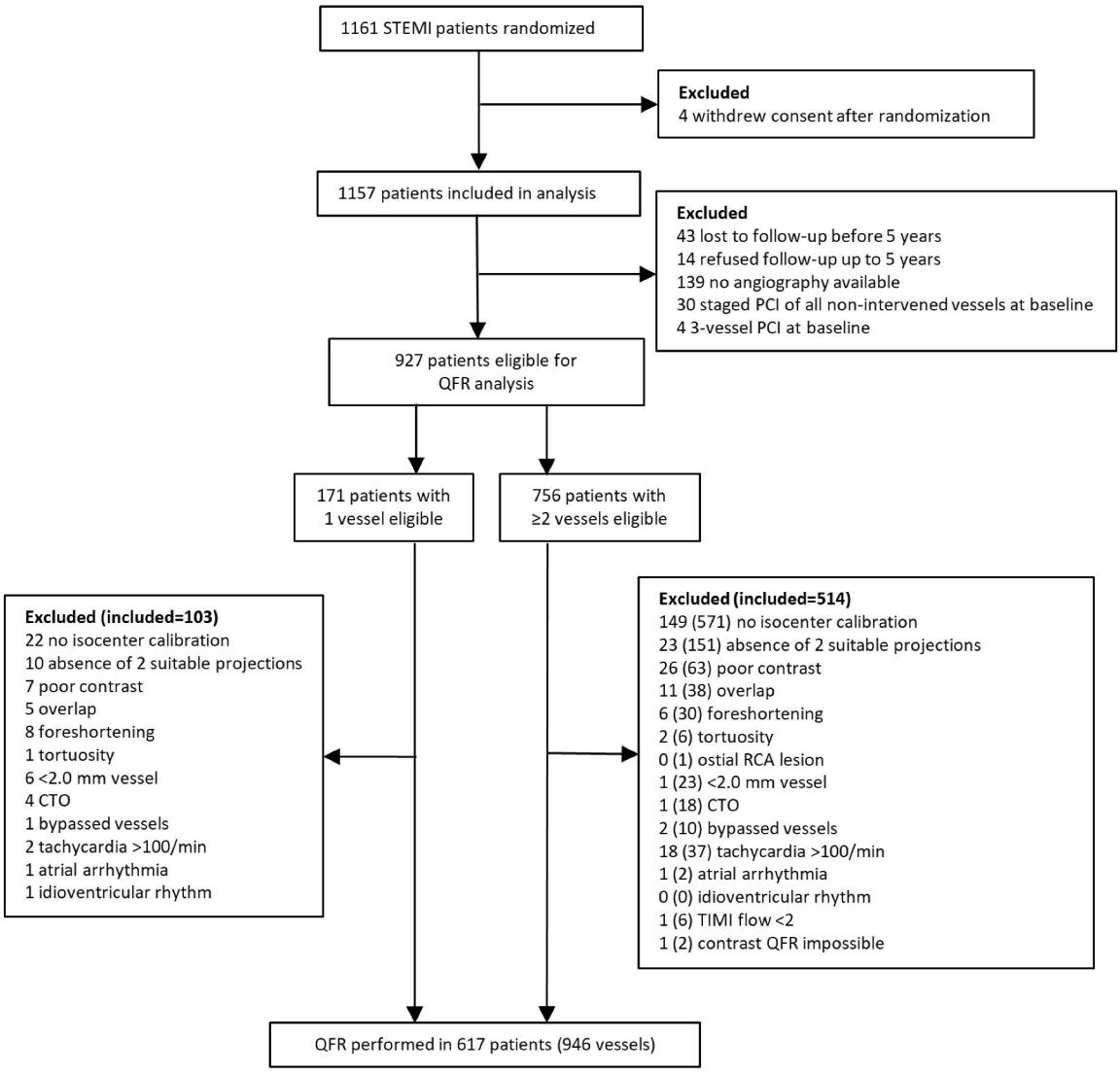


**Figure 5.** Patient flowchart Study I. Depicted are numbers of patients (vessels). CTO = chronic total occlusion, PCI = percutaneous coronary intervention, QFR = quantitative flow ratio, RCA = right coronary artery, STEMI = ST-segment-elevation myocardial infarction, TIMI = Thrombolysis in Myocardial Infarction. Originally published by Bär et al. in J Am Heart Assoc 2021:10:e019052, reprinted with permission.

**Table 1.** Patient- and procedural characteristics Study I.

| PATIENT CHARACTERISTICS | QFR ≤0.80 N=35 | QFR >0.80 N=582 | P-VALUE |
|---|---|---|---|
| SEX (FEMALE), N (%) | 10 (28.6) | 133 (22.9) | 0.415 |
| AGE, YEARS | 63.1 ±11.4 | 60.7 ±11.6 | 0.232 |
| BMI, KG/M2 | 27.3 ±3.5 | 27.0 ±4.0 | 0.730 |
| DIABETES MELLITUS, N (%) | 8 (22.9) | 78 (13.4) | 0.130 |
| HYPERTENSION, N (%) | 22 (62.9) | 262 (45.0) | 0.054 |
| DYSLIPIDEMIA, N (%) | 25 (71.4) | 323 (55.8) | 0.080 |
| FAMILY HISTORY OF CAD, N (%) | 13 (38.2) | 185 (32.2) | 0.457 |
| KILLIP I OR II, N (%) | 33 (94.3) | 577 (99.1) | 0.055 |
| KILLIP III, N (%) | 1 (2.9) | 3 (0.5) | 0.209 |
| LEFT VENTRICULAR EJECTION FRACTION, % | 49.1 ±10.4 | 48.7 ±10.3 | 0.840 |
| MI SYNTAX SCORE | 16.2 ±10.9 | 11.1 ±7.6 | <0.001 |
| PROCEDURAL CHARACTERISTICS (PATIENT-LEVEL) | | | |
| INFARCT VESSEL<br>LM, N (%)<br>LAD, N (%)<br>LCX, N (%)<br>RCA, N (%) | <br>0 (0.0)<br>5 (14.3)<br>7 (20.0)<br>23 (65.7) | <br>1 (0.2)<br>251 (43.1)<br>80 (13.7)<br>250 (43.0) | 0.003 |
| NUMBER OF LESIONS IN INFARCT VESSEL | 1.03 (0.17) | 1.09 (0.33) | 0.236 |
| INTERVENTION<br>IMPLANTATION OF STENT(S), N (%)<br>ONLY BALLOON DILATATION, N (%) | <br>34 (97.1)<br>1 (2.9) | <br>579 (99.5)<br>3 (0.5) | 0.209 |
| NUMBER OF STENTS PER LESION, N | 1.37 ±0.81 | 1.41 ±0.72 | 0.766 |
| TOTAL STENT LENGTH PER LESION, MM | 28.4 ±15.5 | 26.8 ±13.4 | 0.505 |
| AVERAGE STENT DIAMETER, MM | 3.24 ±0.49 | 3.20 ±0.41 | 0.569 |
| DIRECT STENTING, N (%) | 11 (32.4) | 175 (30.2) | 0.848 |
| MAXIMAL BALLOON PRESSURE, ATM | 16.3 ±3.5 | 15.3 ±3.2 | 0.073 |
| THROMBUS ASPIRATION, N (%) | 23 (65.7) | 353 (60.7) | 0.597 |

| NON-TARGET VESSEL (PATIENT-LEVEL) | QFR ≤0.80 N=35 | QFR >0.80 N=582 | |
|---|---|---|---|
| **LAD, N (%)** | 27 (77.1) | 183 (31.4) | |
| **LCX, N (%)** | 1 (2.9) | 255 (43.8) | <0.001 |
| **RCA, N (%)** | 7 (20.0) | 144 (24.7) | |
| **DS ≥50% BY 3D-QCA, N (%)** | 23 (65.7) | 38 (6.5) | <0.001 |
| **NON-TARGET VESSEL (VESSEL-LEVEL)** | **N=36** | **N=910** | |
| **LAD, N (%)** | 28 (77.8) | 226 (24.8) | |
| **LCX, N (%)** | 1 (2.8) | 463 (50.9) | <0.001 |
| **RCA, N (%)** | 7 (19.4) | 221 (24.3) | |
| **DS ≥50% BY 3D-QCA, N (%)** | 24 (66.7) | 43 (4.7) | <0.001 |

Values are mean ±SD or n (%). BMI = body mass index, CAD = coronary artery disease, DS% = diameter stenosis, LAD = left anterior descending artery, LCX = left circumflec artery, LM = left main artery, MI SYNTAX Score = Myocardial Infarction TAXus and Cardiac Surgery Score, PCI = percutaneous coronary intervention, QFR = quantitative flow ratio, RCA = right coronary artery, 3D-QCA = 3D-quantitative coronary angiography. Originally published by Bär et al. in J Am Heart Assoc 2021:10:e019052, reprinted with permission.

### 5.1.2 QFR and 3D-QCA

Mean DS% of non-culprit lesions was 36.5% (±10.5, range 9.5%-70.3%). Only 1 out of 946 (0.1%) vessels revealed DS% above the revascularization threshold of ≥70% (DS 70.3%). Mean QFR of non-culprit lesions was 0.93 (±0.09. range 0.21-1.00). Only in 36 out of 946 (3.8%) vessels QFR was ≤0.80 and in 910 (96.2%) QFR was >0.80. In the QFR ≤0.80 group, left anterior descending artery (LAD) was the most frequent vessel (77.8%) followed by the RCA (19.4%) and the left circumflex (LCX) (2.8%). The majority (66.7%, n=24) of vessels with QFR ≤0.80 exhibited diffuse disease (i.e. lesion length >20mm (Levine et al. 2011)). Most mismatches between angiographic and functional lesion severity (QFR ≤0.80 but DS <50%), were located in in the LAD (83.3%) and fewer in the RCA (16.7%) and none in the LCX (**Figure 6**). QCA analyses indicated that DS% ($p<0.001$) and area stenosis (AS) ($p<0.001$) were higher, minimal lumen diameter (MLD) ($p<0.001$) lower and lesion length ($p<0.001$) longer in vessels with QFR ≤0.80 vs. >0.80 (**Table 2**).

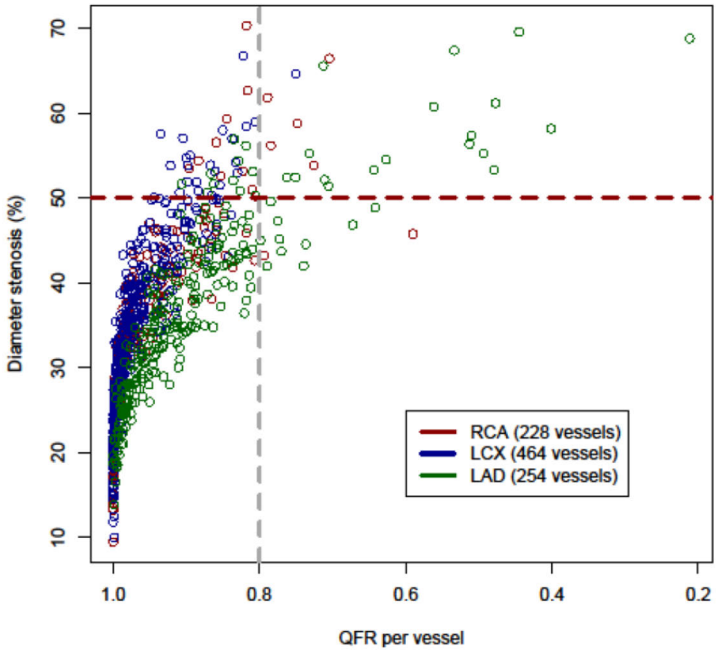


**Figure 6.** Scatterplot DS% vs. QFR (vessel-level). DS% = diameter stenosis, LAD = left anterior descending artery, LCX = left circumflex artery, QFR = quantitative flow ratio, RCA = right coronary artery. Originally published by Bär et al. in J Am Heart Assoc 2021:10:e019052, reprinted with permission.

**Table 2.** 3D-QCA analysis.

| 3D-QCA VARIABLE (PATIENT-LEVEL) | QFR≤0.80 N=35 | QFR>0.80 N=582 | P-VALUE |
|---|---|---|---|
| **DIAMETER STENOSIS, %** | 54.2 ±8.1 | 35.4 ±9.6 | <0.001 |
| **AREA STENOSIS, %** | 69.9 ±8.3 | 45.9 ±15.0 | <0.001 |
| **LESION LENGTH, MM** | 31.0 ±16.9 | 19.9 ±13.2 | <0.001 |
| **PROXIMAL DIAMETER, MM** | 2.77 ±0.61 | 2.90 ±0.63 | 0.264 |
| **MINIMAL LUMEN DIAMETER, MM** | 1.33 ±0.37 | 1.89 ±0.50 | <0.001 |
| **DISTAL DIAMETER, MM** | 2.46 ±0.49 | 2.62 ±0.65 | 0.170 |
| **REFERENCE DIAMETER, MM** | 2.88 ±0.54 | 2.92 ±0.66 | 0.702 |

| 3D-QCA VARIABLE (VESSEL-LEVEL) | QFR≤0.80 N=36 | QFR>0.80 N=910 | P-VALUE |
|---|---|---|---|
| **DIAMETER STENOSIS, %** | 54.2 ±8.1 | 33.3 ±9.6 | <0.001 |
| **AREA STENOSIS, %** | 69.9 ±8.1 | 42.5 ±15.6 | <0.001 |
| **LESION LENGTH, MM** | 30.4 ±17.0 | 18.6 ±13.1 | <0.001 |
| **PROXIMAL DIAMETER, MM** | 2.75 ±0.62 | 2.86 ±0.64 | 0.333 |
| **MINIMAL LUMEN DIAMETER, MM** | 1.32 ±0.37 | 1.92 ±0.51 | <0.001 |
| **DISTAL DIAMETER, MM** | 2.45 ±0.49 | 2.60 ±0.65 | 0.177 |
| **REFERENCE DIAMETER, MM** | 2.86 ±0.55 | 2.88 ±0.66 | 0.797 |

Values are mean ±SD. 3D-QCA = 3D-quantitative coronary angiography, QFR = quantitative flow ratio. Originally published by Bär et al. in J Am Heart Assoc 2021:10:e019052, reprinted with permission.

#### 5.1.2.1 3D-QCA and QFR of treated non-target vessels

As a comparison, 3D-QCA and QFR were also assessed in the non-target vessels that were treated either during the index procedure or as a planned staged procedure. Out of 128 vessels of 105 patients, 89 vessels of 79 patients were eligible for QFR measurement. Mean DS% was 54.2% (±12.4, range 26.2%-92.0%) and mean QFR 0.80 (±11 range 0.40-0.99). Compared to the non-target vessels that were left untreated, QFR was significantly lower ($p<0.001$) and DS% significantly higher ($p<0.001$). 49.4% (n=44) of vessels had QFR ≤0.80.

#### 5.1.2.2 Intra- and interobserver reliability

Intraobserver reliability analysis showed agreement on QFR classification (QFR ≤0.80 vs. >0.80) in 100% of vessels. Intraclass correlation coefficient for continuous QFR was 0.67. Interobserver reliability analysis showed agreement on QFR classification in 90% of vessels, intraclass correlation coefficient was 0.76 and κ coefficient 0.68.

### 5.1.3 Clinical events

Cumulative event rates at 5 years are summarized in **Table 3** and **Figure 7**. At 5 years of follow-up, the rate of the primary endpoint was significantly higher in the QFR ≤0.80 group as compared to the QFR >0.80 group (HR 7.33, 95% CI 4.54–11.83, $p<0.001$). This was driven by significant differences in spontaneous non-TV-MI (HR 4.38, 95% CI 1.47–13.02, $p=0.008$) and non-TVR (HR 10.99, 95% CI 6.39–18.91, $p<0.001$). The non-TV-MIs occurred after a median follow-up of 2.5 years (IQR 1.3-4.3 years). Cardiac death occurred numerically more frequent but

confidence intervals were wide and risk estimates imprecise (HR 1.92, 95% CI 0.58–6.33, p=0.284). Rates of any spontaneous MI (HR 4.38, 95% CI 1.93–9.92, p<0.001) and any revascularization (HR 5.17, 95% CI 3.14–8.52, p<0.001) were significantly higher in the QFR ≤0.80 group. Consistently, exploratory endpoints of cardiac death, any spontaneous MI and any revascularization (HR 4.68, 95% CI 2.96–7.41, p<0.001) as well as cardiac death and any spontaneous MI (HR 3.58, 95% CI 1.82–7.02, p<0.001) showed significantly higher rates in the QFR ≤0.80 group (**Table 3**). When applying a landmark analysis at 1 year, results for the primary endpoint and its components remained consistent.

#### 5.1.3.1 QFR distribution in untreated non-target vessels with a non-TVR event

Out of 109 vessels of 62 patients with a non-TVR during 5 years of follow-up, matched 2D-QCA from the non-TVR angiographies and QFR values from the baseline angiographies were available in 51 (46.8%) vessels of 33 (53.2%) patients. 36 (70.6%) vessels had DS% ≥50% with ischemia and 15 (29.4%) had DS% ≥70%. In vessels with 2D-QCA DS% ≥50% and ischemia at the timepoint of the non-TVR event, mean QFR calculated from baseline angiography was 0.84 (±0.13, range 0.49-1.00). In vessels with 2D-QCA DS% ≥70% at the timepoint of the non-TVR event, mean QFR calculated from baseline angiography was 0.86 (±0.14, range 0.48-1.00).

**Table 3.** Clinical outcomes at 5 years Study I.

| | QFR≤0.80 N=35 | QFR>0.80 N=582 | CRUDE HR (95% CI) | P-VALUE |
|---|---|---|---|---|
| **CARDIAC DEATH, NON-TV-MI, NON-TVR, N (%)** | 22 (62.9) | 72 (12.5) | 7.33 (4.54-11.83) | <0.001 |
| **CARDIAC DEATH, MI (ANY), REVASCULARIZATION (ANY), N (%)** | 22 (62.9) | 108 (18.8) | 4.68 (2.96-7.41) | <0.001 |
| **CARDIAC DEATH OR MI (ANY), N (%)** | 10 (29.6) | 55 (9.7) | 3.58 (1.82-7.02) | <0.001 |
| **CARDIAC DEATH, TV-MI, TVR, N (%)** | 13 (37.5) | 74 (12.9) | 3.50 (1.94-6.30) | <0.001 |
| **DEATH, N (%)** | 4 (11.4) | 54 (9.3) | 1.28 (0.46-3.54) | 0.631 |
| **CARDIAC DEATH, N (%)** | 3 (8.6) | 27 (4.7) | 1.92 (0.58-6.33) | 0.284 |
| **NON-TV-MI, N (%)** | 4 (12.8) | 17 (3.1) | 4.38 (1.47-13.02) | 0.008 |
| **NON-TVR, N (%)** | 19 (58.6) | 43 (7.7) | 10.99 (6.39-18.91) | <0.001 |
| **REVASCULARIZATION (ANY), N (%)** | 19 (58.6) | 85 (15.0) | 5.17 (3.14-8.52) | <0.001 |
| **MI (ANY), N (%)** | 7 (22.4) | 32 (5.8) | 4.38 (1.93-9.92) | <0.001 |
| **MI Q-WAVE, N (%)** | 3 (9.2) | 9 (1.6) | 5.96 (1.61-22.03) | 0.007 |
| **MI NON Q-WAVE, N (%)** | 5 (16.4) | 25 (4.6) | 3.88 (1.49-10.15) | 0.006 |
| **STROKE (ANY), N (%)** | 3 (9.0) | 12 (2.2) | 4.37 (1.23-15.50) | 0.022 |

Depicted are number of patients (%) and hazard ratios (HR) with 95% confidence intervals (CI) from univariable Cox regressions with p-values. MI = myocardial infarction, non-TV-MI = non-target vessel myocardial infarction, non-TVR = non-target vessel revascularization, TV-MI = target vessel myocardial infarction, TVR = target vessel revascularization, QFR = quantitative flow ratio. Originally published by Bär et al. in J Am Heart Assoc 2021:10:e019052, reprinted with permission.

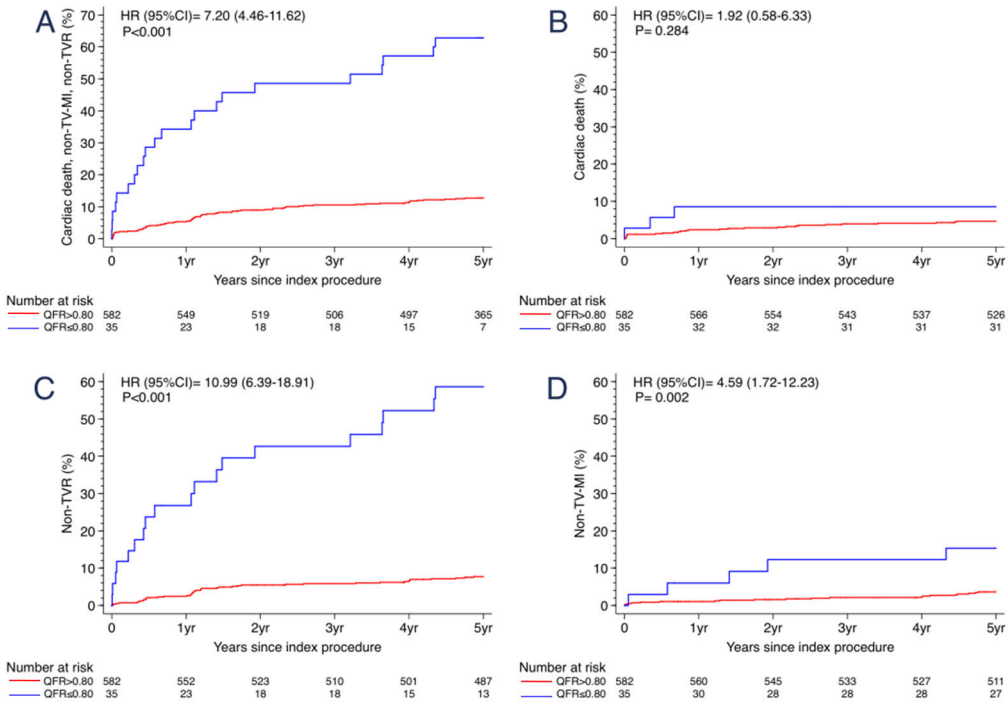


**Figure 7.** Cumulative incidence curves from Cox proportional hazards models through 5 years. A) Primary endpoint: cardiac death, spontaneous non-TV-MI and non-TVR, B) cardiac death, C) non-TVR, D) spontaneous non-TV-MI. CI = confidence interval, HR = hazard ratio, non-TV-MI = non-target-vessel myocardial infarction, non-TVR = non-target vessel revascularization, QFR = quantitative flow ratio. Originally published by Bär et al. in J Am Heart Assoc 2021:10:e019052, reprinted with permission.

### 5.1.3.2 Independent predictor analysis

In multivariable analysis, there was a significant association between QFR ≤0.80 and the primary endpoint with a 7.8 times higher expected hazard for patients with QFR ≤0.80 ($p<0.001$). Further independent predictors of the primary endpoint in multivariable analysis were MI SYNTAX score (per 5 points increase) and left ventricular ejection fraction, but not DS ≥50% by 3D-QCA (**Table 4**).

**Table 4.** Independent predictor analysis.

| CARDIAC DEATH, NON-TV-MI, NON-TVR | UNIVARIABLE ANALYSIS (617 PATIENTS 94 EVENTS) | | MULTIVARIABLE ANALYSIS (571 PATIENTS 94 EVENTS) | |
|---|---|---|---|---|
| | HR (95% CI) | P-VALUE | HR (95% CI) | P-VALUE |
| SEX (FEMALE) | 1.23 (0.78-1.94) | 0.374 | | |
| AGE, YEARS (PER 1 YEAR INCREASE) | 1.03 (1.02-1.05) | <0.001 | 1.02 (1.00-1.04) | 0.061 |
| BMI, KG/M$^2$ (PER 1 KG/M$^2$ INCREASE) | 1.02 (0.97-1.07) | 0.515 | | |
| DIABETES MELLITUS | 2.15 (1.34-3.43) | 0.001 | 1.63 (0.95-2.83) | 0.079 |
| HYPERTENSION | 1.66 (1.11-2.50) | 0.015 | 1.14 (0.71-1.84) | 0.588 |
| HYPERCHOLESTEROLEMIA | 1.26 (0.83-1.92) | 0.277 | | |
| FAMILY HISTORY OF CAD | 0.83 (0.53-1.29) | 0.402 | | |
| KILLIP III OR IV | 7.71 (2.83-20.99) | <0.001 | 3.03 (0.89-10.33) | 0.077 |
| LEFT VENTRICULAR FUNCTION, % (PER 5% DECREASE) | 1.29 (1.17-1.43) | <0.001 | 1.25 (1.13-1.39) | <0.001 |
| MI SYNTAX SCORE (PER 5 POINTS INCREASE) | 1.39 (1.25-1.54) | <0.001 | 1.19 (1.05-1.34) | 0.007 |
| QFR ≤0.80 | 7.33 (4.54-11.83) | <0.001 | 7.75 (3.89-15.42) | <0.001 |
| DS ≥50% BY 3D-QCA | 2.63 (1.59-4.35) | <0.001 | 0.60 (0.28-1.28) | 0.187 |

Depicted are hazard ratios (HR) with 95% confidence intervals (CI) of the primary endpoint (cardiac death, spontaneous non-TV-MI, non-TVR) from uni- and multivariable Cox models. BMI = body mass index, CAD = coronary artery disease, DS% = diameter stenosis by 3D-QCA, MI SYNTAX Score = Myocardial Infarction TAXus and Cardiac Surgery Score, non-TV-MI = non-target vessel myocardial infarction, non-TVR = non-target vessel revascularization, QFR = quantitative flow ratio, 3D-QCA = 3D-quantiative coronary angiography. Originally published by Bär et al. in J Am Heart Assoc 2021:10:e019052, reprinted with permission.

### 5.1.4 Diagnostic Performance of QFR

Using the conventional QFR cut-off point of ≤0.80 for the prediction of the primary endpoint (cardiac death, spontaneous non-TV-MI, non-TVR) at 5 years, accuracy was 86.2%, sensitivity 23.4%, specificity 97.5%, PPV 62.9% and NPV 87.6%. ROC analysis yielded an AUC of 0.64 (95% CI 0.58-0.70) (**Figure 8**). Expressed in absolute patient numbers, in 532 out of 617 (86.2%) patients, QFR ≤0.80 vs. QFR >0.80 correctly identified patients with vs. without a subsequent event (i.e. occurrence of the primary endpoint), whereas in 72 out of 617 (11.7%) patients, QFR was >0.80 despite a subsequent event (false negatives), and in 13 out of 617 (2.1%) patients, QFR was ≤0.80 although no event occurred (false positives). Best QFR cut-

off to predict the primary endpoint was 0.93 with accuracy 64.2%, sensitivity 55.3%, specificity 65.8%, PPV 22.5%, and NPV 89.1%. As a comparator to QFR ≤0.80, we added the diagnostic ability of DS ≥50% by 3D-QCA (**Figure 8**), which yielded markedly lower PPV (32.8%) for DS ≥50% as compared to QFR ≤0.80 (62.9%), but similar AUC (DS ≥50% 0.65 (0.59-0.72), QFR ≤0.80 0.64 (0.58-0.70)).

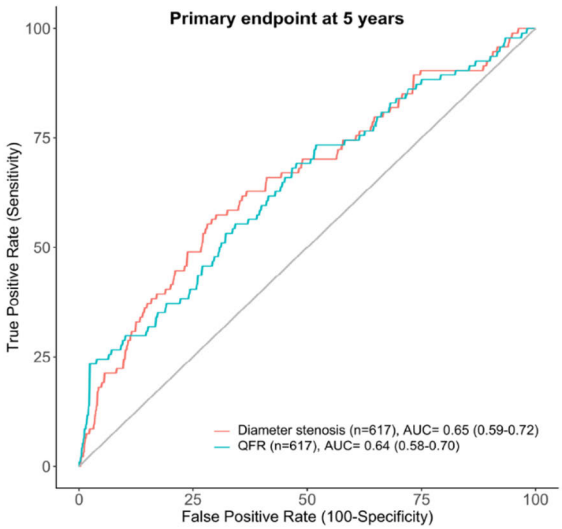


| | QFR | DS |
|---|---|---|
| **Cut-off** | 0.80 | 50% |
| **Accuracy, %** | 86.2 | 81.2 |
| **Sensitivity, %** | 23.4 | 22.3 |
| **Specificity, %** | 97.5 | 91.8 |
| **PPV, %** | 62.9 | 32.8 |
| **NPV, %** | 87.6 | 86.8 |

**Figure 8.** ROC analyses for QFR ≤0.80 vs. DS ≥50% by 3D-QCA predicting the primary endpoint (cardiac death, spontaneous, non-TV-MI, non-TVR) at 5 years. AUC = area under the curve, DS% = diameter stenosis, NPV = negative predictive value, PPV = positive predictive value, QFR = quantitative flow ratio, ROC = receiver operating curve. 3D-QCA = 3D-quantitative coronary angiography. Originally published by Bär et al. in J Am Heart Assoc 2021:10:e019052, reprinted with permission.

To account for changing event risk over time, we additionally performed time-dependent ROC analysis at 1, 2, 3, 4, and 5 years, respectively, which showed similar results (AUC range 0.61-0.64).

## 5.2 QFR to predict non-target-vessel events prior to planned staged PCI in ACS patients (Study II)

### 5.2.1 Patient population

Between January 2009 and December 2017, 8657 ACS patients (STEMI and NSTE-ACS) were consecutively enrolled into the Cardiobase Bern PCI Registry. Staged PCI was scheduled for 1764 patients of whom 1432 patients (1702 vessels, 2197 lesions) fulfilled the clinical eligibility criteria (Otsuka et al. 2021) and were evaluated for QFR measurements. A total of 1262 vessels with 1558 lesions from 1093 patients were analyzable by QFR. Most frequent exclusion criteria were absence of 2 appropriate projections, missing angiographic data, or missing isocenter calibration (**Figure 9**).

Baseline clinical characteristics and medical treatment at hospital discharge are summarized in **Table 5**. There were no significant differences in clinical characteristics between patients with QFR analysis available (n=1093) and those fulfilling the clinical eligibility criteria (n=1432) (Otsuka et al. 2021). Mean patient age was 65 years, 78% were male, 17% had diabetes mellitus, 56% of patients presented with STEMI and 44% with NSTE-ACS. Median duration to planned staged PCI was 28 days (IQR 28-42 days), similar as for the total cohort (Otsuka et al. 2021).

The indication for urgent premature non-TV-PCI (n=52) was most frequently unstable angina (n=31, 60%), followed by MI (n=9, 17%). In 13% (n=7) it was related to congestive heart failure, and only in a minority to refractory arrhythmia (n=3, 6%) or cardiogenic shock (n=2, 4%). Total clinical events throughout 1 year, premature events occurring before planned staged PCI for patients scheduled <4 weeks vs. ≥4 weeks from index PCI, and treatment adherence at 1 year of this cohort have been reported previously (Otsuka et al. 2021).

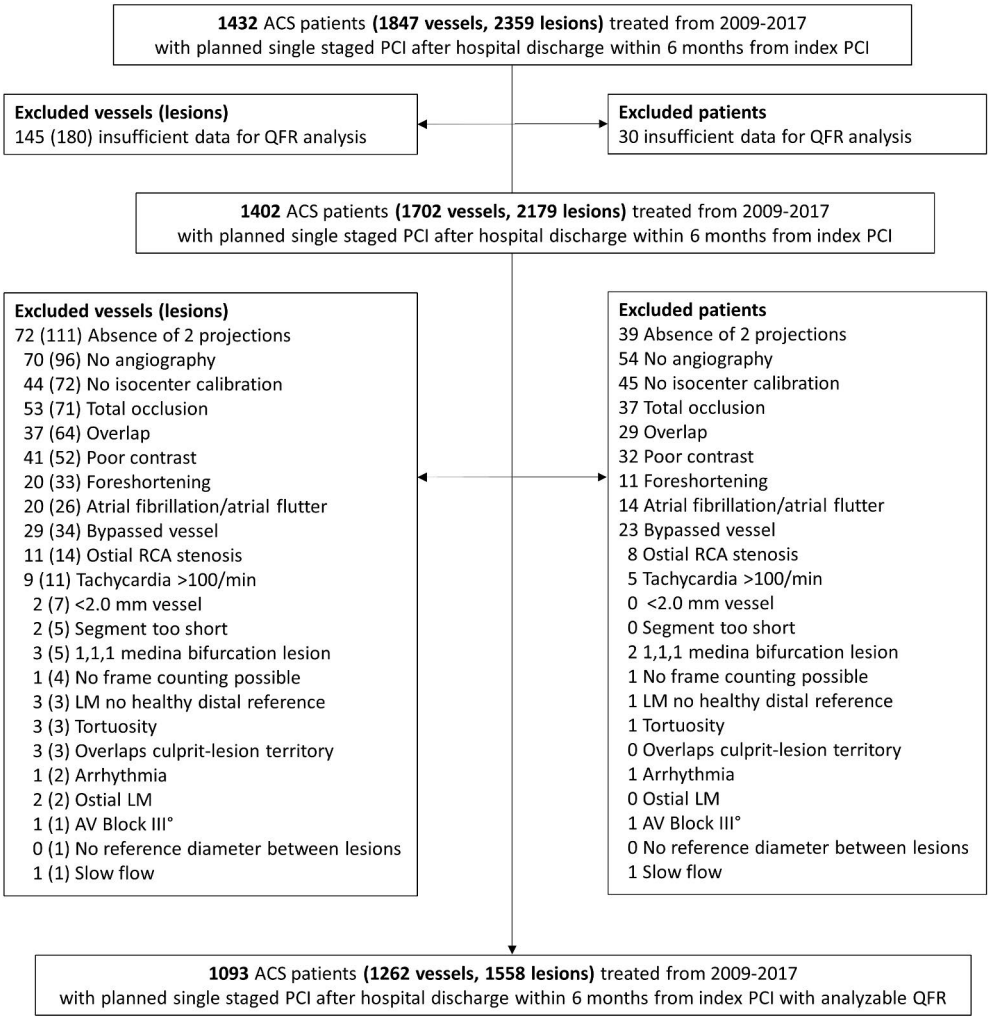


**Figure 9.** Flowchart Study II. ACS = acute coronary syndrome, LM = left main, PCI = percutaneous coronary intervention, QFR = quantitative flow ratio, RCA = right coronary artery. Originally published by Bär et al. in J Am Heart Assoc 2024;2:e031847, reprinted with permission.

**Table 5.** Patient characteristics and medical treatment Study II.

| PATIENT CHARACTERISTICS | N=1093 |
|---|---|
| AGE, YEARS | 65 ±11 |
| FEMALE, N (%) | 238 (22%) |
| BMI, KG/M$^2$ | 27.3 ±4.2 |
| SMOKER, N (%) | 403 (37%) |
| HYPERCHOLESTEROLEMIA, N (%) | 564 (52%) |
| HYPERTENSION, N (%) | 633 (58%) |
| DIABETES MELLITUS, N (%) | 188 (17%) |
| FAMILY HISTORY OF CAD, N (%) | 267 (24%) |
| PREVIOUS MI, N (%) | 62 (5.7%) |
| PREVIOUS PCI, N (%) | 92 (8.4%) |
| PREVIOUS CABG, N (%) | 12 (1.1%) |
| LEFT VENTRICULAR EJECTION FRACTION, % | 51 ±11 |
| INDICATION, N (%) | |
| UNSTABLE ANGINA | 45 (4.1%) |
| NSTEMI | 440 (40%) |
| STEMI | 608 (56%) |
| CONGESTIVE HEART FAILURE, N (%) | |
| KILLIP I | 948 (87%) |
| KILLIP II | 113 (10%) |
| KILLIP III | 32 (2.9%) |
| RENAL FAILURE (GFR <60 ML/MIN), N (%) | 172 (16%) |
| RENAL FAILURE REQUIRING DIALYSIS, N (%) | 15 (1.4%) |
| PERIPHERAL ARTERIAL DISEASE, N (%) | 42 (3.8%) |
| HISTORY OF STROKE OR TIA, N (%) | 46 (4.2%) |
| HISTORY OF GI BLEEDING, N (%) | 13 (1.2%) |
| HISTORY OF MALIGNANCY, N (%) | 93 (8.5%) |
| COPD, N% | 57 (5.2%) |
| ANEMIA*, N (%) | 155 (14%) |
| DAYS FROM INDEX TO PLANNED STAGED PCI | 28 [28, 42] |

| MEDICATION AT HOSPITAL DISCHARGE | N=1093 |
|---|---|
| **ASPIRIN, N (%)** | 1082 (99%) |
| **POTENT P2Y12 INHIBITOR (PRASUGREL OR TICAGRELOR), N (%)** | 851 (78%) |
| **CLOPIDOGREL, N (%)** | 240 (22%) |
| **ANY DAPT, N (%)** | 1081 (99%) |
| **ORAL ANTICOAGULATION (VITAMIN K ANTAGONISTS OR NOAC), N (%)** | 60 (5.5%) |
| **STATIN, N (%)** | 1043 (95%) |

Values are n (%), mean ± standard deviations (SD), or median [interquartile range (IQR)]. *Anemia was defined as hemoglobin <130 g/l in men and <120 g/l in women. ACS = acute coronary syndrome, BMI = body mass index, CABG = coronary artery bypass graft, CAD = coronary artery disease, COPD = chronic obstructive pulmonary disease, DAPT = dual antiplatelet therapy, GFR = glomerular filtration rate, GI = gastrointestinal, NOAC = novel oral anticoagulant, NSTEMI = non-ST-segment-elevation myocardial infarction, PCI = percutaneous coronary intervention, STEMI = ST-elevation-segment myocardial infarction, TIA = transitory ischemic attack. Originally published by Bär et al. in J Am Heart Assoc 2024;2:e031847, reprinted with permission.

### 5.2.2 QFR and 3D-QCA

Of 1262 vessels analyzed by QFR, 41.1% were LAD (n=519), 30.6% LCX (n=386), 27.1% RCA (n=342), and 1.2% (n=15) LM vessels. Mean QFR per patient was QFR 0.73±0.17, mean DS% 54.8 ±11.2%, and ACC/AHA angiographic lesion complexity (lesion-level) was most frequently C, followed by B1 (**Figure 10, Table 6**).

**Table 6.** 3D-QCA and QFR Study II.

| | PATIENTS N=1093 | VESSELS N=1262 |
|---|---|---|
| **DIAMETER STENOSIS, %** | 54.8 ±11.2 | 53.6 ±11.5 |
| **AREA STENOSIS, %** | 70.4 ±12.6 | 69.0 ±13.4 |
| **LESION LENGTH, MM** | 26.1 ±12.1 | 25.0 ±12.0 |
| **PROXIMAL DIAMETER, MM** | 2.86 ±0.59 | 2.82 ±0.59 |
| **DISTAL DIAMETER, MM** | 2.45 ±0.57 | 2.47 ±0.57 |
| **MINIMUM LUMEN DIAMETER, MM** | 1.36 ±0.57 | 1.34 ±0.56 |
| **QFR** | 0.73 ±0.17 | 0.75 ±0.17 |

Values are mean ±standard deviation (SD). QFR = quantitative flow ratio. 3D-QCA = 3D-Quantitative Coronary Angiography. Originally published by Bär et al. in J Am Heart Assoc 2024;2:e031847, reprinted with permission.

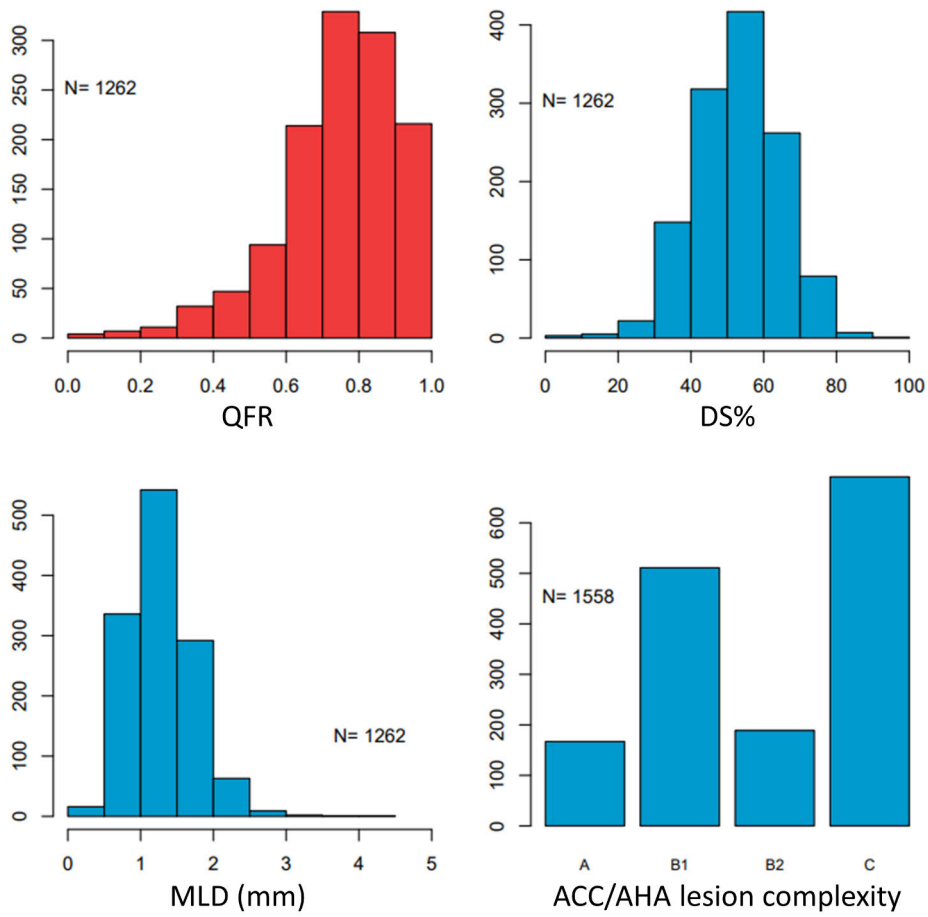


**Figure 10.** QFR and 3D-QCA charcteristics Study II. ACC/AHA = American College of Cardiology/American Heart Association, DS% = diameter stenosis, MLD = minimum lumen diameter, QFR = Quantitative Flow Ratio, 3D-QCA =3D-Quantitative Coronary Angiography. Originally published by Bär et al. in J Am Heart Assoc 2024;2:e031847, reprinted with permission.

### 5.2.3 Primary and secondary analyses

A total of 55 (5.0%) primary endpoint events (non-TV-MI or urgent unplanned non-TV-PCI) had occurred within median 11 days (IQR 5-16 days) prior to planned staged PCI. In multivariable analysis (1018 patients 51 events), there was no independent association between linear or non-linear QFR and the primary endpoint (adjusted HR ($HR_{adj}$) 0.87, 95% CI 0.69-1.05, p=0.125; QFR non-linear p=0.648) (**Figure 11, Table 7**). Overall, none of the variables in the model showed a significant association with the primary endpoint composite (**Table 7**). The sensitivity analysis on patient-level using ACC/AHA lesion complexity instead of

DS% showed consistent results ($HR_{adj}$ 0.90, 95% CI 0.74-1.05, p=0.173; QFR non-linear p=0.603) (**Table 7**). Also, in the sensitivity analysis on vessel-level, there was no independent association between QFR and the primary endpoint ($HR_{adj}$ 0.84, 95% CI 0.65-1.04, p=0.083) (**Table 7**). Cumulative event curves of the primary endpoint components and planned staged PCI are shown in **Figure 12**.

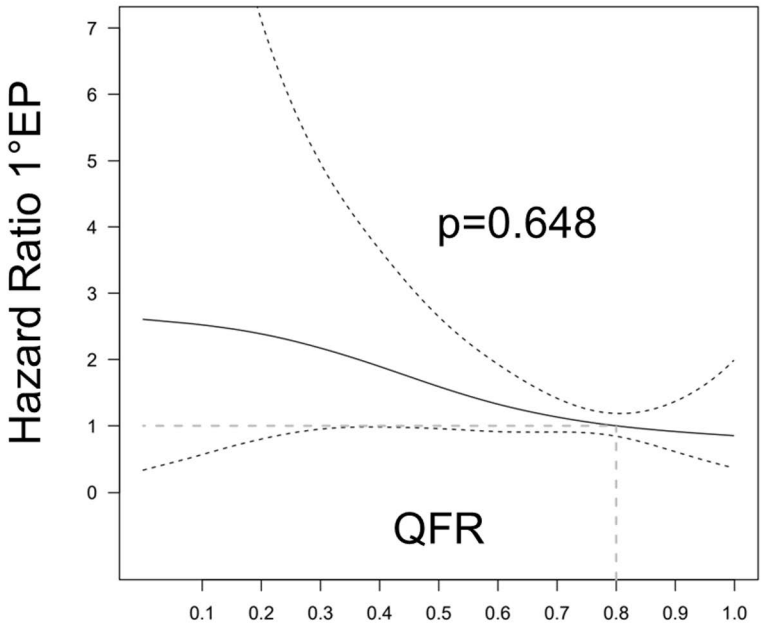


**Figure 11.** Non-linear QFR analysis. Hazard ratios were calculated using the reference hazard corresponding to QFR=0.80 (grey dashed line) from a Cox proportional hazards model with penalized splines. QFR = quantitative flow ratio, 1°EP = primary endpoint. Adapted from Bär et al. in J Am Heart Assoc 2024;2:e031847, reprinted with permission.

**Table 7.** Cox regressions primary endpoint.

| PRIMARY ANALYSIS | N PATIENTS (EVENTS) | UNIVARIABLE | | N PATIENTS (EVENTS) | MULTIVARIABLE | |
|---|---|---|---|---|---|---|
| | | HR (95% CI) | P VALUE | | HR (95% CI) | P VALUE |
| AGE (PER 1 YEAR) | 1093 (55) | 1.01 (0.99 - 1.03) | 0.419 | 1018 (51) | 1.00 (0.98 - 1.03) | 0.750 |
| FEMALE SEX | 1093 (55) | 1.12 (0.60 - 2.08) | 0.723 | 1018 (51) | 1.17 (0.52 – 1.83) | 0.637 |
| DIABETES MELLITUS | 1092 (55) | 0.79 (0.37 - 1.67) | 0.536 | 1018 (51) | 0.80 (0.04 - 1.56) | 0.573 |
| RENAL FAILURE | 1018 (51) | 1.35 (0.69 - 2.64) | 0.373 | 1018 (51) | 1.15 (0.36 - 1.94) | 0.728 |
| DS% (PER 5% INCREASE) | 1093 (55) | 1.01 (0.90 - 1.13) | 0.925 | 1018 (51) | 0.97 (0.83 - 1.12) | 0.726 |
| QFR (PER 0.1 INCREASE) | 1093 (55) | 0.90 (0.78 - 1.04) | 0.141 | 1018 (51) | 0.87 (0.69 - 1.05) | 0.125 |
| SENSITIVITY ANALYSIS I | N PATIENTS (EVENTS) | UNIVARIABLE | | N PATIENTS (EVENTS) | MULTIVARIABLE | |
| | | HR (95% CI) | P VALUE | | HR (95% CI) | P VALUE |
| AGE (PER 1 YEAR) | 1093 (55) | 1.01 (0.99 - 1.03) | 0.419 | 1018 (51) | 1.00 (0.98 - 1.03) | 0.774 |
| FEMALE SEX | 1093 (55) | 1.12 (0.60 - 2.08) | 0.723 | 1018 (51) | 1.17 (0.51 - 1.82) | 0.642 |
| DIABETES MELLITUS | 1092 (55) | 0.79 (0.37 - 1.67) | 0.536 | 1018 (51) | 0.81 (0.05 - 1.57) | 0.588 |
| RENAL FAILURE | 1018 (51) | 1.35 (0.69 - 2.64) | 0.373 | 1018 (51) | 1.16 (0.37 - 1.95) | 0.710 |
| LESION COMPLEXITY (B2 OR C VS. A OR B1) | 1093 (55) | 1.17 (0.68 - 2.01) | 0.577 | 1018 (51) | 1.10 (0.48 - 1.73) | 0.764 |
| QFR (PER 0.1 INCREASE) | 1093 (55) | 0.90 (0.78 - 1.04) | 0.141 | 1018 (51) | 0.90 (0.74 - 1.05) | 0.173 |

| SENSITIVITY ANALYSIS II | N VESSELS (EVENTS) | UNIVARIABLE | | N VESSELS (EVENTS) | MULTIVARIABLE | |
|---|---|---|---|---|---|---|
| | | HR (95% CI) | P VALUE | | HR (95% CI) | P VALUE |
| QFR (PER 0.1 INCREASE) | 1262 (59) | 0.84 (0.61 - 1.14) | 0.265 | 1262 (59) | 0.83 (0.52 - 1.32) | 0.422 |
| DS% (PER 5% INCREASE) | 1262 (59) | 1.01 (0.84 - 1.22) | 0.885 | 1262 (59) | 0.82 (0.58 - 1.16) | 0.257 |
| MLD (PER 1MM INCREASE) | 1262 (59) | 0.54 (0.15 - 1.96) | 0.351 | 1262 (59) | 0.31 (0.06 - 1.72) | 0.181 |
| RESIDUAL QFR (PER 0.1 INCREASE) | 1177 (54) | 0.83 (0.53 - 1.28) | 0.392 | 1262 (59) | 1.05 (0.56 - 1.96) | 0.883 |
| LESION COMPLEXITY (B2 OR C VS. A OR B1) | 1262 (59) | 1.09 (0.47 - 2.52) | 0.839 | 1262 (59) | 0.89 (0.37 - 2.16) | 0.801 |
| QFR (PER 0.1 INCREASE) | 1262 (59) | 0.84 (0.61 - 1.14) | 0.265 | 1262 (59) | 0.83 (0.52 - 1.32) | 0.422 |

Values are hazard ratios (HR) and associated 95% confidence intervals (95% CI) from Cox models. Main analysis and sensitivity analysis 1 correspond to Cox proportional hazards regressions. Sensitivity analysis 2 corresponds to a mixed-effects Cox model including patient identity as random factor to correct for multiple vessels per patient. Sample size for the multivariable model corresponds to the lowest sample size in the univariable models (i.e. renal failure). DS% = diameter stenosis, MLD = minimum lumen diameter, QFR = quantitative flow ratio. Originally published by Bär et al. in J Am Heart Assoc 2024;2:e031847, reprinted with permission.

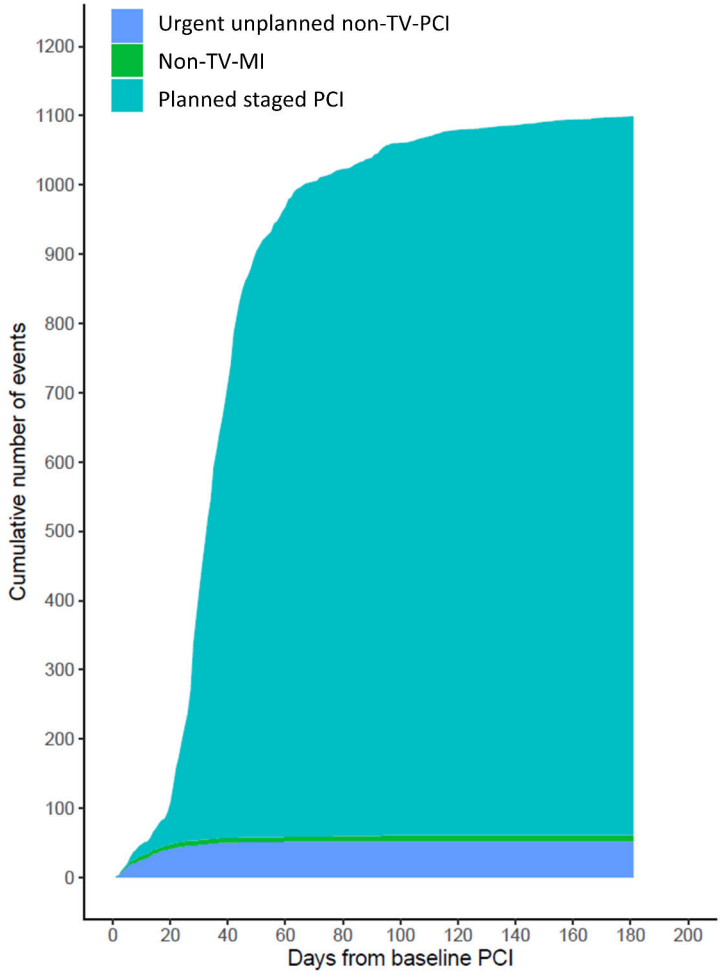


**Figure 12.** Cumulative event curves. Shown are urgent unplanned non-target-vessel (non-TV) staged percutaneous coronary intervention (PCI), non-TV myocardial infarction (MI), and planned staged PCI analysis. Originally published by Bär et al. in J Am Heart Assoc 2024;2:e031847, reprinted with permission.

With respect to the individual primary endpoint components, there was a significant univariable association between linear QFR (per 0.1) and non-TV-MI (HR 0.69, 95% CI 0.52-0.91, p=0.008), but not with urgent premature non-TV-PCI (HR 0.92, 95% CI 0.79-1.07, p=0.299) (**Table 8**). Owing to the limited sample size, non-linear QFR terms and multivariable associations were not assessed.

**Table 8.** Univariable Cox regressions primary endpoint components

| **NON-TV-MI** | **N PATIENTS (EVENTS)** | **UNIVARIABLE HR (95% CI)** | **P-VALUE** |
|---|---|---|---|
| **AGE (PER 1 YEAR)** | 1093 (9) | 1.03 (0.97 - 1.09) | 0.377 |
| **FEMALE SEX** | 1093 (9) | 1.88 (0.47 - 7.52) | 0.374 |
| **DIABETES MELLITUS** | 1093 (9) | - | - |
| **RENAL FAILURE** | 1093 (9) | 2.41 (0.60 - 9.64) | 0.214 |
| **DS% (PER 5% INCREASE)** | 1093 (9) | 1.07 (0.80 - 1.42) | 0.650 |
| **QFR (PER 0.1 INCREASE)** | 1093 (9) | 0.69 (0.52 - 0.91) | 0.008 |
| **URGENT PREMATURE NON-TV-PCI** | **N PATIENTS (EVENTS)** | **UNIVARIABLE HR (95% CI)** | **P-VALUE** |
| **AGE (PER 1 YEAR)** | 1093 (52) | 1.01 (0.98 - 1.03) | 0.480 |
| **FEMALE SEX** | 1093 (52) | 1.20 (0.64 - 2.24) | 0.576 |
| **DIABETES MELLITUS** | 1093 (52) | 0.84 (0.40 - 1.78) | 0.649 |
| **RENAL FAILURE** | 1093 (48) | 1.30 (0.65 - 2.61) | 0.458 |
| **DS% (PER 5% INCREASE)** | 1093 (52) | 1.02 (0.91 - 1.15) | 0.758 |
| **QFR (PER 0.1 INCREASE)** | 1093 (52) | 0.92 (0.79 - 1.07) | 0.299 |

Values are hazard ratios (HR) and associated 95% confidence intervals (95% CI), from Cox models. DS% = diameter stenosis, non-TV-MI = non-target-vessel myocardial infarction, non-TV-PCI = non-target-vessel percutaneous coronary intervention, QFR = quantitative flow ratio. Originally published by Bär et al. in J Am Heart Assoc 2024;2:e031847, reprinted with permission.

## 5.3 Prognostic value of AI-QCT$_{ischemia}$ for patients with suspected coronary artery disease (Study III)

### 5.3.1 Patient population

Out of 2411 patients who underwent CCTA for suspected CAD at Turku University Hospital from February 2007 to December 2016, 2274 patients had CCTA image data available for AI-QCT$_{ischemia}$ analysis. Three patients were lost to follow-up, resulting in the final cohort of 2271 patients eligible for AI-QCT$_{ischemia}$ analysis (full-analysis set). 1880/2271 (83%) patients had conclusive AI-QCT$_{ischemia}$ result (per-protocol set). 509/1880 (27.1%) patients had abnormal and 1371/1880 (72.9%) patients had normal AI-QCT$_{ischemia}$ result (**Figure 13**). The decision on possible early (6-month) revascularization was based on functionally significant stenosis according to $^{15}$O-$H_2O$ PET perfusion or invasive FFR. Out of 1880 patients, 662 (35.2%) were referred for $^{15}$O-$H_2O$ PET perfusion, and subsequently 413 (22.0%) of the patients were referred for ICA and 204 (10.9%) underwent early elective revascularization within 6 months. Since for most patients undergoing ICA, the PET perfusion result was available, the use of invasive FFR was not systematically collected.

Patients with abnormal AI-QCT$_{ischemia}$ result were significantly older, more frequently male, had more frequently hypertension, diabetes mellitus, dyslipidemia, smoking history, typical angina pectoris, higher NYHA class, and were more frequently on an antiplatelet agent, oral anticoagulation, lipid-lowering, anti-anginal and/or anti-hypertensive drug. Agatston Coronary Calcium Score as well as diameter stenosis were remarkably higher in patients with abnormal vs. normal AI-QCT$_{ischemia}$ result (**Table 9**). Patients with an abnormal AI-QCT$_{ischemia}$ result were also more frequently referred for downstream $^{15}$O-$H_2O$ PET perfusion imaging, and ICA. 36.0% of the patients with abnormal AI-QCT$_{ischemia}$ result as compared to 1.5% of patients with normal AI-QCT$_{ischemia}$ result underwent early elective revascularization ($p<0.001$) (**Table 9**).

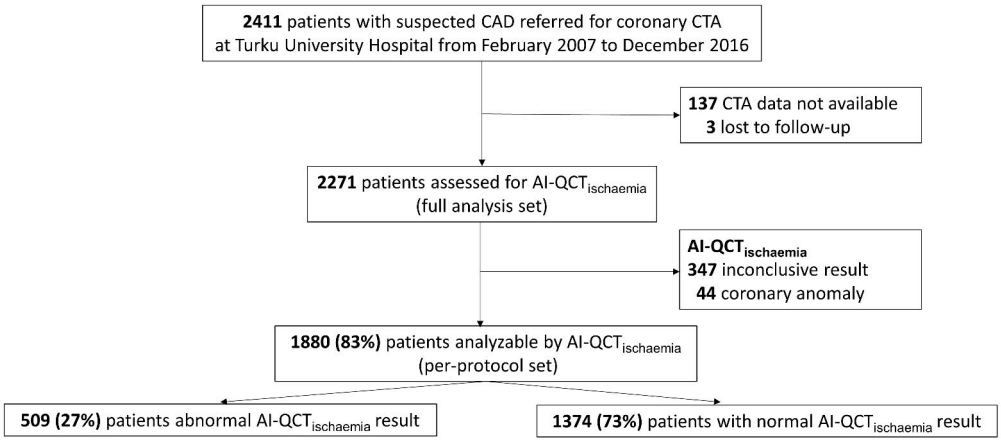


**Figure 13.** Flowchart Study III. AI-QCT = artificial intelligence-guided quantitative computed tomography, CAD = coronary artery disease, CCTA = coronary computed tomography angiography. Originally published by Bär et al. in Eur Heart J Cardiovasc Imaging 2024;25:657-667, reprinted with permission.

**Table 9.** Patient characteristics and medication Study III.

| PATIENT CHARACTERISTICS | N | ABNORMAL AI-QCT$_{ISCHEMIA}$ RESULT N=509 | N | NORMAL AI-QCT$_{ISCHEMIA}$ RESULT N=1371 | P-VALUE |
|---|---|---|---|---|---|
| **AGE, YEARS** | 509 | 67 [61-72] | 1371 | 62 [55-68] | <0.001 |
| **SEX (FEMALE), N (%)** | 509 | 200 (38.3%) | 1371 | 846 (61.7%) | <0.001 |
| **HYPERTENSION, N (%)** | 509 | 352 (69.2%) | 1371 | 707 (51.6%) | <0.001 |
| **DYSLIPIDEMIA, N (%)** | 509 | 370 (72.7%) | 1371 | 848 (61.9%) | <0.001 |
| **CURRENT SMOKER, N (%)** | 509 | 74 (14.5%) | 1371 | 165 (12.0%) | 0.148 |
| **PREVIOUS SMOKER, N (%)** | 509 | 138 (27.1%) | 1371 | 256 (18.7%) | <0.001 |
| **BMI, KG/M2** | 435 | 27.8 [24.8-30.8] | 773 | 27.4 [24.6-31.1] | 0.549 |
| **DIABETES MELLITUS, N (%)** | 509 | 109 (21.4%) | 1371 | 180 (13.1%) | <0.001 |
| **PREDIABETES*, N (%)** | 509 | 92 (18.1%) | 1371 | 176 (12.8%) | 0.004 |
| **FAMILY HISTORY OF CAD, N (%)** | 509 | 228 (44.8%) | 1371 | 660 (48.1%) | 0.197 |
| **TYPICAL ANGINA, N (%)** | 509 | 160 (31.4%) | 1371 | 283 (20.6%) | <0.001 |
| **NYHA CLASS, N (%)**<br>**I**<br>**II**<br>**III** | 319 | <br>153 (48.0%)<br>140 (43.9%)<br>26 (8.1%) | 840 | <br>547 (65.1%)<br>271 (32.3%)<br>22 (2.6%) | <0.001 |
| **VISUAL DS%, N (%)**<br>**0%**<br>**1-50%**<br>**>50%** | 491 | <br>1 (0.2%)<br>112 (22.8%)<br>378 (77.0%) | 1356 | <br>542 (40.0%)<br>718 (53.0%)<br>96 (7.0%) | <0.001 |
| **AGATSTON CORONARY CALCIUM SCORE** | 416 | 500 [242-1215] | 1133 | 6 [0-87] | <0.001 |
| **DOWNSTREAM PET PERFORMED, N (%)** | 509 | 416 (81.7%) | 1371 | 246 (17.9%) | <0.001 |
| **ELECTIVE REFERRAL FOR ICA (WITHIN 6 MONTHS), N (%)** | 509 | 268 (52.7%) | 1371 | 145 (10.6%) | <0.001 |
| **EARLY REVASCULARIZATION (WITHIN 6 MONTHS, PCI OR CABG), N (%)** | 509 | 183 (36.0%) | 1371 | 21 (1.5%) | <0.001 |
| **EARLY PCI (WITHIN 6 MONTHS), N (%)** | 509 | 149 (29.3%) | 1371 | 20 (1.5%) | <0.001 |
| **EARLY CABG (WITHIN 6 MONTHS), N (%)** | 509 | 38 (7.5%) | 1371 | 2 (0.1%) | <0.001 |

| **MEDICATION** | | | | | |
|---|---|---|---|---|---|
| **ANTIPLATELET DRUG (ASPIRIN OR OTHER), N (%)** | 509 | 283 (55.6%) | 1371 | 555 (40.5) | <0.001 |
| **ANTICOAGULATION, N (%)** | 509 | 48 (9.4%) | 1371 | 90 (6.6%) | 0.034 |
| **LIPID-LOWERING DRUG, N (%)** | 509 | 277 (54.4%) | 1371 | 506 (36.9%) | <0.001 |
| **BETABLOCKER, N (%)** | 509 | 272 (53.4%) | 1371 | 558 (40.7%) | <0.001 |
| **LONG-ACTING NITRATE, N (%)** | 509 | 55 (10.8%) | 1371 | 99 (7.2%) | 0.012 |
| **CALCIUM CHANNEL BLOCKER, N (%)** | 509 | 105 (20.6%) | 1371 | 163 (11.9%) | <0.001 |
| **ACE INHIBITOR, N (%)** | 509 | 114 (22.4%) | 1371 | 206 (15.0%) | <0.001 |
| **AT II ANTAGONIST, N (%)** | 509 | 122 (24.0%) | 1371 | 263 (19.2%) | 0.022 |
| **DIURETIC, N (%)** | 509 | 120 (23.6%) | 1371 | 215 (15.7%) | <0.001 |
| **ANTIARRHYTHMIC DRUG, N (%)** | 509 | 13 (2.6%) | 1371 | 33 (2.4%) | 0.855 |

Values are n (%) or mean (±standard deviation (SD)) or median [interquartile range (IQR)]. P-values are from Mann-Withney U tests or Chi-square tests. *Prediabetes was defined as HbA1c 6.0-6.5%, or fasting glucose 6.1-6.9 mmol/l or impaired glucose tolerance (2h plasma glucose 7.8-11.0 mmol/l in a 75 oral glucose tolerance test). AI-QCT= artificial intelligence-guided quantitative computed tomography, ACE= angiotensin converting enzyme, AP= angina pectoris, AT II = angiotensin II, BMI= body mass index, CABG = coronary artery bypass grafting, CAD= coronary artery disease, DS = diameter stenosis, FFR= fractional flow reserve, ICA= invasive coronary angiography, NYHA= New York Heart Association. PCI= percutaneous coronary intervention, PET= positron emission tomography. Originally published by Bär et al. in Eur Heart J Cardiovasc Imaging 2024;25:657-667, reprinted with permission.

### 5.3.2 Primary endpoint

Patients with an abnormal AI-QCT$_{ischemia}$ result (27.1%, n=509/1880) as compared to patients with a normal AI-QCT$_{ischemia}$ result (72.9%, n=1371/1880) had a significantly higher crude rate of the primary endpoint (HR 3.01, 95% CI 2.29-3.97, p<0.001) (**Figure 14, Table 10**), driven by significantly higher rates of all primary endpoint components (death: HR 2.00, 95% CI 1.42-2.81, p<0.001; MI: HR 6.50, 95% CI 3.64-11.25, p<0.001; uAP: HR 8.94, 95% CI 3.85-20.77, p<0.001) (**Figure 14, Table 10**). Age, sex, hypertension, diabetes, smoking, and typical angina showed significant associations with the primary endpoint composite in univariable Cox regressions and were used as adjusting covariates in the multivariable analysis. Results of this adjusted analysis remained consistent (primary endpoint HR$_{adj}$1.96, 95% CI 1.46-2.63, p<0.001). Adjusted analyses also showed consistent results for MI (HR$_{adj}$ 4.61, 95% CI 2.56-8.28, p<0.001), and uAP (HR$_{adj}$ 6.52, 95% CI 2.74-15.50, p<0.001), but statistical significance was lost for death alone (HR$_{adj}$1.27, 95% CI 0.89-1.82, p=0.182) (**Table 10**).

The analysis was repeated using the full-analysis set (n=2271) in an intention-to-diagnose approach (i.e. classifying those patients with inconclusive AI-QCT$_{ischemia}$ result or those excluded due to coronary anomalies (n=391) as having an abnormal AI-QCT$_{ischemia}$ result). Results of the full-analysis set were consistent, except for the adjusted rate of death, which was significantly higher in patients with an abnormal as compared to a normal AI-QCT$_{ischemia}$ result (**Table 11)**.

C-indexes for three different Cox regressions for the primary endpoint were as follows: Clinical model (1): 0.707, Clinical+Stenosis model (2): 0.736, and Clinical+Stenosis+AI-QCT$_{ischemia}$ model (3): 0.739. The improvement in C-index was statistically significant for model 2 vs. model 1 (p=0.001) and model 3 vs. model 1 (p=0.001), but not for model 3 vs. model 2 (p=0.332). However, AI-QCT$_{ischemia}$ remained an independent predictor of the primary endpoint on top of visual stenosis and clinical factors in model 3 (HR 1.52, 95% CI 1.03-2.25, p=0.036) (**Table 12**).

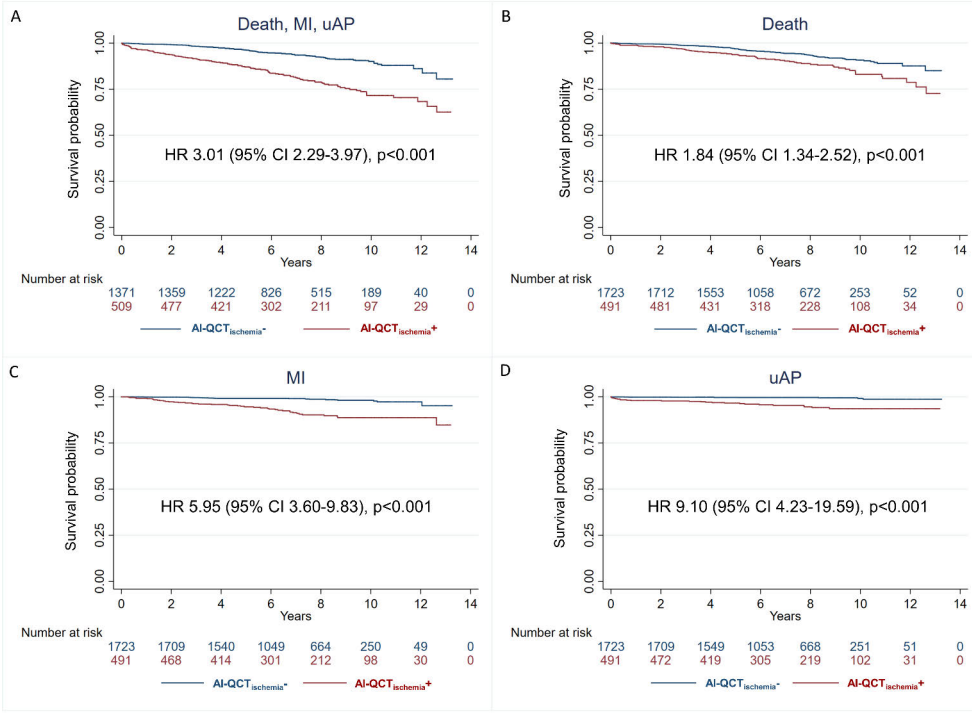


**Figure 14.** Crude Kaplan-Meier curves Study III. Primary endpoint (A), death (B), myocardial infarction (MI) (C), and unstable angina pectoris (uAP) (D). AI-QCTischemia- denotes normal AI-QCT$_{ischemia}$ result and AI-QCTischemia+ denotes abnormal AI-QCT$_{ischemia}$ result. AI-QCT = artificial intelligence-guided quantitative computed tomography, CI = confidence interval, HR = hazard ratio. Originally published by Bär et al. in Eur Heart J Cardiovasc Imaging 2024;25:657-667, reprinted with permission.

**Table 10.** Per-protocol set Study III.

| **ALL PATIENTS N=1880** | **CRUDE HAZARD RATIOS** | | | | **ADJUSTED HAZARD RATIOS** | | |
|---|---|---|---|---|---|---|---|
| | **ABNORMAL AI-QCT$_{ISCHEMIA}$ RESULT N=509** | **NORMAL AI-QCT$_{ISCHEMIA}$ RESULT N=1371** | **HR (95% CI)** | **P-VALUE** | **N PATIENTS (EVENTS)** | **HR (95% CI) ADJUSTED** | **P-VALUE ADJUSTED** |
| **DEATH, MI OR UAP, N (%)** | 110 (21.6%) | 96 (7.0%) | 3.01 (2.29-3.97) | <0.001 | 1880 (206) | 1.96 (1.46-2.63) | <0.001[1] |
| **DEATH, N (%)** | 61 (12.0%) | 74 (5.4%) | 2.00 (1.42-2.81) | <0.001 | 1880 (135) | 1.27 (0.89-1.82) | 0.182[2] |
| **MI, N (%)** | 42 (8.3%) | 17 (1.2%) | 6.40 (3.64-11.25) | <0.001 | 1880 (59) | 4.61 (2.56-8.28) | <0.001[3] |
| **UAP, N (%)** | 24 (4.7%) | 7 (0.5%) | 8.94 (3.85-20.77) | <0.001 | 1880 (31) | 6.52 (2.74-15.50) | <0.001[4] |
| **PATIENTS WITH VISUAL DS ≤50% N=1373** | **ABNORMAL AI-QCT$_{ISCHEMIA}$ RESULT N=113** | **NORMAL AI-QCT$_{ISCHEMIA}$ RESULT N=1260** | **HR (95% CI)** | **P-VALUE** | **N PATIENTS (EVENTS)** | **HR (95% CI) ADJUSTED** | **P-VALUE ADJUSTED** |
| **DEATH, MI OR UAP, N (%)** | 20 (17.7%) | 79 (6.3%) | 2.86 (1.75-4.67) | <0.001 | 1373 (99) | 1.81 (1.09-3.00) | 0.022[3] |
| **DEATH, N (%)** | 12 (10.6%) | 61 (4.8%) | 2.16 (1.16-4.02) | 0.015 | 1373 (73) | 1.53 (0.82-2.86) | 0.185[5] |
| **MI, N (%)** | 6 (5.3%) | 13 (1.0%) | 5.18 (1.97-13.62) | 0.001 | 1373 (19) | 4.79 (1.81-12.64) | 0.002[6] |
| **UAP, N (%)** | 3 (2.7%) | 6 (0.5%) | 5.48 (1.37-21.93) | 0.016 | 1373 (9) | 3.93 (0.96-16.00) | 0.056[7] |

| PATIENTS WITH VISUAL DS >50% N=474 | ABNORMAL AI-QCT$_{ISCHEMIA}$ RESULT N=378 | NORMAL AI-QCT$_{ISCHEMIA}$ RESULT N=96 | HR (95% CI) | P-VALUE | N PATIENTS (EVENTS) | HR (95% CI) ADJUSTED | P-VALUE ADJUSTED |
|---|---|---|---|---|---|---|---|
| **DEATH, MI OR UAP, N (%)** | 90 (23.8%) | 17 (17.7%) | 1.33 (0.79-2.24) | 0.279 | 474 (107) | 1.26 (0.75-2.12) | 0.386[7] |
| **DEATH, N (%)** | 49 (13.0%) | 13 (13.5%) | 0.89 (0.48-1.64) | 0.700 | 474 (62) | 0.83 (0.45-1.54) | 0.557[8] |
| **MI, N (%)** | 36 (9.5%) | 4 (4.2%) | 2.25 (0.80-6.32) | 0.125 | 474 (40) | - | - |
| **UAP, N (%)** | 21 (5.6%) | 1 (1.0%) | 5.29 (0.71-39.30) | 0.104 | 474 (22) | - | - |

Displayed are numbers (percentage) of first events and hazard ratios (HR) with 95% confidence intervals (CI) from Cox proportional hazards models. HRs were adjusted for covariates with significant univariable associations with the reported endpoints: [1]age, sex, hypertension, diabetes, smoking, typical angina; [2]age, hypertension, diabetes, smoking, family history of coronary artery disease (CAD). [3]age, hypertension, smoking, typical angina; [4]age, hypertension, typical angina; [5]age, family history of CAD; [6]typical angina; [7]age; [8]age, diabetes. AI-QCT= artificial intelligence-guided quantitative computed tomography, DS% = diameter stenosis, MI= myocardial infarction, uAP= unstable angina pectoris. Originally published by Bär et al. in Eur Heart J Cardiovasc Imaging 2024;25:657-667, reprinted with permission.

**Table 11.** Full-analysis set Study III.

| ALL PATIENTS N=2271 | CRUDE HAZARD RATIOS | | | | ADJUSTED HAZARD RATIOS | | |
|---|---|---|---|---|---|---|---|
| | ABNORMAL AI-QCT$_{ISCHEMIA}$ RESULT N=900 | NORMAL AI-QCT$_{ISCHEMIA}$ RESULT N=1371 | HR (95% CI) | P-VALUE | N PATIENTS (EVENTS) | HR (95% CI) ADJUSTED | P-VALUE ADJUSTED |
| **DEATH, MI OR UAP, N (%)** | 159 (17.7%) | 96 (7.0%) | 2.47 (1.91-3.18) | <0.001 | 2271 (255) | 1.81 (1.40-2.36) | <0.001[1] |
| **DEATH, N (%)** | 68 (12.4%) | 105 (6.1%) | 1.89 (1.40-2.56) | <0.001 | 2271 (173) | 1.37 (1.01-1.87) | 0.044[2] |
| **MI, N (%)** | 51 (5.7%) | 17 (1.2%) | 4.45 (2.57-7.70) | <0.001 | 2271 (68) | 3.46 (1.98-6.05) | <0.001[3] |
| **UAP, N (%)** | 27 (3.0%) | 7 (0.5%) | 5.71 (2.49-13.13) | <0.001 | 2271 (34) | 4.48 (1.93-10.41) | <0.001[4] |

Displayed are numbers (percentage) of first events and hazard ratios (HR) with 95% confidence intervals (CI) from Cox proportional hazards models. Patients with unevaluable AI-QCT$_{ischemia}$ (n=391) were classified as having an abnormal AI-QCT$_{ischemia}$ result. HRs were adjusted for covariates with significant univariable associations with the reported endpoints: [1]age, sex, hypertension, diabetes, smoking, typical angina; [2]age, hypertension, diabetes, smoking, family history of coronary artery diease; [3]age, hypertension, smoking, dyslipidemia, typical angina; [4]age, hypertension, typical angina. AI-QCT = artificial intelligence-guided quantitative computed tomography, MI = myocardial infarction, uAP = unstable angina pectoris. Originally published by Bär et al. in Eur Heart J Cardiovasc Imaging 2024;25:657-667, reprinted with permission.

**Table 12.** Multivariable Cox models and C-indexes for the primary endpoint.

| DEATH, MI, UAP<br><br>1847 PATIENTS<br>206 EVENTS | CLINICAL MODEL (1) | | CLINICAL<br>+STENOSIS MODEL (2) | | CLINICAL+STENOSIS<br>+AI-QCT$_{ISCHEMIA}$ MODEL (3) | |
|---|---|---|---|---|---|---|
| | **HR (95% CI)** | **P-VALUE** | **HR (95% CI)** | **P-VALUE** | **HR (95% CI)** | **P-VALUE** |
| **AI-QCT$_{ISCHEMIA}$** | - | - | - | - | 1.52 (1.03-2.25) | 0.036 |
| **VISUAL DS >50%** | - | - | 1.97 (1.47-2.65) | <0.001 | 1.49 (1.01-2.21) | 0.045 |
| **AGE, PER 1 YEAR** | 1.07 (1.06-1.09) | <0.001 | 1.07 (1.05-1.09) | <0.001 | 1.06 (1.04-1.08) | <0.001 |
| **SEX (MALE VS. FEMALE)** | 1.48 (1.11-1.97) | 0.007 | 1.27 (0.95-1.70) | 0.104 | 1.24 (0.92-1.66) | 0.153 |
| **HYPERTENSION** | 1.35 (1.00-1.83) | 0.050 | 1.29 (0.95-1.74) | 0.099 | 1.27 (0.94-1.72) | 0.116 |
| **DIABETES MELLITUS** | 1.32 (0.94-1.85) | 0.104 | 1.19 (0.85-1.67) | 0.310 | 1.20 (0.86-1.69) | 0.285 |
| **SMOKER** | 1.67 (1.25-2.22) | <0.001 | 1.59 (1.20-2.12) | 0.001 | 1.57 (1.18-2.09) | 0.002 |
| **TYPICAL ANGINA** | 1.42 (1.06-1.91) | 0.019 | 1.31 (0.97-1.76) | 0.079 | 1.29 (0.95-1.73) | 0.098 |
| **C-INDEX (95% CI)** | 0.707<br>(0.672-0.742) | <0.001 | 0.736<br>(0.702-0.769) | <0.001 | 0.739<br>(0.706-0.773) | <0.001 |
| **C-INDEX DIFFERENCE (95% CI)** | **MODEL 2-MODEL 1** | **P-VALUE** | **MODEL 3-MODEL 2** | **P-VALUE** | **MODEL 3-MODEL 1** | **P-VALUE** |
| | 0.029 (0.011-0.046) | 0.001 | 0.003 (-0.004-0.011 | 0.332 | 0.032 (0.013-0.051) | 0.001 |

Displayed are hazard ratios (HR) with 95% confidence intervals (CI) from multivariable Cox regressions, C-index per model, and difference in C-indexes between the models. The clinical variables were chosen based on significant univariable associations with the primary endpoint. The sample size is given by the number of patients with available visual stenosis reading (n=1847). AI-QCT= artificial intelligence-guided quantitative computed tomography, DS = diameter stenosis, MI= myocardial infarction, uAP= unstable angina pectoris. Originally published by Bär et al. in Eur Heart J Cardiovasc Imaging 2024;25:657-667, reprinted with permission.

### 5.3.3 Primary endpoint among patients with ≤50% or >50% visual diameter stenosis

Visual stenosis reading was available for 1847/1880 (98.2%) of the per-protocol population. Overall, 1373/1847 (74.3%) of patients had no/non-obstructive CAD on CCTA (i.e. visual DS ≤50%) and 474/1847 (25.7%) had obstructive CAD on CCTA (i.e. visual DS >50%).

Among the 1373 patients with no/non-obstructive CAD, AI-$QCT_{ischemia}$ result was normal in 1260 (91.8%) and abnormal in 113 (8.2%) patients. In contrast, among the 474 patients with obstructive CAD on CCTA, AI-$QCT_{ischemia}$ result was normal in 96 (20.3%) and abnormal in 378 (79.7%) patients. An abnormal AI-$QCT_{ischemia}$ result as compared with a normal AI-$QCT_{ischemia}$ result was associated with a significantly higher crude rate of the primary endpoint among patients with no/non-obstructive CAD (HR 2.86, 95% CI 1.75-4.67, p<0.001), but not among those with obstructive CAD (HR 1.33, 95% CI 0.79-2.24, p=0.279 (p-interaction=0.032) (**Figure 15 A-B, Table 10**). According to univariable Cox regressions, age, hypertension, smoking, and typical angina were used as adjusting covariates for the subgroup with no/non-obstructive CAD, and age for the subgroup with obstructive CAD. Results of the adjusted analyses remained consistent (**Table 10**).

Among patients with no/non-obstructive disease, C-index of the Clinical model (1) was 0.722 and for the Clinical+AI-$QCT_{ischemia}$ model (2) 0.726. This improvement in C-index was statistically not significant (p=0.535), but AI-$QCT_{ischemia}$ remained an independent predictor of the primary endpoint (HR 1.74, 95% CI 1.04-2.90, p=0.035) (**Table 13**). Among patients with obstructive disease, C-index of the Clinical model (1) was 0.602, similar to that of the Clinical+AI-$QCT_{ischemia}$ model (2) of 0.604 (p =0.741). However, in model 2, AI-$QCT_{ischemia}$ was no independent predictor of the primary endpoint (HR 1.27, 95% CI 0.75-2.14, p=0.374) (**Table 14**).

**Table 13.** Multivariable Cox models and C-indexes for the primary endpoint for patients with visual no/non-obstructive stenosis (≤50%)

| **VISUAL NO/NON-OBSTRUCTIVE STENOSIS (≤50%)**<br>**1373 PATIENTS**<br>**99 EVENTS** | **CLINICAL MODEL (1)** | | **CLINICAL +STENOSIS MODEL (2)** | |
|---|---|---|---|---|
| | **HR (95% CI)** | **P-VALUE** | **HR (95% CI)** | **P-VALUE** |
| **AI-QCT$_{ISCHEMIA}$** | - | - | 1.74 (1.04-2.90) | 0.035 |
| **AGE, PER 1 YEAR** | 1.09 (1.06-1.12) | <0.001 | 1.08 (1.06-1.11) | <0.001 |
| **SEX (MALE VS. FEMALE)** | 1.44 (0.95-2.18) | 0.085 | 1.38 (0.91-2.09) | 0.128 |
| **HYPERTENSION** | 1.21 (0.80-1.84) | 0.371 | 1.19 (0.78-1.82) | 0.411 |
| **DIABETES MELLITUS** | 1.04 (0.57-1.90) | 0.888 | 1.00 (0.55-1.82) | 0.995 |
| **SMOKER** | 1.92 (1.26-2.94) | 0.003 | 1.85 (1.21-2.82) | 0.005 |
| **TYPICAL ANGINA** | 1.59 (1.03-2.46) | 0.036 | 1.53 (0.99-2.38) | 0.055 |
| **C-INDEX (95% CI)** | 0.722 (0.670-0.774) | <0.001 | 0.726 (0.674-0.777) | <0.001 |
| **C-INDEX DIFFERENCE (95% CI)** | **MODEL 2-MODEL 1** | | **P-VALUE** | |
| | 0.004 (-0.009 to 0.017) | | 0.535 | |

Displayed are hazard ratios (HR) with 95% confidence intervals (CI) from multivariable Cox regressions, C-index per model, and difference in C-indexes between the models. AI-QCT = artificial intelligence-guided quantitative computed tomography, MI = myocardial infarction, uAP = unstable angina pectoris. Originally published by Bär et al. in Eur Heart J Cardiovasc Imaging 2024;25:657-667, reprinted with permission.

**Table 14.** Multivariable Cox models and C-indexes for the primary endpoint for patients with visual obstructive stenosis (>50%)

| VISUAL OBSTRUCTIVE STENOSIS (>50%) 474 PATIENTS 107 EVENTS | CLINICAL MODEL (1) | | CLINICAL +STENOSIS MODEL (2) | |
|---|---|---|---|---|
| | HR (95% CI) | P-VALUE | HR (95% CI) | P-VALUE |
| AI-QCT$_{ISCHEMIA}$ | - | - | 1.27 (0.75-2.14) | 0.374 |
| AGE, PER 1 YEAR | 1.04 (1.01-1.07) | 0.003 | 1.04 (1.01-1.07) | 0.004 |
| SEX (MALE VS. FEMALE) | 1.07 (0.71-1.61) | 0.747 | 1.05 (0.70-1.58) | 0.814 |
| HYPERTENSION | 1.26 (0.81-1.96) | 0.301 | 1.26 (0.81-1.96) | 0.306 |
| DIABETES MELLITUS | 1.36 (0.90-2.07) | 0.146 | 1.38 (0.91-2.11) | 0.129 |
| SMOKER | 1.35 (0.92-1.9) | 0.129 | 1.35 (0.92-1.99) | 0.128 |
| TYPICAL ANGINA | 1.13 (0.75-1.69) | 0.557 | 1.12 (0.75-1.68) | 0.575 |
| C-INDEX (95% CI) | 0.602 (0.548-0.656) | <0.001 | 0.604 (0.550-0.659) | <0.001 |
| C-INDEX DIFFERENCE (95% CI) | MODEL 2-MODEL 1 | | P-VALUE | |
| | 0.002 (-0.012 to 0.017) | | 0.741 | |

Displayed are hazard ratios (HR) with 95% confidence intervals (CI) from multivariable Cox regressions, C-index per model, and difference in C-indexes between the models. AI-QCT = artificial intelligence-guided quantitative computed tomography, MI = myocardial infarction, uAP = unstable angina pectoris. Originally published by Bär et al. in Eur Heart J Cardiovasc Imaging 2024;25:657-667, reprinted with permission.

### 5.3.4 Subgroup analysis for patients with vs. without early revascularization

Among the 1676 patients not undergoing early revascularization, 326 (19.5%) patients had an abnormal, 1350 (80.5%) patients had a normal AI-QCT$_{ischemia}$ result, and there was incremental risk stratification for the primary endpoint by AI-QCT$_{ischemia}$ (HR 3.29, 95% CI 2.40-4.67, p<0.001) (**Figure 15, C**). Contrarily, among the 204 patients who underwent early revascularization, 183 (89.7%) had an abnormal, 21 (10.3%) had a normal AI-QCT$_{ischemia}$ result, and AI-QCT$_{ischemia}$ showed no incremental risk stratification (HR 1.09, 95% CI 0.39-3.05, p=0.872) (p-interaction=0.043) (**Figure 15, D**). These results also remained consistent in adjusted analyses based on significant univariable associations with the primary endpoint (no revascularization group: HR$_{adj}$ 2.06, 95% CI 1.48-2.85, p<0.001; covariates: age,

sex, hypertension, diabetes, smoking, typical angina; revascularization group: $HR_{adj}$ 0.87, 95% CI 0.31-2.49, p=0.802; covariate: age).

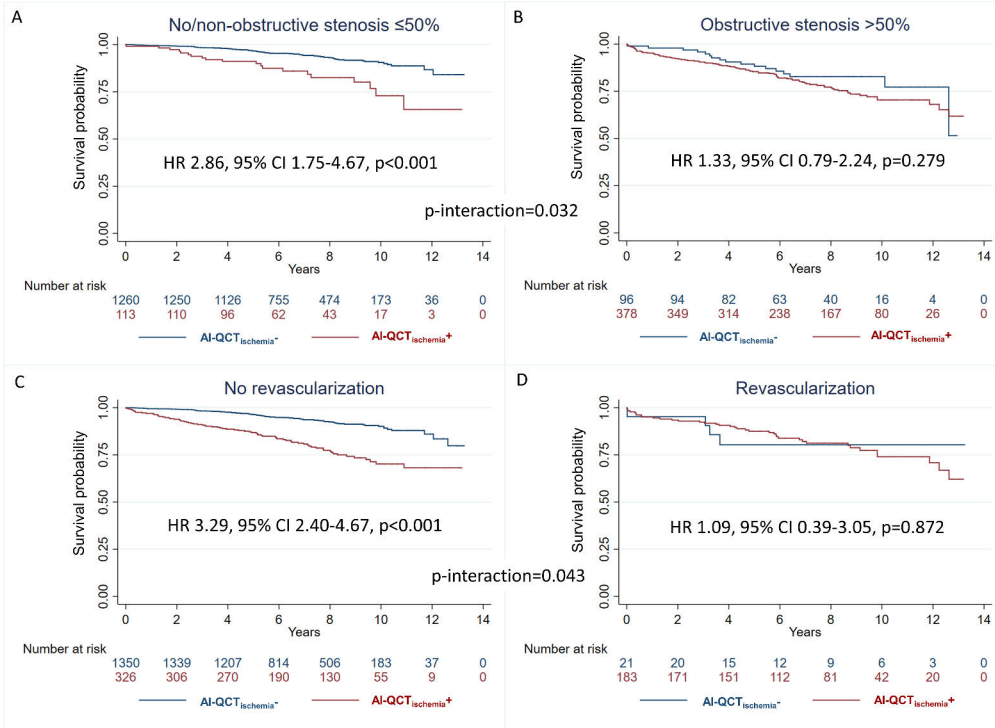


**Figure 15.** Subgroup analyses Study III. Crude Kaplan Meier curves and hazard ratios (HR) for the primary endpoint (death, myocardial infarction, unstable angina pectoris) are shown among patients with ≤50% (A) vs. >50% (B) visual diameter stenosis, as well as without early reavascularization (C) vs. with early revascularization (D) within 6 months from coronary computed tomography angiography. AI-QCTischemia- denotes normal AI-QCTischemia result and AI-QCTischemia+ denotes abnormal AI-QCTischemia result. AI-QCT = artificial intelligence-guided quantitative computed tomography, CI = confidence interval. Originally published by Bär et al. in Eur Heart J Cardiovasc Imaging 2024;25:657-667, reprinted with permission.

## 5.4 Prognostic value of AI-QCT$_{ischemia}$ for patients with obstructive CAD and normal or abnormal PET perfusion (Study IV)

### 5.4.1 Patient population

Out of 768 patients (full analysis set), 17 patients patients were excluded due to coronary anomalies and 89 patients due to inconclusive AI-QCT$_{ischemia}$, resulting in 662/768 (86%) with conclusive AI-QCT$_{ischemia}$ result (per-protocol set) (**Figure 16**). Of these, 331 (50.0%) patients had abnormal and 331 (50.0%) patients had normal PET perfusion.

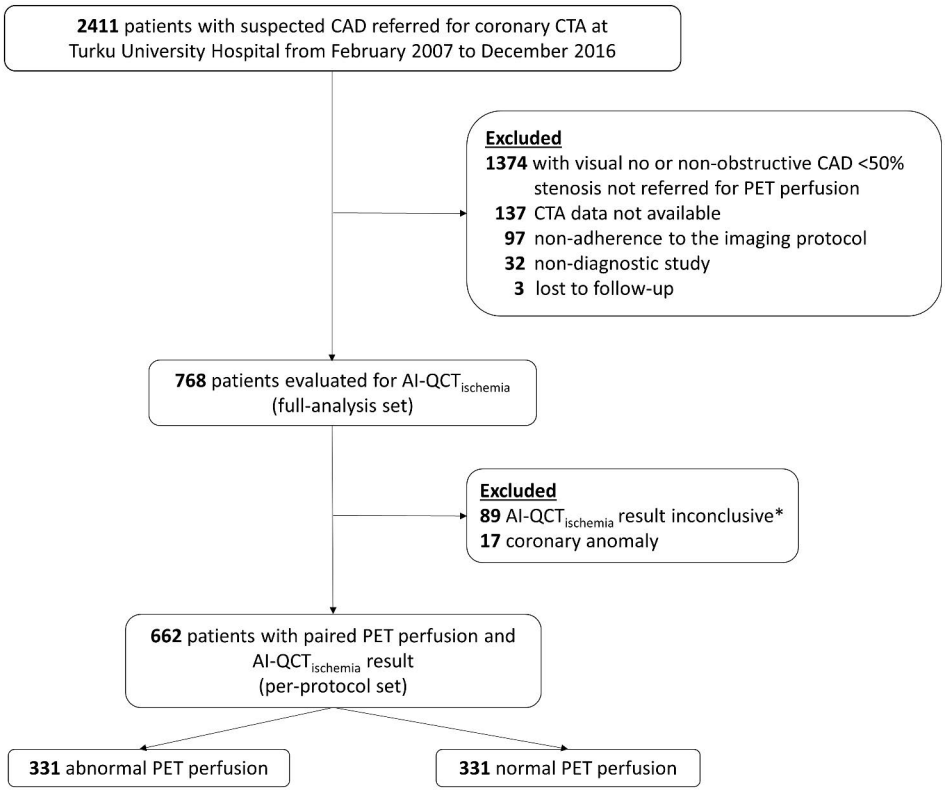


**Figure 16.** Flowchart Study IV. *Indicates absence of a conclusive result for all vessels in the absence of any ischemic vessel. AI-QCT = artificial intelligence quantitative computed tomography, CAD = coronary artery disease, CTA = computed tomography angiography, PET = positron emission tomography. Originally published by Bär et al. in J Cardiovasc Comput Tomogr 2024 Apr 24:S1934-5925(24)00075-3, reprinted with permission.

In the group with normal PET perfusion (n=331) (**Table 15**), 147 (44.4%) had an abnormal and 184 (55.6%) had a normal AI-$QCT_{ischemia}$ result. The prevalence of cardiovascular risk factors and medical therapy was similar between those with an abnormal as compared to those with a normal AI-$QCT_{ischemia}$ result.

However, patients with an abnormal AI-$QCT_{ischemia}$ result were slightly younger (66 vs. 68 years, p<0.001), were more frequently referred for ICA (26.5% vs. 7.6%, p<0.001), and underwent more frequently early elective revascularization within 6 months (11.6% vs. 0.5%, p<0.001). Also, they had higher Agatston calcium score (407 vs. 124, p<0.001) and AI-QCT diameter stenosis (59% vs. 31%, p<0.001), more frequently ≥50% diameter stenosis by AI-QCT (93.9% vs. 8.7%, p<0.001), higher percent atheroma volume (PAV) (13.8% vs. 6.1%, p<0.001), percent calcified plaque volume (CPV) (5.6% vs. 1.6%, p<0.001), and NCPV (7.4% vs. 3.8%, p<0.001).

In the group with abnormal PET perfusion (n=331) (**Table 16**), 269 (81.3%) had an abnormal and 62 (18.7%) had a normal AI-$QCT_{ischemia}$ result. Clinical characteristics between those with an abnormal vs. normal AI-$QCT_{ischemia}$ result were similar. However, patients with an abnormal AI-$QCT_{ischemia}$ result were more frequently prescribed an antiplatelet agent (61.7% vs. 41.9%, p<0.001), referred for ICA (68.4% vs. 35.5%, p<0.001), and underwent more frequently early revascularization (50.9% vs. 17.7%, p<0.001). Also, they had higher Agatston calcium score (656 vs. 194, p<0.001) and AI-QCT diameter stenosis (72% vs. 36%, p<0.001), more frequently ≥50% diameter stenosis by AI-QCT (95.2% vs. 14.5%, p<0.001), higher PAV (18.9% vs. 7.9%, p<0.001), CPV (6.8% vs. 2.0%, p<0.001), and NCPV (10.1% vs. 5.6%, p<0.001).

**Table 15.** Baseline characteristics and medication of patients with normal PET perfusion.

| PATIENT CHARACTERISTICS | N | ABNORMAL AI-QCT$_{ISCHEMIA}$ RESULT N=147 | N | NORMAL AI-QCT$_{ISCHEMIA}$ RESULT N=184 | P-VALUE |
|---|---|---|---|---|---|
| **AGE, YEARS** | 147 | 66 [59-71] | 184 | 68 [64-73] | <0.001 |
| **SEX (FEMALE), N (%)** | 147 | 76 (51.7%) | 184 | 98 (53.3%) | 0.778 |
| **HYPERTENSION, N (%)** | 147 | 109 (74.2%) | 184 | 119 (64.7%) | 0.064 |
| **DYSLIPIDEMIA, N (%)** | 147 | 105 (71.4%) | 184 | 127 (69.0%) | 0.635 |
| **CURRENT SMOKER, N (%)** | 147 | 17 (11.6%) | 184 | 22 (12.0%) | 0.913 |
| **PREVIOUS SMOKER, N (%)** | 147 | 41 (27.9%) | 184 | 45 (24.5%) | 0.479 |
| **BMI, KG/M$^2$** | 139 | 27.5 [24.8-30.1] | 166 | 27.3 [24.8-30.9] | 0.898 |
| **DIABETES MELLITUS, N (%)** | 147 | 33 (22.5%) | 184 | 33 (17.9%) | 0.307 |
| **PREDIABETES*, N (%)** | 147 | 16 (10.9%) | 184 | 35 (19.0%) | 0.042 |
| **FAMILY HISTORY OF CAD, N (%)** | 147 | 70 (47.6%) | 184 | 81 (44.0%) | 0.514 |
| **TYPICAL ANGINA, N (%)** | 147 | 33 (22.5%) | 184 | 42 (22.8%) | 0.935 |
| **NYHA CLASS, N (%)**<br>**I**<br>**II**<br>**III** | 101 | <br>51 (50.5%)<br>39 (38.6%)<br>11 (10.9%) | 117 | <br>73 (62.4%)<br>40 (34.2%)<br>4 (3.4%) | 0.049 |
| **AGATSTON CORONARY CALCIUM SCORE** | 118 | 407 [224-980] | 160 | 124 [33-259] | <0.001 |
| **ELECTIVE REFERRAL FOR ICA (WITHIN 6 MONTHS), N (%)** | 147 | 39 (26.5%) | 184 | 14 (7.6%) | <0.001 |
| **EARLY REVASCULARIZATION (WITHIN 6 MONTHS, PCI OR CABG), N (%)** | 147 | 17 (11.6%) | 184 | 1 (0.5%) | <0.001 |
| **EARLY PCI (WITHIN 6 MONTHS), N (%)** | 147 | 17 (11.6%) | 184 | 1 (0.5%) | <0.001 |
| **EARLY CABG (WITHIN 6 MONTHS), N (%)** | 147 | - | 184 | - | - |

| **MEDICATION** | | | | | |
|---|---|---|---|---|---|
| **ANTIPLATELET DRUG (ASPIRIN OR OTHER), N (%)** | 147 | 74 (50.3%) | 184 | 77 (41.9%) | 0.123 |
| **ANTICOAGULATION, N (%)** | 147 | 19 (12.9%) | 184 | 14 (7.6%) | 0.109 |
| **LIPID-LOWERING DRUG, N (%)** | 147 | 72 (49.0%) | 184 | 85 (46.2%) | 0.614 |
| **BETABLOCKER, N (%)** | 147 | 76 (51.7%) | 184 | 90 (48.9%) | 0.614 |
| **LONG-ACTING NITRATE, N (%)** | 147 | 15 (10.2%) | 184 | 21 (11.4%) | 0.726 |
| **CALCIUM CHANNEL BLOCKER, N (%)** | 147 | 32 (21.8%) | 184 | 36 (19.6%) | 0.622 |
| **ACE INHIBITOR, N (%)** | 147 | 31 (21.1%) | 184 | 35 (19.0%) | 0.640 |
| **AT II ANTAGONIST, N (%)** | 147 | 33 (22.5%) | 184 | 46 (25.0%) | 0.589 |
| **DIURETIC, N (%)** | 147 | 38 (25.9%) | 184 | 35 (19.0%) | 0.137 |
| **ANTIARRHYTHMIC DRUG, N (%)** | 147 | 5 (3.4%) | 184 | 5 (2.7%) | 0.718 |
| **AI-QCT** | | | | | |
| **AI-QCT DS, %** | 147 | 59 [54-71] | 184 | 31 [23-41] | <0.001 |
| **AI-QCT DIAMETER STENOSIS ≥30%, N (%)** | 147 | 147 (100%) | 184 | 103 (56.0%) | <0.001 |
| **AI-QCT DIAMETER STENOSIS ≥50%, N (%)** | 147 | 138 (93.9%) | 184 | 16 (8.7%) | <0.001 |
| **AI-QCT DIAMETER STENOSIS ≥70%, N (%)** | 147 | 40 (27.2%) | 184 | 0 (0.0%) | <0.001 |
| **VESSELS WITH AI-QCT DIAMETER STENOSIS ≥50%[§], N (%)** | | | | | |
| **LM** | 144 | 5 (3.5%) | 181 | 0 (0.0%) | 0.012 |
| **LAD** | 147 | 113 (76.9%) | 184 | 12 (6.7%) | <0.001 |
| **LCX** | 147 | 20 (13.6%) | 184 | 3 (1.6%) | <0.001 |
| **RCA** | 147 | 40 (27.2%) | 184 | 3 (1.6%) | <0.001 |
| **AREA STENOSIS, %** | 147 | 84 [79-92] | 184 | 58 [47-69] | <0.001 |
| **PERCENT ATHEROMA VOLUME, %** | 147 | 13.8 [8.8-20.3] | 184 | 6.1 [3.3-9.3] | <0.001 |
| **PERCENT CALCIFIED PLAQUE VOLUME, %** | 147 | 5.6 [2.6-9.9] | 184 | 1.6 [0.4-3.6] | <0.001 |
| **PERCENT NON-CALCIFIED PLAQUE VOLUME, %** | 147 | 7.4 [5.3-10.5] | 184 | 3.8 [2.5-5.9] | <0.001 |

| | | | | | |
|---|---|---|---|---|---|
| **POSITIVE REMODELING, N (%)** | 147 | 147 (100%) | 184 | 182 (98.9%) | 0.205 |
| **TOTAL VESSEL VOLUME, MM$^3$** | 147 | 3162 [2652-3814] | 184 | 3168 [2640-3811] | 0.700 |
| **TOTAL LUMEN VOLUME, MM$^3$** | 147 | 2621 [2187-3250] | 184 | 2909 [2404-3534] | 0.006 |
| **TOTAL VESSEL LENGTH, MM** | 147 | 616 ±105 | 184 | 632 ±89 | 0.135 |

Values are n (%) or mean (±standard deviation (SD)) or median [interquartile range (IQR)]. P-values are from Mann-Withney U tests, T-tests, or Chi-square tests. *Prediabetes was defined as HbA1c 6.0-6.5%, or fasting glucose 6.1-6.9 mmol/l or impaired glucose tolerance (2h plasma glucose 7.8-11.0 mmol/l in a 75 oral glucose tolerance test). §Including side branches with diameter ≥1.5 mm. In some patients, left main was either absent or too short to be assessed as separate segment. Percent plaque volume (%) = plaque volume (mm$^3$)/vessel volume (mm$^3$)*100. AI-QCT= artificial intelligence-guided quantitative computed tomography, ACE= angiotensin converting enzyme, AP= angina pectoris, AT II = angiotensin II, BMI= body mass index, CABG = coronary artery bypass grafting, CAD= coronary artery disease, DS = diameter stenosis, FFR= fractional flow reserve, ICA= invasive coronary angiography, LAD = left anterior descending, LCX = left circumflex artery, LM = left main artery, NYHA= New York Heart Association. PCI= percutaneous coronary intervention, PET= positron emission tomography, RCA = right coronary artery. Originally published by Bär et al. in J Cardiovasc Comput Tomogr 2024 Apr 24:S1934-5925(24)00075-3, reprinted with permission.

**Table 16.** Baseline characteristics and medication of patients with abnormal PET perfusion.

| **PATIENT CHARACTERISTICS** | **N** | **ABNORMAL AI-QCT$_{ISCHEMIA}$ RESULT N=269** | **N** | **NORMAL AI-QCT$_{ISCHEMIA}$ RESULT N=62** | **P-VALUE** |
|---|---|---|---|---|---|
| **AGE, YEARS** | 269 | 66 [60-71] | 62 | 65 [57-69] | 0.162 |
| **SEX (FEMALE), N (%)** | 269 | 80 (30.1%) | 62 | 22 (35.5%) | 0.410 |
| **HYPERTENSION, N (%)** | 269 | 182 (67.6%) | 62 | 42 (67.7%) | 0.990 |
| **DYSLIPIDEMIA, N (%)** | 269 | 203 (75.5%) | 62 | 46 (74.2%) | 0.834 |
| **CURRENT SMOKER, N (%)** | 269 | 38 (14.1%) | 62 | 12 (19.4%) | 0.300 |
| **PREVIOUS SMOKER, N (%)** | 269 | 77 (28.6%) | 62 | 20 (32.3%) | 0.571 |
| **BMI, KG/M$^2$** | 251 | 27.7 [24.8-30.8] | 56 | 26.6 [25.8-29.8] | 0.499 |
| **DIABETES MELLITUS, N (%)** | 269 | 61 (22.7%) | 62 | 9 (14.5%) | 0.156 |
| **PREDIABETES*, N (%)** | 269 | 51 (19.0%) | 62 | 12 (19.4%) | 0.943 |
| **FAMILY HISTORY OF CAD, N (%)** | 269 | 119 (44.2%) | 62 | 33 (53.2%) | 0.200 |
| **TYPICAL ANGINA, N (%)** | 269 | 91 (33.8%) | 62 | 19 (30.7%) | 0.631 |

| | | | | | |
|---|---|---|---|---|---|
| **NYHA CLASS, N (%)**<br>**I**<br>**II**<br>**III** | **166** | **77 (46.4%)**<br>**79 (47.6%)**<br>**10 (6.0%)** | **30** | **18 (19.0%)**<br>**11 (36.7%)**<br>**1 (3.3%)** | **0.762** |
| **AGATSTON CORONARY CALCIUM SCORE** | 227 | 656 [293-1419] | 80 | 194 [40-576] | <0.001 |
| **ELECTIVE REFERRAL FOR ICA (WITHIN 6 MONTHS), N (%)** | 269 | 184 (68.4%) | 62 | 22 (35.5%) | <0.001 |
| **EARLY REVASCULARIZATION (WITHIN 6 MONTHS, PCI OR CABG), N (%)** | 269 | 137 (50.9%) | 62 | 11 (17.7%) | <0.001 |
| **EARLY PCI (WITHIN 6 MONTHS), N (%)** | 269 | 108 (40.2%) | 62 | 10 (16.1%) | <0.001 |
| **EARLY CABG (WITHIN 6 MONTHS), N (%)** | 269 | 32 (11.9%) | 62 | 1 (1.6%) | 0.015 |
| **MEDICATION** | | | | | |
| **ANTIPLATELET DRUG (ASPIRIN OR OTHER), N (%)** | 269 | 166 (61.7%) | 62 | 26 (41.9%) | 0.004 |
| **ANTICOAGULATION, N (%)** | 269 | 20 (7.4%) | 62 | 5 (8.1%) | 0.866 |
| **LIPID-LOWERING DRUG, N (%)** | 269 | 160 (59.5%) | 62 | 29 (46.8%) | 0.068 |
| **BETABLOCKER, N (%)** | 269 | 155 (57.6%) | 62 | 29 (46.8%) | 0.121 |
| **LONG-ACTING NITRATE, N (%)** | 269 | 33 (12.3%) | 62 | 11 (17.7%) | 0.252 |
| **CALCIUM CHANNEL BLOCKER, N (%)** | 269 | 55 (20.5%) | 62 | 10 (16.1%) | 0.440 |
| **ACE INHIBITOR, N (%)** | 269 | 62 (23.1%) | 62 | 12 (19.4%) | 0.529 |
| **AT II ANTAGONIST, N (%)** | 269 | 68 (25.3%) | 62 | 18 (29.0%) | 0.543 |
| **DIURETIC, N (%)** | 269 | 61 (22.7%) | 62 | 14 (22.6%) | 0.987 |
| **ANTIARRHYTHMIC DRUG, N (%)** | 269 | 7 (2.6%) | 62 | 2 (3.2%) | 0.785 |
| **AI-QCT** | | | | | |
| **AI-QCT DS, %** | 269 | 72 [60-79] | 62 | 36 [27-43] | <0.001 |
| **AI-QCT DIAMETER STENOSIS ≥30%, N (%)** | 269 | 269 (100%) | 62 | 44 (71.0%) | <0.001 |
| **AI-QCT DIAMETER STENOSIS ≥50%, N (%)** | 269 | 256 (95.2%) | 62 | 9 (14.5%) | <0.001 |
| **AI-QCT DIAMETER STENOSIS ≥70%, N (%)** | 269 | 163 (60.6%) | 62 | 0 (0.0%) | <0.001 |

| | | | | | |
|---|---|---|---|---|---|
| **VESSELS WITH AI-QCT DIAMETER STENOSIS ≥50%§, N (%)** | | | | | |
| **LM** | 262 | 13 (5.0%) | 61 | 0 (0.0%) | 0.076 |
| **LAD** | 269 | 215 (79.9%) | 62 | 5 (8.1%) | <0.001 |
| **LCX** | 269 | 93 (34.6%) | 62 | 1 (1.6%) | <0.001 |
| **RCA** | 269 | 139 (51.7%) | 62 | 4 (6.5%) | <0.001 |
| **AREA STENOSIS, %** | 269 | 92 [85-96] | 62 | 58 [47-69] | <0.001 |
| **PERCENT ATHEROMA VOLUME, %** | 269 | 18.9 [11.5-27.1] | 62 | 7.9 [4.1-13.2] | <0.001 |
| **PERCENT CALCIFIED PLAQUE VOLUME, %** | 269 | 6.8 [3.1-12.6] | 62 | 2.0 [0.9-6.1] | <0.001 |
| **PERCENT NON-CALCIFIED PLAQUE VOLUME, %** | 269 | 10.1 [7.5-14.6] | 62 | 5.6 [3.0-8.1] | <0.001 |
| **POSITIVE REMODELING, N (%)** | 269 | 269 (100%) | 62 | 62 (100%) | - |
| **TOTAL VESSEL VOLUME, MM³** | 269 | 3209 [2677-3838] | 62 | 3167 [2797-3167] | 0.840 |
| **TOTAL LUMEN VOLUME, MM³** | 269 | 2520 [2073-3017] | 62 | 2856 [2439-3310] | <0.001 |
| **TOTAL VESSEL LENGTH, MM** | 269 | 638 ±104 | 62 | 638 ±83 | 0.800 |

Values are n (%) or mean (±standard deviation (SD)) or median [interquartile range (IQR)]. P-values are from Mann-Withney U tests, T-tests, or Chi-square tests. *Prediabetes was defined as HbA1c 6.0-6.5%, or fasting glucose 6.1-6.9 mmol/l or impaired glucose tolerance (2h plasma glucose 7.8-11.0 mmol/l in a 75 oral glucose tolerance test). §Including side branches with diameter ≥1.5 mm. In some patients, left main was either absent or too short to be assessed as separate segment. Percent plaque volume (%) = plaque volume ($mm^3$)/vessel volume ($mm^3$)*100. AI-QCT= artificial intelligence-guided quantitative computed tomography, ACE= angiotensin converting enzyme, AP= angina pectoris, AT II = angiotensin II, BMI= body mass index, CABG = coronary artery bypass grafting, CAD= coronary artery disease, DS = diameter stenosis, FFR= fractional flow reserve, ICA= invasive coronary angiography, LAD = left anterior descending, LCX = left circumflex artery, LM = left main artery, NYHA= New York Heart Association. PCI= percutaneous coronary intervention, PET= positron emission tomography, RCA = right coronary artery. Originally published by Bär et al. in J Cardiovasc Comput Tomogr 2024 Apr 24:S1934-5925(24)00075-3, reprinted with permission.

### 5.4.2 Primary endpoint among all patients undergoing PET perfusion

In the total study population undergoing PET perfusion (n=662), 20.2% (n=84/416) of patients with an abnormal AI-$QCT_{ischemia}$ result and 8.9% (n=24/246) of patients with a normal AI-$QCT_{ischemia}$ result experienced the primary endpoint. The crude rate of the primary endpoint was significantly higher among patients with an abnormal vs. normal AI-$QCT_{ischemia}$ result (HR 2.25, 95% CI 1.40-3.60, p=0.001) (**Table 17**). Results remained consistent after adjusting for age, sex, diabetes mellitus, and

smoking according to significant associations with the primary endpoint in univariable models ($HR_{adj}$ 1.95, 95% CI 1.21-3.13, p=0.006) (**Table 17**). The rate of death alone was not significantly different between the groups (HR 1.26, 95% CI 0.74-2.16, p=0.402). The crude rate of MI alone was higher for patients with an abnormal AI-$QCT_{ischemia}$ result (HR 3.82, 95% CI 1.49-9.78, p=0.005), and remained significant after adjusting for age ($HR_{adj}$ 3.60, 95% CI 1.40-9.23, p=0.008). uAP alone could not be compared between groups, since none occurred in the group with a normal AI-$QCT_{ischemia}$ result (**Table 17**).

The results of the full-analysis set analyzed in an intention-to-diagnose approach, i.e. classifying those patients with an inconclusive AI-$QCT_{ischemia}$ or those excluded due to coronary anomalies (n=106) as having an abnormal AI-$QCT_{ischemia}$ result, was consistent with the main results (**Table 18**).

### 5.4.3 Primary endpoint among patients with normal PET perfusion

In the group with normal PET perfusion (n=331), 17.0% (n=25/147) of patients with an abnormal AI-$QCT_{ischemia}$ result and 5.4% (n=10/184) of patients with a normal AI-$QCT_{ischemia}$ result experienced the primary endpoint. The crude rate of the primary endpoint was significantly higher among patients with an abnormal vs. normal AI-$QCT_{ischemia}$ result (HR 3.11, 95% CI 1.49-6.47, p=0.002) (**Figure 17, Table 17**). Results remained consistent after adjusting for age and diabetes mellitus according to significant associations with the primary endpoint in univariable models ($HR_{adj}$ 2.47, 95% CI 1.17-5.21, p=0.018) (**Table 17**). The rate of death alone was not significantly different between the groups (HR 2.37, 95% CI 0.95-5.88, p=0.064). The crude rate of MI alone was higher for patients with an abnormal AI-$QCT_{ischemia}$ result (HR 5.08, 95% CI 1.43-18.00, p=0.012) and remained significant after adjusting for age ($HR_{adj}$ 3.93, 95% CI 1.10-14.07, p=0.036). uAP alone could not be compared between groups, since none occurred in the group with a normal AI-$QCT_{ischemia}$ result (**Table 17**).

Analyses censored at 2 years (HR 3.16, 95% CI 0.61-16.26, p=0.170) and 6 years showed that the rate of the primary endpoint starts to diverge between the AI-$QCT_{ischemia}$ groups from 6 years of follow-up onwards (HR 2.45, 95% CI 1.09-5.49, p=0.030).

The main analysis was repeated in the full-analysis set as an intention-to-diagnose approach, i.e. classifying those patients with an inconclusive AI-$QCT_{ischemia}$ or those excluded due to coronary anomalies (n=64) as having an abnormal AI-$QCT_{ischemia}$ result. This analysis remained consistent with the main results (**Table 18**).

### 5.4.4 Primary endpoint among patients with abnormal PET perfusion

In the group with abnormal PET perfusion (n=331), 21.9% (n=59/269) of patients with an abnormal AI-QCT$_{ischemia}$ result and 19.4%% (n=12/62) of patients with a normal AI-QCT$_{ischemia}$ result experienced the primary endpoint. There was no significant difference in the crude rate of the primary endpoint (HR 1.14, 95% CI 0.61-2.12, p=0.679) (**Figure 17, Table 17**). Results remained consistent after adjusting for age according to a significant association with the primary endpoint in the univariable model (HR$_{adj}$ 1.09, 95% CI 0.58-2.02, p=0.794) (**Table 17**). There were also no significant differences in the rates of death or MI alone between groups (death: HR 0.57, 95% CI 0.28-1.13, p=0.108; MI: 4.83, 95% CI 0.65-35.93, p=0.124). uAP alone could not be compared between groups, since none occurred in the group with a normal AI-QCT$_{ischemia}$ result (**Table 17**).

Analyses censored at 2 years (22 (8.2%) primary endpoint events in the abnormal AI-QCT$_{ischemia}$ group vs. 0 (0.0%) in the normal AI-QCT$_{ischemia}$ group) and 6 years (HR 1.37, 95% CI 0.65-2.91, p=0.409) showed similar results.

Results of the full-analysis set (i.e. by classifying 42 patients with inconclusive AI-QCT$_{ischemia}$ result or those excluded due to coronary anomalies as having an abnormal AI-QCT$_{ischemia}$ result) remained consistent with the main results (**Table 18**).

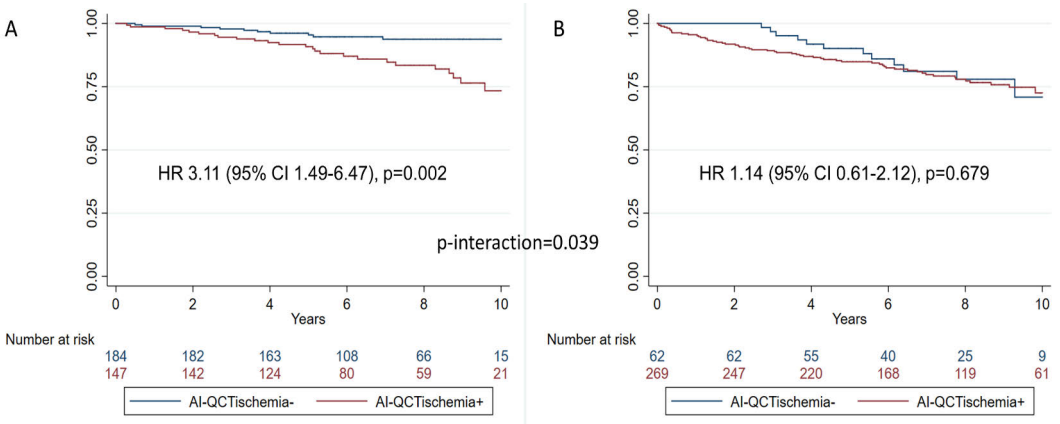


**Figure 17.** Crude Kaplan-Meier curves Study IV. Shown is the primary endpoint death, myocardial infarction (MI), and unstable angina pectoris (uAP) among patients with A) normal positron emission tomography (PET) perfusion, and B) abnormal PET perfusion. AI-QCTischemia- denotes normal and AI-QCTischemia+ denotes abnormal AI-QCT$_{ischemia}$ result. AI-QCT = artificial intelligence quantitative computed tomography, CI = confidence interval, HR = hazard ratio. Originally published by Bär et al. in J Cardiovasc Comput Tomogr 2024 Apr 24:S1934-5925(24)00075-3, reprinted with permission.

**Table 17.** Per-protocol set Study IV at 10 years.

| ALL PATIENTS N=662 | CRUDE HAZARD RATIOS | | | | ADJUSTED HAZARD RATIOS | | |
|---|---|---|---|---|---|---|---|
| | ABNORMAL AI-QCT$_{ISCHEMIA}$ RESULT N=416 | NORMAL AI-QCT$_{ISCHEMIA}$ RESULT N=246 | HR (95% CI) | P-VALUE | N PATIENTS (EVENTS) | HR (95% CI) ADJUSTED | P-VALUE ADJUSTED |
| DEATH, MI OR UAP, N (%) | 84 (20.2%) | 22 (8.9%) | 2.04 (1.30-3.22) | 0.002 | 662 (106) | 1.95 (1.21-2.3.13)[1] | 0.006[1] |
| DEATH, N (%) | 44 (10.6%) | 18 (7.3%) | 1.32 (0.76-2.29) | 0.322 | 662 (62) | 1.19 (0.63-1.92)[2] | 0.726[2] |
| MI, N (%) | 33 (7.9%) | 4 (1.6%) | 4.85 (1.72-13.69) | 0.003 | 662 (37) | 4.57 (1.62-12.92)[3] | 0.004[3] |
| UAP, N (%) | 20 (4.8%) | 0 (0.0%) | - | - | 662 (20) | - | - |
| PATIENTS WITH NORMAL PET PERFUSION N=331 | ABNORMAL AI-QCT$_{ISCHEMIA}$ RESULT N=147 | NORMAL AI-QCT$_{ISCHEMIA}$ RESULT N=184 | HR (95% CI) | P-VALUE | N PATIENTS (EVENTS) | HR (95% CI) ADJUSTED | P-VALUE ADJUSTED |
| DEATH, MI OR UAP, N (%) | 25 (17.0%) | 10 (5.4%) | 3.11 (1.49-6.47) | 0.002 | 331 (35) | 2.47 (1.17-5.21)[4] | 0.018[4] |
| DEATH, N (%) | 14 (9.5%) | 7 (3.8%) | 2.37 (0.95-5.88) | 0.064 | 331 (21) | 2.27 (0.91-5.64)[5] | 0.077[5] |
| MI, N (%) | 12 (8.2%) | 3 (1.7%) | 5.08 (1.43-18.00) | 0.012 | 331 (15) | 3.93 (1.10-14.07)[3] | 0.036[3] |
| UAP, N (%) | 3 (2.0%) | 0 (0.0%) | - | - | 331 (3) | - | - |
| PATIENTS WITH ABNORMAL PET PERFUSION N=331 | ABNORMAL AI-QCT$_{ISCHEMIA}$ RESULT N=269 | NORMAL AI-QCT$_{ISCHEMIA}$ RESULT N=62 | HR (95% CI) | P-VALUE | N PATIENTS (EVENTS) | HR (95% CI) ADJUSTED | P-VALUE ADJUSTED |
| DEATH, MI OR UAP, N (%) | 59 (21.9%) | 12 (19.4%) | 1.14 (0.61-2.12) | 0.679 | 331 (71) | 1.09 (0.58-2.02)[3] | 0.794[3] |
| DEATH, N (%) | 30 (11.2%) | 11 (17.7%) | 0.57 (0.28-1.13) | 0.108 | 331 (41) | 0.55 (0.27-1.10)[6] | 0.091[6] |
| MI, N (%) | 21 (8.2%) | 1 (1.6%) | 4.83 (0.65-35.93) | 0.124 | 331 (22) | - | - |
| UAP, N (%) | 17 (6.3%) | 0 (0.05) | - | - | 331 (17) | - | - |

Displayed are numbers (percentage) of first events and hazard ratios (HR) with 95% confidence intervals (CI) from Cox proportional hazards models. Results were adjusted for variables with a significant association with the reported endpoints in univariable Cox regressions: [1]age, sex, diabetes mellitus, smoking; [2]age, diabetes mellitus, smoking, family history of coronary artery disease; [3]age; [4]age, diabetes mellitus; [5]diabetes mellitus (only strongest univariable predictor due to the limited event number), [6]age, smoking. AI-QCT = artificial intelligence quantitative computed tomography, MI = myocardial infarction, PET = positron emission tomography, uAP = unstable angina pectoris. Originally published by Bär et al. in J Cardiovasc Comput Tomogr 2024 Apr 24:S1934-5925(24)00075-3, reprinted with permission.

**Table 18.** Full-analysis set Study IV at 10 years.

| ALL PATIENTS N=768 | CRUDE HAZARD RATIOS | | | | ADJUSTED HAZARD RATIOS | | |
|---|---|---|---|---|---|---|---|
| | ABNORMAL AI-QCT$_{ISCHEMIA}$ RESULT N=522 | NORMAL AI-QCT$_{ISCHEMIA}$ RESULT N=246 | HR (95% CI) | P-VALUE | N PATIENTS (EVENTS | HR (95% CI) ADJUSTED | P-VALUE ADJUSTED |
| DEATH, MI OR UAP, N (%) | 103 (19.7%) | 22 (9.8%) | 2.19 (1.38-3.47) | 0.001 | 768 (125) | 1.97 (1.24-3.14)[1] | 0.004[1] |
| DEATH, N (%) | 56 (10.7%) | 18 (7.3%) | 1.34 (0.79-2.28) | 0.280 | 768 (74) | 1.15 (0.67-1.96)[2] | 0.614[2] |
| MI, N (%) | 38 (7.3%) | 4 (1.6%) | 4.45 (1.59-12.46) | 0.005 | 768 (42) | 4.26 (1.52-11.94)[3] | 0.006[3] |
| UAP, N (%) | 22 (4.2%) | 0 (0.0%) | - | - | 768 (22) | - | - |
| **PATIENTS WITH NORMAL PET PERFUSION N=395** | **ABNORMAL AI-QCT$_{ISCHEMIA}$ RESULT N=211** | **NORMAL AI-QCT$_{ISCHEMIA}$ RESULT N=184** | **HR (95% CI)** | **P-VALUE** | **N PATIENTS (EVENTS)** | **HR (95% CI) ADJUSTED** | **P-VALUE ADJUSTED** |
| DEATH, MI OR UAP, N (%) | 37 (17.5%) | 10 (5.4%) | 3.21 (1.60-6.46) | 0.001 | 395 (47) | 2.72 (1.34-5.51)[4] | 0.005[4] |
| DEATH, N (%) | 22 (10.4%) | 7 (3.8%) | 2.61 (1.11-6.13) | 0.027 | 395 (29) | 2.30 (0.98-5.45)[5] | 0.059[5] |
| MI, N (%) | 16 (7.6%) | 3 (1.6%) | 4.71 (1.37-16.17) | 0.014 | 395 (19) | 4.03 (1.17-13.92)[6] | 0.028[6] |
| UAP, N (%) | 3 (1.4%) | 0 (0.0%) | - | - | 395 (3) | - | - |
| **PATIENTS WITH ABNORMAL PET PERFUSION N=373** | **ABNORMAL AI-QCT$_{ISCHEMIA}$ RESULT N=311** | **NORMAL AI-QCT$_{ISCHEMIA}$ RESULT N=62** | **HR (95% CI)** | **P-VALUE** | **N PATIENTS (EVENTS)** | **HR (95% CI) ADJUSTED** | **P-VALUE ADJUSTED** |
| DEATH, MI OR UAP, N (%) | 66 (21.2%) | 12 (19.4%) | 1.09 (0.59-2.03) | 0.775 | 373 (78) | 1.05 (0.57-1.95)[3] | 0.875[3] |
| DEATH, N (%) | 34 (10.9%) | 11 (17.7%) | 0.55 (0.28-1.09) | 0.085 | 373 (45) | 0.55 (0.28-1.09)[6] | 0.086[6] |
| MI, N (%) | 22 (7.1%) | 1 (1.6%) | 4.37 (0.59-32.43) | 0.149 | 373 (23) | - | - |
| UAP, N (%) | 19 (6.1%) | 0 (0.0%) | - | - | 373 (19) | - | - |

Displayed are numbers (percentage) of first events and hazard ratios (HR) with 95% confidence intervals (CI) from Cox proportional hazards models. Results were adjusted for variables with a significant association with the reported endpoints in univariable Cox regressions: [1]age, sex, diabetes mellitus, smoking; [2]age, sex, diabetes mellitus, smoking, family history of coronary artery disease; [3]age; [4]age, diabetes mellitus; [5]age, diabetes mellitus, family history of coronary artery disease; [6]age smoking. AI-QCT = artificial intelligence quantitative computed tomography, MI = myocardial infarction, PET = positron emission tomography, uAP = unstable angina pectoris. Originally published by Bär et al. in J Cardiovasc Comput Tomogr 2024 Apr 24:S1934-5925(24)00075-3, reprinted with permission.

### 5.4.5 Sensitivity analysis without patients undergoing early revascularization

Overall, 25.1% (n=166/662) of patients underwent early revascularization within 6 months. 31 patients (18.7%) who underwent early revascularization and 75 (15.1%) of patients who did not undergo early revascularization experienced the primary endpoint and event rates were similar (HR 1.15, 95% CI 0.75-1.74, p=0.523). The main analysis was repeated among the 496 patients without early revascularization and results were consistent. Among patients with normal PET perfusion (n=313), 16.9% (n=22/130) of patients with an abnormal AI-$QCT_{ischemia}$ result and 5.5% (n=10/183) of patients with a normal AI-$QCT_{ischemia}$ result experienced the primary endpoint. The crude and adjusted rates of the primary endpoint were significantly higher for patients with an abnormal as compared to a normal AI-$QCT_{ischemia}$ result ($HR_{adj}$ 2.70, 95% CI 1.26-5.80, p=0.011) (**Table 19**). Among patients with abnormal PET perfusion (n=183), 25.0% (n=33/132) of patients with an abnormal AI-$QCT_{ischemia}$ result and 19.6% (n=10/51) of patients with a normal AI-$QCT_{ischemia}$ result experienced the primary endpoint. The crude rate of the primary endpoint was similar for patients with an abnormal vs. normal AI-$QCT_{ischemia}$ result (HR 1.35, 95% CI 0.66-2.74, p=0.407). Adjusted analyses were not performed, since none of the variables showed a significant association with the primary endpoint (**Table 19**).

**Table 19.** Cox regressions among patients without early revascularization at 10 years Study IV.

| DEATH, MI, UAP | NORMAL PET PERFUSION (313 PATIENTS, 32 EVENTS) | | NORMAL PET PERFUSION (313 PATIENTS, 32 EVENTS) | | ABNORMAL PET PERFUSION (183 PATIENTS, 43 EVENTS) | |
|---|---|---|---|---|---|---|
| | UNIVARIABLE | | MULTIVARIABLE | | UNIVARIABLE | |
| | HR (95% CI) | P-VALUE | HR (95% CI) | P-VALUE | HR (95% CI) | P-VALUE |
| AI-QCT$_{ISCHEMIA}$ | 3.12 (1.48-6.60) | 0.003 | 2.70 (1.26-5.80) | 0.011 | 1.35 (0.66-2.74) | 0.407 |
| AGE, PER 1 YEAR | 1.09 (1.03-1.14) | 0.001 | 1.07 (1.01-1.12) | 0.011 | 1.04 (1.00-1.07) | 0.056 |
| SEX (MALE VS. FEMALE) | 1.82 (0.89-3.71) | 0.103 | - | - | 1.32 (0.69-2.54) | 0.400 |
| HYPERTENSION | 1.96 (0.81-4.76) | 0.138 | - | - | 1.19 (0.60-2.37) | 0.641 |
| DIABETES MELLITUS | 2.45 (1.18-5.09) | 0.016 | 2.26 (1.08-4.72) | 0.030 | 1.53 (0.75-3.11) | 0.237 |
| SMOKER | 1.83 (0.91-3.66) | 0.089 | - | - | 1.74 (0.95-3.16) | 0.071 |
| DYSLIPIDEMIA | 0.74 (0.36-1.51) | 0.406 | - | - | 0.85 (0.45-1.60) | 0.606 |
| FAMILY HISTORY OF CAD | 0.38 (0.17-0.84) | 0.017 | 0.45 (0.20-1.03) | 0.058 | 0.90 (0.49-1.64) | 0.722 |
| TYPICAL ANGINA | 0.51 (0.18-1.44) | 0.202 | - | - | 1.41 (0.73-2.70) | 0.305 |

AI-QCT = artificial intelligence quantitative computed tomography, CI = confidence interval, CAD = coronary artery disease, HR = hazard ratio, MI = myocardial infarction, uAP = unstable angina pectoris, PET = positron emission tomography. Originally published by Bär et al. in J Cardiovasc Comput Tomogr 2024 Apr 24:S1934-5925(24)00075-3, reprinted with permission.

# 6 Discussion

## 6.1 QFR to predict non-target-vessel-related events at 5-years in STEMI patients (Study I)

The main findings of Study I can be summarized as follows: 1) In STEMI patients undergoing primary PCI and angiography-guided complete revascularization, QFR ≤0.80 in non-target vessels was associated with a 7 times higher rate of the primary endpoint cardiac death, spontaneous non-TV-MI and non-TVR throughout 5 years. 2) Differences were driven by a 4-fold increased rates of spontaneous non-TV-MI and 11-fold increased rates of non-TVR. 3) Multivariable analysis identified QFR ≤0.80, but not DS ≥50% by 3D-QCA, as independent predictor for the occurrence of the primary endpoint. 4) The conventional QFR cut-off ≤0.80 showed high specificity (97.5%) and good NPV (87.6%) but low sensitivity (23.4%) and moderate PPV (62.9%) in the prediction of the primary endpoint.

The results of this study suggest that QFR in addition to angiographic assessment identifies patients at risk for future non-target-vessel related adverse events including spontaneous MI and revascularization in a patient population of STEMI patients undergoing angiography-guided complete revascularization. The lowest DS% in the group of patients with QFR ≤0.80 was 42%, suggesting that STEMI patients may possibly not only benefit from treatment of stenoses ≥70% or ≥50% and positive FFR ≤0.80, but also of lower grade stenoses in the range of ≥40-70% in the presence of a positive QFR ≤0.80. Interestingly, among the non-target vessels that were treated either during the index or as a planned staged procedure, 49.4% exhibited QFR ≤0.80.

In our study, 33% (n=12) of vessels in the QFR ≤0.80 group exhibited <50% stenosis, 67% (n=24) ≥50-70% stenosis, and the majority of vessels (67%) diffuse disease (i.e. lesion length >20mm) which may explain, why the significance was underestimated based on angiographic criteria alone. Of note, diffuse disease may be less amenable to revascularization and thus limit realizable treatment options. Mismatch between angiographic and functional lesion severity (i.e. QFR ≤0.80 but DS <50%) occurred most frequently (83%) in the LAD, which is in line with previous FFR investigations (Park et al. 2012).

Previous studies have shown that QFR outperforms 2D-QCA (Xu et al. 2017), and 3D-QCA outperforms 2D-QCA (Ding et al. 2019) in the in the prediction of FFR ≤0.80. In our study, as QFR ≤0.80 and DS ≥50% by 3D-QCA had similar sensitivity and specificity for the detection of the primary clinical endpoint, and ROC analysis yielded also similar AUC for QFR and DS%. However, QFR ≤0.80 proofed to be the better predictive variable, as shown by the markedly higher PPV for QFR ≤0.80 as for DS ≥50% (62.9% vs. 32.8%). This was also confirmed in multivariable analysis, where only QFR ≤0.80, but not DS ≥50% was independently associated with the primary endpoint.

The results for the present study are in line with other studies on the prognostic value of QFR in ACS patients (Chu et al. 2022). However, at variance to the other studies, the endpoint selection in our study focused on non-target vessel related events, allowing for a more direct mechanistic assessment of the association between the QFR value and the adverse events. Indeed, our results revealed that in the QFR ≤0.80 group, 71.4% (n=5) of MIs were related to the vessel with QFR ≤0.80. Furthermore, we extended QFR calculation to all eligible non-target vessels, whereas in the other studies, QFR was usually calculated after stenosis-based pre-selection (Chu et al. 2022).

Collectively, the current evidence on QFR in non-culprit lesions of STEMI patients suggests a diagnostic and prognostic incremental benefit over angiography alone. It is noteworthy that the safe and non-invasive QFR procedure is able to predict future adverse events including spontaneous MI and revascularization related to non-culprit lesions without the need of additional measures beyond diagnostic angiography and a dedicated software, which may be of particular importance to streamline the effective workflow for STEMI patients. Reliability of QFR in the acute vs. stable setting in STEMI patients has been shown previously to outperform FFR (Wang et al. 2023). This may be related to the fact that QFR mathematically assumes stable conditions, whereas the response of the microvasculature at the timepoint of the STEMI can be blunted and lead to falsely high FFR (van der Hoeven et al. 2019).

As an important limitation to the widespread use of QFR, it has to be acknowledged, that QFR calculation in our retrospective dataset was possible in only 56% of patients. However, this was mostly related to missing isocenter calibration or missing optimal angiographic projections, which can be addressed in prospective studies, where QFR calculation was shown to be possible in 96-99% (Xu et al. 2017; Westra et al. 2018).

In this STEMI population, the NPV of QFR >0.80 to preclude the primary endpoint was high (87.6%), but further prospective research is warranted to investigate whether revascularization of lesions with QFR >0.80 in this setting can safely be deferred. The moderate PPV of QFR ≤0.80 to predict primary endpoint

events may be at least in part related to the low number of lesions with QFR ≤0.80 (n=36, 5.7%). Furthermore, the very low sensitivity to detect the primary endpoint may reflect the low prevalence of higher grade stenoses (mean DS 36.5% (±10.5)). When conducting ROC analysis including only patients with higher degrees of stenosis (>25%, >30%, >40%, >50%), sensitivity incrementally increased reaching a maximum of 76.2% in stenoses >50%. The best QFR cut-off to detect the primary endpoint was 0.93, which may warrant further investigation in future studies.

### 6.1.1 Limitations

The results of this study must be considered in the light of several limitations. 1) This was a retrospective post-hoc analysis and therefore optimal angiographic projections for QFR calculation were not always available. 2) QFR was computable in only 56.1% of patients mostly due to missing isocenter calibration or inadequate angiographic quality, aspects that can be addressed, as shown in previous prospective studies (successful QFR calculation in 96-99% of vessels) (Xu et al. 2017; Westra et al. 2018). 3) The study population consisted of unbalanced comparator groups, which may weaken the reliability of statistical analyses, led to wide confidence intervals, and, owing to the low event number in the large QFR >0.80 group, might have biased the overall study results away from the null hypothesis. However, we have addressed this by performing all analyses including only patients with >30% stenosis and results for this lesser skewed population were consistent with the overall study results. Furthermore, the study design of a QFR investigation regardless of stenosis was chosen to investigate the benefit of a truly physiologic assessment without an angiographic/QCA stenosis pre-selection, which is, to our knowledge, unique in the field of QFR. 4) Lesions left untreated according to an angiographic assessment could consist of more complex lesions less/not amenable to revascularization, which would affect the practical implications of QFR detecting these lesions. 5) As the original study design included no FFR analyses, comparison between QFR and FFR was not possible and therefore no statement regarding the accuracy of QFR as compared to FFR in the setting of STEMI can be made. However, previous studies addressed this question sufficiently (Wang et al. 2023; Chu et al. 2022). 6) More recent evidence indicates no benefit of FFR-guided non-culprit PCI in STEMI patients (Puymirat et al. 2021). However, in this study we assessed the incremental value of QFR on top of and not versus an angiographic assessment. Furthermore, there is some evidence that QFR could be more accurate as FFR in the acute setting of STEMI, potentially explained by the fact that QFR mathematically assumes stable conditions, and may be less dependent on the full dilatation capacity of the microvasculature than FFR (Wang et al. 2023). 7) In this cohort, the protocol required revascularization of non-culprit lesions was visual DS

≥70% and lesions with DS ≥50% were treated according to the operators' discretion. However, the data shows that adherence to the ≥50% threshold was very high, because only 24/946 assessed vessels had DS ≥50% by 3D-QCA.

## 6.2 QFR to predict non-target-vessel events prior to planned staged PCI in ACS patients (Study II)

The main findings of Study II can be summarized as follows: In this cohort study of patients with ACS and MVD scheduled to undergo out-of-hospital staged PCI within a median of 28 (IQR 28-42) days from index presentation, non-TV QFR of vessels scheduled for staged PCI using the index procedure angiogram did not show an independent association with non-TV events occurring prior to the planned staged PCI. Therefore, this study does not provide conceptual evidence for QFR being able to optimize the timing of staged PCI (i.e. to plan earlier in case of lower QFR) on top of clinical judgement. These results apply to patients scheduled on average 4 weeks after the index procedure and mean QFR value of 0.73 in the untreated non-target vessel.

In a subanalysis of the COMPARE-ACUTE (Comparison Between FFR Guided Revascularization Versus Conventional Strategy in Acute STEMI Patients With MVD) trial (Piróth et al. 2020), an inverse non-linear relationship between deferred lesions among STEMI patients investigated by FFR and non-TV events was observed which plateaued at FFR 0.60. Additional evidence exists from retrospective analyses from mixed populations including 29% ACS, where FFR was shown to be continuously and inversely related to ischemic event risk (Johnson et al. 2014). These analyses support the concept that the functional significance of non-culprit lesions may represent an ischemic continuum with increasing inverse event risk, rather than a dichotomous state dividing at FFR 0.80. In STEMI patients, acute QFR shows even better agreement with 30-day FFR as acute FFR itself (Wang et al. 2023), which in addition to its non-invasive and hyperemia-free nature, makes it an interesting diagnostic tool for the ACS population.

However, in our investigation, we did not observe any independent association between QFR and non-TV events occurring before staged PCI. These findings suggest that non-TV QFR may not be able to refine the timing of staged PCI, among patients undergoing operators' scheduled out-of-hospital staged PCI within a median of 28 days from index PCI. The overall event rate was 5%, the number of very low QFR values (i.e. <0.60) small, and the timeframe for the events to occur short with a median of 28 days. Therefore, we cannot definitely exclude a potential association between QFR and non-TV events prior to staged PCI in a larger patient population with more pronounced hemodynamic impairment and longer duration to staged PCI.

Along these lines, we observed a significant univariable association between linear QFR and non-TV-MI, as well as a trend towards higher risk of clinical events with lower QFR, but these investigations are limited by low sample size. Further, there was a small trend, also impacted by the sample size, that patients with lower QFR seemed to be scheduled slightly earlier for staged PCI. This may have diluted outcomes and further studies are required. Lastly, none of the other classical covariates in the prediction models showed an independent association with the primary endpoint, and also patient characteristics of patients with vs. without a primary endpoint event were similar, implying that, taking into account all limitations of the current study, other factors may drive this type of event.

At variance to the clinical setting of CCS demonstrating improved short- and middle-term outcomes with physiology-guided compared to angiography-guided revascularization using FFR (Pijls et al. 2010) and QFR (Xu et al. 2021; Song Lei et al. 2022), no superiority of FFR-guided vs. angiography-guided complete non-culprit lesion revascularization has been observed in the STEMI population (Puymirat et al. 2021). Vulnerable non-culprit plaque features such as high plaque burden, thin fibrous cap and low minimal lumen area are highly prevalent in ACS patients (Stone et al. 2011) and have been shown to be associated with subsequent events (Stone et al. 2011). Therefore, and based on the findings of this study, it may be hypothesized, that plaque morphology may play a more important role as compared to physiology in driving early non-TV events occurring before planned staged PCI. This should be investigated in future studies.

### 6.2.1 Limitations

The study results need to be considered in light of several limitations. 1) It is an observational, non-randomized, post-hoc, single-center study. 2) The timepoint of staged PCI (and thus time to event) was defined by operators' judgement, however the aim of the study was to investigate potential add-on value of QFR for the timing of staged PCI on top of clinical judgement and not QFR alone. 3) A small trend towards staged PCIs scheduled later in case of higher QFR was observed, which may have diluted QFR-related outcomes, highlighting the need for further studies. 4) The number of vessels with very low QFR was limited and we observed a significant univariable association between linear QFR and non-TV-MI as well as a trend towards a higher percentage of events with lower QFR, so that we cannot exclude a potential association between QFR and non-TV events occurring before staged PCI in larger patient populations with more pronounced hemodynamic impairment and longer duration to staged PCI. 5) Highest-risk patients, i.e. those undergoing in-hospital staged PCI (n=139) or those with cardiogenic shock at index presentation (n=70), were excluded from this study (Otsuka et al. 2021). 6) FFR and intracoronary

imaging were used clinically upon the discretion of the operators and could not be collected systematically. 7) 24% of the patients had to be excluded due to unanalyzable QFR, most frequently angiographic quality related (absence of 2 suitable projections, overlap, poor contrast, foreshortening) (148 patients, 10%). Further issues were incomplete patient-related and/or angiographic data (84 patients, 6%) or missing isocenter calibration, which was sometimes not available in the angiograms from 2009-2011 (45 patients, 3%). However, the proportion of excluded patients is even smaller as compared to previous post-hoc QFR analyses (Spitaleri et al. 2018; Lauri et al. 2020), and we have compared the characteristics of in- vs. excluded patients from this cohort study with no relevant differences. Importantly, these technical issues do not represent a limitation to the QFR technique per se, since in prospective QFR studies, analyzability of the angiograms is usually 96-99% (Tu et al. 2016; Xu et al. 2017). 8) The percentage of female patients was lower than in unselected cohorts of ACS patients (Fokkema et al. 2016).

## 6.3 Prognostic value of AI-QCT$_{ischemia}$ for patients with suspected coronary artery disease (Study III)

The main findings of Study III can be summarized as follows: 1) Calculation of AI-QCT$_{ischemia}$ was feasible from real-world CCTA data in 83% of patients. 2) An abnormal AI-QCT$_{ischemia}$ result was associated with a 2-fold adjusted rate of all-cause death, MI, or uAP throughout median 7 years of follow-up, driven by higher rates of MI and uAP. 3) AI-QCT$_{ischemia}$ remained an independent predictor of the primary endpoint on top of visual stenosis and clinical factors, and the risk differentiation was most prominent among patients with no or non-obstructive CAD (i.e. visual DS ≤50%).

AI-based analyses for the assessment of CAD are increasingly being developed (Carin and Pencina 2018; Slart et al. 2021) and they may revolutionize image analysis in the future. In this regard, we tested the prognostic value of a recently developed AI-algorithm based on morphology from CCTA images to identify whether coronary lesions will likely be functionally significant. Our analysis shows, that AI-QCT$_{ischemia}$ calculation was feasible from CCTA data obtained during the clinical routine in 83% of cases, which is comparable to CT-FFR (Nørgaard et al. 2014; Min et al. 2015; Curzen et al. 2021). AI-QCT$_{ischemia}$ also proofed its prognostic power with a 2-fold increased adjusted long-term rate of the primary endpoint. This is consistent with previous data on quantitative PET perfusion (Juárez-Orozco et al. 2018). Furthermore, C-index improvement with the addition of AI-QCT$_{ischemia}$ was significant in comparison to clinical variables and similar to that of visual obstructive

stenosis. However, AI-QCT$_{ischemia}$ remained an independent predictor of the primary endpoint on top of clinical variables and visual stenosis.

In the validation study, the diagnostic agreement of AI-QCT$_{ischemia}$ with invasive FFR outperformed that of FFR-CT and was similar to $^{15}O$-$H_2O$ PET perfusion (Nurmohamed et al. 2024a). The prognostic value of AI-QCT$_{ischemia}$ as compared FFR-CT should be investigated in future studies. Also, in order to investigate the prognostic value of two different approaches to model functionally significant CAD (i.e. with CFD by FFR-CT and with AI by AI-QCT$_{ischemia}$), a combined prognostic model with AI-QCT$_{ischemia}$ and FFR-CT could shed light on to what extent the functionality by both methods agree with each other, i.e. if AI-QCT$_{ischemia}$ would improve the prediction of FFR-CT, it could be argued that the AI-based model is not specifically a functional but also/rather a morphological estimate.

The second aim of this investigation was to determine whether AI-QCT$_{ischemia}$ had differential risk stratification among patients with no/non-obstructive or obstructive CAD. First of all, in this analysis, 79.8% of patients with >50% stenosis had "ischemia" according to AI-QCT$_{ischemia}$. This is a substantially higher proportion of patients having "ischemia" as commonly reported, where agreement between anatomically obstructive disease and (invasively or non-invasively determined) functional significance is usually 30-47% (Gaemperli et al. 2007, 2008; Meijboom et al. 2008). This may be explained by the fact that DS% is the highest ranked feature in the AI-QCT$_{ischemia}$ algorithm, and it has been reported previously, that obstructive disease according to AI-QCT stenosis is related to functional significance in up to 76% of the cases (Lipkin et al. 2022). Despite using visual and not AI-QCT stenosis, it appears plausible that the higher classification agreement between obstructive and "functionally" significant disease according AI-QCT$_{ischemia}$ is related to the high feature importance of stenosis in the AI-QCT$_{ischemia}$ algorithm.

Among patients with no/non-obstructive disease, we found incremental risk stratification by AI-QCT$_{ischemia}$. And, although sample size and event numbers are small and confidence intervals wide, the results indicate that this risk difference was driven by a significantly higher adjusted rate of spontaneous MI, whereas adjusted mortality rates were similar. Revascularization was performed in <1% in this patient group without obstructive disease (in 5.3% of patients with abnormal AI-QCT$_{ischemia}$ and 0.3% with normal AI-QCT$_{ischemia}$ result). These results are in line with current evidence, that ischemia based on contemporary non-invasive methods is associated with an increased risk of spontaneous MI if managed medically (Chaitman et al. 2021; Navarese et al. 2021), whereas all-cause mortality is similar among revascularized vs. medically treated patients with ischemic CAD (Maron et al. 2020; Chacko et al. 2020; Hochman et al. 2023). Vice versa, the absence of incremental risk stratification by AI-QCT$_{ischemia}$ among patients with obstructive disease could be explained by the 39.7% of patients who underwent early revascularization (45.5%

of patients with abnormal AI-QCT$_{ischemia}$ and 16.7% with normal AI-QCT$_{ischemia}$ result). These considerations are also supported by the subgroup analysis in the total cohort for patients with vs. without early revascularization, where incremental risk stratification by AI-QCT$_{ischemia}$ was only found among those without revascularization. However, these are observations from a post hoc analysis of cohort data and only an adequate, prospective, RCT could demonstrate the effect of revascularization among patients with an abnormal AI-QCT$_{ischemia}$ result. Nevertheless, the findings highlight the utility of a test to determine the hemodynamic consequences of CAD also in the non-obstructive range, and the results are also in agreement with earlier findings that non-obstructive CAD on CCTA is associated with increased overall event risk (Min et al. 2011; Nielsen et al. 2017; The SCOT-HEART Investigators 2018; Mortensen et al. 2020).

Together with its good calculability from real-world clinical CCTA data, as well as radiation and hyperemia-free nature, AI-QCT$_{ischemia}$ may thus represent a promising tool for improved risk stratification among patients with coronary atherosclerosis and may become an alternative to other functional CCTA tests consisting to date of myocardial CTP and FFR-CT. Further research on its agreement with other functional tests and prognostic power in different patient populations are warranted.

### 6.3.1 Limitations

The results of this study must be considered in the light of several limitations: 1) It was a single-center re-analysis of observational study cohort data. 2) In 17% of the patients AI-QCT$_{ischemia}$ was not analyzable, however, we have included these patients in an intention-to-diagnose approach. 3) The algorithm is binary and does currently not quantify the magnitude of hemodynamic impairment. 4) Subgroups (visual DS ≤50% with abnormal AI-QCT$_{ischemia}$ result, n=113; visual DS >50% with normal AI-QCT$_{ischemia}$ result, n=96) were relatively small, which hampers the evaluation of different event types (death vs. MI vs. uAP). 5) Different treatment strategies for non-obstructive vs. obstructive CAD in accordance with current guidelines may have reduced event rates in the subgroup of patients with obstructive disease and diluted the prognostic value of AI-QCT$_{ischemia}$. Therefore, the evidence from this study may not allow to generally conclude on the absence of risk stratification by AI-QCT$_{ischemia}$ among patients with obstructive CAD. 6) The functional nature of AI-QCT$_{ischemia}$ that integrates morphological variables may need to be proven by more evidence. However, test characteristics of AI-QCT$_{ischemia}$ for the detection of invasive FFR ≤0.80 were superior to those of FFR-CT and SPECT, comparable to $^{15}$O-$H_2O$ PET (Nurmohamed et al. 2024a) and clearly better than those expected for obstructive stenosis on CCTA alone (Knuuti et al. 2018). Furthermore, AI-algorithms in cardiac

imaging were previously shown to provide value beyond that of traditional mathematical models when using exactly the same variables (Juarez-Orozco et al. 2020).

## 6.4 Prognostic value of AI-QCT$_{ischemia}$ for patients with visually obstructive stenosis and normal or abnormal PET perfusion (Study IV)

The main findings of this Study IV can be summarized as follows: Among patients with visually obstructive stenosis on CCTA and normal downstream $^{15}O$-$H_2O$ PET perfusion, an abnormal AI-QCT$_{ischemia}$ result was associated with a 2.5-fold higher adjusted rate of all-cause death, MI, or uAP throughout 6.2 median years of follow-up. In contrast, incremental risk stratification by AI-QCT$_{ischemia}$ was not observed for patients with abnormal PET perfusion.

AI-QCT$_{ischemia}$ aims at estimating the presence of functional significant CAD directly from anatomical CCTA images (Nurmohamed et al. 2024a). In a previous preliminary analysis, the test characteristics of AI-QCT$_{ischemia}$ for ischemic CAD based on hybrid CCTA/PET were accuracy 83%, sensitivity 74%, specificity 86%, PPV 66%, and NPV 90% (Nabeta et al. 2023). However, the prognostic value of AI-QCT$_{ischemia}$ in a typical population that needs downstream functional testing after CCTA was unknown so far. Therefore, in Study IV, we assessed the prognostic value of AI-QCT$_{ischemia}$ according to the PET perfusion result.

Selective hybrid coronary CTA/$^{15}O$-$H_2O$-PET imaging (Maaniitty et al. 2017) and pooled quantitative PET perfusion across various radiotracers (Juárez-Orozco et al. 2018) have proven prognostic value. Also, plaque burden according to AI-QCT has been shown to be independently associated with 10-year cardiovascular outcomes (Nurmohamed et al. 2023). In Study III of this thesis, AI-QCT$_{ischemia}$ showed incremental prognostic value among symptomatic patients with suspected CAD undergoing CCTA, and specifically among those with anatomically no/non-obstructive disease (≤50% stenosis), but not among those with anatomically obstructive disease (>50% stenosis).

In Study IV we have extended these previous findings by investigating the prognostic value of AI-QCT$_{ischemia}$ among patients referred for downstream PET perfusion due to visually suspected obstructive disease adopting the threshold of ≥50% stenosis according to the institutional hybrid CCTA/PET imaging protocol. We found that, overall, the risk stratification by AI-QCT$_{ischemia}$ in this patient subgroup with an indication for functional imaging was preserved. Furthermore, among patients with normal PET perfusion, an abnormal AI-QCT$_{ischemia}$ result identified those patients with a higher event risk, despite median 2 years younger

patients, as well as equally prevalent cardiovascular risk factors and medical therapy in both AI-$QCT_{ischemia}$ groups. The prognostic power of AI-$QCT_{ischemia}$ accrued over the long-term with event rates diverging from 6 years of follow-up onwards. In contrast, in the abnormal PET perfusion group, no additional risk stratification by AI-$QCT_{ischemia}$ was found.

Integrating the results of Study III and IV, it appears, that the grouping of patients with visual borderline stenosis 50% impacts the prognostic value of AI-$QCT_{ischemia}$. These are typically also the patients for whom functional imaging is indicated and most necessary for clinical management.

Furthermore, 95% of patients with normal PET perfusion in Study IV and >99% of patients with anatomically no/non-obstructive disease in Study III, where AI-$QCT_{ischemia}$ had incremental prognostic value, did not undergo early revascularization. In contrast, 45% of the patients with abnormal PET perfusion in Study IV and 40% of the patients with anatomically obstructive disease in Study III underwent early revascularization. Additionally, among patients with abnormal PET perfusion in Study IV, antiplatelet therapy was more frequently prescribed for those with an abnormal AI-$QCT_{ischemia}$ result. Therefore, it could be argued, that the absence of risk stratification among patients with >50% anatomical disease or those with an abnormal PET perfusion result is related to the differential treatment strategies that follow the current guidelines.

This concept is further supported by the interaction with revascularization demonstrated in Study III, which may imply that revascularization importantly affects prognosis and the risk stratification by AI-$QCT_{ischemia}$. Also, it has been shown previously in this registry, that patients revascularized based on the hybrid CCTA/PET imaging protocol attained a similar prognosis as those patients without an indication for revascularization (Maaniitty et al. 2017). And in Study IV, the risk stratification by AI-$QCT_{ischemia}$ in the normal PET perfusion group was numerically increased after excluding the patients undergoing revascularization.

However, only an appropriate prospective RCT could demonstrate whether revascularization improves outcomes among patients with an abnormal AI-$QCT_{ischemia}$ result. Alternatively, since AI-$QCT_{ischemia}$ is derived from the epicardial atherosclerotic burden on CCTA, rather more aggressive medical therapy could be warranted given the higher burden of non-obstructive or non-flow-limiting atherosclerotic disease, known to be related to poor clinical outcome (Min et al. 2011; Nielsen et al. 2017; The SCOT-HEART Investigators 2018; Mortensen et al. 2020).

Of note, only 63% of the population of Study IV had ≥50% diameter stenosis according to AI-QCT. This is in line with a previous report, that stenosis assessment with AI-QCT vs. visual analysis generally leads to a downgrade in stenosis severity (Nurmohamed et al. 2024b). However, the findings of the current study support the

concept, that the prognostic value of AI-QCT$_{ischemia}$ is not only related to the more accurate diagnosis of obstructive CAD by AI-QCT vs. visual analysis, because in both PET perfusion groups, where AI-QCT$_{ischemia}$ had different prognostic value, ~94-95% of patients with abnormal AI-QCT$_{ischemia}$ result also had AI-QCT diameter stenosis ≥50%. But, since AI-QCT diameter stenosis is the highest ranked feature in the AI-QCT$_{ischemia}$ algorithm (Nurmohamed et al. 2024a) the prognostic value of AI-QCT diameter stenosis vs. AI-QCT$_{ischemia.}$ should be the target of future studies in unselected populations.

In the total cohort, 50% of the patients had "ischemia" according to PET and 63% according to AI-QCT$_{ischemia}$, but these two techniques disagreed in 32% of the patients. It has been acknowledged previously, that some CCTA-derived plaque parameters like non-calcified plaque volume or positive remodeling are independently associated with impaired MBF on PET and invasive FFR, while others, like low-attenuation plaque or spotty calcification, are only associated with impaired invasive FFR, but not with PET (Driessen et al. 2018). Thus, varying phenotypes of atherosclerosis may impact myocardial perfusion imaging and FFR in different ways. Since AI-QCT$_{ischemia}$ uses AI to detect atherosclerosis features from CCTA that have a certain probability to be found in a lesion with invasive FFR ≤0.80, some disagreement between AI-QCT$_{ischemia}$ and PET is consistent with the current evidence. Furthermore, in contrast to AI-QCT$_{ischemia}$, which was trained to detect flow-limiting epicardial atherosclerosis from CCTA, PET detects myocardial perfusion abnormalities that are not only caused by epicardial but also microvascular disease. And since both, microvascular (Del Buono et al. 2021) and epicardial coronary disease (Min et al. 2011; Nielsen et al. 2017; The SCOT-HEART Investigators 2018; Mortensen et al. 2020) are known to be associated with impaired prognosis, it could be hypothesized, that these techniques may act complementary.

This is also supported by the current data showing that the event rate for patients with preserved PET perfusion but an abnormal AI-QCT$_{ischemia}$ result was close to those with abnormal PET perfusion. Indeed, these patients proved to have more advanced epicardial atherosclerosis, as evidenced by higher plaque burden (PAV, CPV, and NCPV) and more severe lumen impairment (DS%, area stenosis, lumen volume). However, while AI-QCT$_{ischemia}$ successfully risk stratifies patients with normal PET perfusion, among the patients with abnormal PET perfusion, 20% experienced the primary endpoint regardless of the AI-QCT$_{ischemia}$ result. Consistently, in a preliminary analysis from this cohort, AI-QCT$_{ischemia}$ showed similar prognostic value as hybrid CCTA/PET perfusion imaging. But when AI-QCT$_{ischemia}$ and hybrid CCTA/PET were combined into the same multivariable Cox regression, only ischemic CAD by hybrid CCTA/PET remained an independent predictor of death, MI, or uAP, whereas AI-QCT$_{ischemia}$ did not reach statistical significance (Maaniitty 2023 et al). Some of the patients detected only by PET, but

not AI-QCT$_{ischemia}$ are expected to have microvascular disease (Stenström et al. 2017), that should be managed according to the current recommendations (Del Buono et al. 2021).

However, the detailed underlying factors to the discrepancies between PET perfusion and AI-QCT$_{ischemia}$ require future dedicated investigation. Also, appropriate prospective studies are warranted to test the impact of AI-QCT$_{ischemia}$ on outcomes in unselected populations.

### 6.4.1 Limitations

The results of this study must be considered in the light of several limitations. 1) It was a single-center, observational study associated with all limitations of a retrospective analysis. However, for AI-QCT$_{ischemia}$, the CTAs were re-analyzed blinded to clinical data, PET perfusion results, and outcome. 2) The study population represents a highly selected cohort of symptomatic patients having visually obstructive CAD on a CCTA therefore referred for downstream ischemia testing with PET perfusion imaging, and the results do not pertain to patients without obstructive CAD on CCTA or those undergoing PET perfusion imaging for another indication. 3) The clinical CCTA reading as basis for PET perfusion referral was performed visually by experienced clinical readers. Therefore, intra- or interobserver reproducibility in stenosis assessment, that could have introduced variability in the current analysis, was not assessed. 4) The clinical CTA reading was performed according to the AHA recommendations valid during the enrolment period (Austen et al. 1975). However, the segmenting system used should not impact the overall interpretation of the CCTA. 5) AI-QCT$_{ischemia}$ is binary and does currently not quantify the magnitude of hemodynamic impairment. 6) Invasive FFR was not routinely performed as the patients had non-invasive functional information available based on PET.

# 7 Conclusions

The major findings and conclusions of Studies I-IV are as follows:

I. Among 617 STEMI patients undergoing primary PCI and angiography-guided complete revascularization, QFR ≤0.80 in untreated non-target vessels was associated with a 7 times higher rate of cardiac death, spontaneous non-TV-MI and non-TVR throughout 5 years. These findings suggest, that QFR on top of traditional ICA identifies STEMI patients at risk for future adverse cardiovascular events.

II. Among 1093 patients with ACS and MVD scheduled to undergo out-of-hospital staged PCI within median 28 days, QFR from non-target vessels planned for staged PCI was not independently associated with non-target vessel related events prior to staged PCI. Therefore, this study does not provide conceptual evidence, that QFR may be able to help refine the timing of staged PCI on top of clinical judgement.

III. Among 1880 symptomatic patients with suspected CAD undergoing CCTA, an abnormal AI-$QCT_{ischemia}$ result was associated with a 2-fold increased adjusted rate of long-term death, MI, or uAP. This risk stratification was observed among patients with no/non-obstructive CAD, but not among those with obstructive CAD. AI-$QCT_{ischemia}$ may thus be useful to improve risk stratification, especially among patients with no/non-obstructive CAD on CCTA.

IV. Among 662 patients with visually obstructive CAD on CCTA undergoing downstream PET myocardial perfusion imaging, an abnormal AI-$QCT_{ischemia}$ result was associated with a 2.5-fold increased adjusted rate of long-term death, MI, or uAP in case of a normal PET perfusion result. This incremental risk stratification was not observed for patients with abnormal PET perfusion.

# Acknowledgements

The research of this thesis has been conducted at the Department of Cardiology at Bern University Hopsital, Switzerland, from 2019 to 2023, and at Turku PET Centre and Heart Center at Turku University Hospital, Finland, from 2023 to 2024. I thank Professor Juhani Knuuti, Director of Turku PET Centre, and Professor Lorenz Räber, Director of Interventional Cardiology in Bern, and for the facilities and the opportunity to conduct research in their groups. I also thank Professor Stephan Windecker, Head of Cardiology Department in Bern, for the facilities in Bern in general and his supportive attitude towards this academic collaboration between Switzerland and Finland.

For this work, I have received personal support from the Swiss National Science Foundation and the University of Turku. Cleerly inc. has provided the AI-QCT$_{ischemia}$ analyses without costs.

I am very grateful for all support of Professor Juhani Knuuti, for the unique chance to work in this research group, for kind guidance through the thesis, and the inspiring academic atmosphere at Turku PET Centre. I was blessed to get in touch with such fantastic data that you have in Turku. I hope to be able to learn from you ever on, and for that I really regret, that my journey takes be back to Switzerland – at least for now.

I am very thankful for all the work of my supervisor Doctor Teemu Maaniitty. For set up of the database many years ago, for kind introduction into a new research field, for your sharp mind and critical eyes in the review process of the articles, and friendly company. I really hope that we can continue our collaboration.

A special word is owned to Professor Lorenz Räber, who has unrestrictedly supported me from the first day we met in 2019. Since for me, unexpectedly, all the academic and clinical challenges of a young cardiologist came together with the "rush hour of life" (two babies born within 20 months), it needed your specific skill to guide me through the challenges of the last years. Sometimes I think, it comes close to a miracle, that my passion for research keeps on growing alongside with my kids. Thank you.

I thank both reviewers of this thesis, Professor Oliver Gaemperli from the University of Zurich, Switzerland, and Doctor Helena Rajala from the University of Helsinki, Finland, who have helped to increase the quality of the thesis.

I thank the opponent of this thesis Professor Göran Bergström from the University of Gothenburg, Sweden, for all effort and input.

I thank Professor Antti Saraste for all support, and specifically for guidance through the administrative processes at the university. I thank Professor Jeroen Bax from Leiden University, the Netherlands, and Doctor Tanja Kero from the University of Uppsala, Sweden. I thank Heli Louhi, research coordinator at Turku PET Centre, for collaboration and kind company.

I thank all co-authors for collaboration and insightful inputs for the articles. Specifically, Yasushi Ueki, Tatsuhiko Otsuka, and Raminta Kavaliauskaite for endless hours spent together in the Corelab in Bern.

Lastly, I thank my family. My husband Christian for all love and support, it is a privilege to raise a family with you. Also, the professional and personal sacrifices you made during this year in Finland, need to be honored specifically. Our kids Jari and Ella for bringing sunshine and purpose into our life. My father Matthias for outstanding efforts and excellence in supporting our family in Turku, and for sharing and understanding my passion for research. My mother Erja for greatest support through the last years. My sister Mirjam for all good moments. My mother-in-law Christine for all help with the kids and countless books read to them.

Ultimately, I thank my childcare network, without which, none of this would ever have been possible. I could not count all the hours you indirectly worked on this thesis. Thank you grandparents, Ursula, and Tyksilän päiväkoti.

Turku, 24.04.2024
*Sarah Bär*

# References


Abbara S, Blanke P, Maroules CD, et al (2016). SCCT guidelines for the performance and acquisition of coronary computed tomographic angiography: A report of the Society of Cardiovascular Computed Tomography Guidelines Committee: Endorsed by the North American Society for Cardiovascular Imaging (NASCI). J Cardiovasc Comput Tomogr 10:435–449. https://doi.org/10.1016/j.jcct.2016.10.002

Ahmadi A, Leipsic J, Øvrehus KA, et al (2018). Lesion-Specific and Vessel-Related Determinants of Fractional Flow Reserve Beyond Coronary Artery Stenosis. JACC Cardiovasc Imaging 11:521–530. https://doi.org/10.1016/j.jcmg.2017.11.020

Ahmadi A, Senoner T, Correa A, et al (2020). How atherosclerosis defines ischemia: Atherosclerosis quantification and characterization as a method for determining ischemia. J Cardiovasc Comput Tomogr 14:394–399. https://doi.org/10.1016/j.jcct.2019.10.006

Antoniadis M, Stader J, Ussat M, et al (2022). Comparison of quantitative flow ratio (QFR) and instantaneous wave-free ratio (iFR) or resting full-cycle ratio (RFR) during daily routine in the catheterization laboratory. Eur Heart J 43:ehac544.1369. https://doi.org/10.1093/eurheartj/ehac544.1369

Arbab-Zadeh A, Nakano M, Virmani R, Fuster V (2012). Acute Coronary Events. Circulation 125:1147–1156. https://doi.org/10.1161/CIRCULATIONAHA.111.047431

Austen W, Edwards J, Frye R, et al (1975). A reporting system on patients evaluated for coronary artery disease. Report of the Ad Hoc Committee for Grading of Coronary Artery Disease, Council on Cardiovascular Surgery, American Heart Association. Circulation 51:5–40. https://doi.org/10.1161/01.CIR.51.4.5

Steg PhG, James SK, Atar D, et al (2012). ESC Guidelines for the management of acute myocardial infarction in patients presenting with ST-segment elevation. Eur Heart J 33:2569–2619. https://doi.org/10.1093/eurheartj/ehs215

Bangalore S, Maron DJ, Stone GW, Hochman JS (2020). Routine Revascularization Versus Initial Medical Therapy for Stable Ischemic Heart Disease. Circulation 142:841–857. https://doi.org/10.1161/CIRCULATIONAHA.120.048194

Bär S, Kavaliauskaite R, Ueki Y, et al (2021). Quantitative Flow Ratio to Predict Nontarget Vessel-Related Events at 5 Years in Patients With ST-Segment-Elevation Myocardial Infarction Undergoing Angiography-Guided Revascularization. J Am Heart Assoc 10:e019052. https://doi.org/10.1161/JAHA.120.019052

Barbato E, Toth GG, Johnson NP, et al (2016). A Prospective Natural History Study of Coronary Atherosclerosis Using Fractional Flow Reserve. J Am Coll Cardiol 68:2247–2255. https://doi.org/10.1016/j.jacc.2016.08.055

Baskaran L, Al'Aref SJ, Maliakal G, et al (2020). Automatic segmentation of multiple cardiovascular structures from cardiac computed tomography angiography images using deep learning. PLOS ONE 15:e0232573. https://doi.org/10.1371/journal.pone.0232573

Berntorp K, Rylance R, Yndigegn T, et al (2023). Clinical Outcome of Revascularization Deferral With Instantaneous Wave-Free Ratio and Fractional Flow Reserve: A 5-Year Follow-Up Substudy From the iFR-SWEDEHEART Trial. J Am Heart Assoc 12:e028423. https://doi.org/10.1161/JAHA.122.028423

Berry C, van 't Veer M, Witt N, et al (2013). VERIFY (VERification of Instantaneous Wave-Free Ratio and Fractional Flow Reserve for the Assessment of Coronary Artery Stenosis Severity in EverydaY Practice): A Multicenter Study in Consecutive Patients. J Am Coll Cardiol 61:1421–1427. https://doi.org/10.1016/j.jacc.2012.09.065

Boden WE, O'Rourke RA, Teo KK, et al (2007). Optimal Medical Therapy with or without PCI for Stable Coronary Disease. N Engl J Med 356:1503–1516. https://doi.org/10.1056/NEJMoa070829

Byrne RA, Rossello X, Coughlan JJ, et al (2023). 2023 ESC Guidelines for the management of acute coronary syndromes: Developed by the task force on the management of acute coronary syndromes of the European Society of Cardiology (ESC). Eur Heart J 44:3720-3826. https://doi.org/10.1093/eurheartj/ehad191

Carin L, Pencina MJ (2018). On Deep Learning for Medical Image Analysis. JAMA 320:1192–1193. https://doi.org/10.1001/jama.2018.13316

Celeng C, Leiner T, Maurovich-Horvat P, et al (2019). Anatomical and Functional Computed Tomography for Diagnosing Hemodynamically Significant Coronary Artery Disease: A Meta-Analysis. JACC Cardiovasc Imaging 12:1316–1325. https://doi.org/10.1016/j.jcmg.2018.07.022

Cerqueira MD, Weissman NJ, Dilsizian V, et al (2002). Standardized myocardial segmentation and nomenclature for tomographic imaging of the heart. A statement for healthcare professionals from the Cardiac Imaging Committee of the Council on Clinical Cardiology of the American Heart Association. Int J Cardiovasc Imaging 18:539–542

Chacko L, P. Howard J, Rajkumar C, et al (2020). Effects of Percutaneous Coronary Intervention on Death and Myocardial Infarction Stratified by Stable and Unstable Coronary Artery Disease. Circ Cardiovasc Qual Outcomes 13:e006363. https://doi.org/10.1161/CIRCOUTCOMES.119.006363

Chaitman BR, Alexander KP, Cyr DD, et al (2021). Myocardial Infarction in the ISCHEMIA Trial. Circulation 143:790–804. https://doi.org/10.1161/CIRCULATIONAHA.120.047987

Chang H-J, Lin FY, Gebow D, et al (2019). Selective Referral Using CCTA Versus Direct Referral for Individuals Referred to Invasive Coronary Angiography for Suspected CAD: A Randomized, Controlled, Open-Label Trial. JACC Cardiovasc Imaging 12:1303–1312. https://doi.org/10.1016/j.jcmg.2018.09.018

Chang H-J, Lin FY, Lee S-E, et al (2018). Coronary Atherosclerotic Precursors of Acute Coronary Syndromes. J Am Coll Cardiol 71:2511–2522. https://doi.org/10.1016/j.jacc.2018.02.079

Chen MY, Rochitte CE, Arbab-Zadeh A, et al (2017). Prognostic Value of Combined CT Angiography and Myocardial Perfusion Imaging versus Invasive Coronary Angiography and Nuclear Stress Perfusion Imaging in the Prediction of Major Adverse Cardiovascular Events: The CORE320 Multicenter Study. Radiology 284:55–65. https://doi.org/10.1148/radiol.2017161565

Chiong J, Ramkumar PG, Weir NW, et al (2023). Evaluating Radiation Exposure in Patients with Stable Chest Pain in the SCOT-HEART Trial. Radiology 308:e221963. https://doi.org/10.1148/radiol.221963

Choi AD, Marques H, Kumar V, et al (2021). CT Evaluation by Artificial Intelligence for Atherosclerosis, Stenosis and Vascular Morphology (CLARIFY): A Multi-center, international study. J Cardiovasc Comput Tomogr 15:470–476. https://doi.org/10.1016/j.jcct.2021.05.004

Chu J, Lin H, Yan W, et al (2022). Angiographic quantitative flow ratio in acute coronary syndrome: beyond a tool to define ischemia-causing stenosis-a literature review. Cardiovasc Diagn Ther 12:892–907. https://doi.org/10.21037/cdt-22-334

Cleerly ISCHEMIA; United States Food and Drug Administration; https://www.accessdata.fda.gov/cdrh_docs/pdf23/K231335.pdf, accessed Dec 22, 2023.

Cleerly LABS, United States Food and Drug Administration; https://www.accessdata.fda.gov/cdrh_docs/pdf19/K190868.pdf, accessed Dec 22, 2023.

Collet C, Onuma Y, Sonck J, et al (2018). Diagnostic performance of angiography-derived fractional flow reserve: a systematic review and Bayesian meta-analysis. Eur Heart J 39:3314–3321. https://doi.org/10.1093/eurheartj/ehy445

Collet J-P, Thiele H, Barbato E, et al (2021). 2020 ESC Guidelines for the management of acute coronary syndromes in patients presenting without persistent ST-segment elevation. Eur Heart J 42:1289–1367. https://doi.org/10.1093/eurheartj/ehaa575

Commandeur F, Goeller M, Razipour A, et al (2019). Fully Automated CT Quantification of Epicardial Adipose Tissue by Deep Learning: A Multicenter Study. Radiol Artif Intell 1:e190045. https://doi.org/10.1148/ryai.2019190045

Cortés C, Carrasco-Moraleja M, Aparisi A, et al (2021). Quantitative flow ratio—Meta-analysis and systematic review. Catheter Cardiovasc Interv 97:807–814. https://doi.org/10.1002/ccd.28857

Curzen N, Nicholas Z, Stuart B, et al (2021). Fractional flow reserve derived from computed tomography coronary angiography in the assessment and management of stable chest pain: the FORECAST randomized trial. Eur Heart J 42:3844–3852. https://doi.org/10.1093/eurheartj/ehab444

Danad I, Raijmakers PG, Appelman YE, et al (2013). Hybrid imaging using quantitative H215O PET and CT-based coronary angiography for the detection of coronary artery disease. J Nucl Med 54:55–63. https://doi.org/10.2967/jnumed.112.104687

Danad I, Raijmakers PG, Driessen RS, et al (2017). Comparison of Coronary CT Angiography, SPECT, PET, and Hybrid Imaging for Diagnosis of Ischemic Heart Disease Determined by Fractional Flow Reserve. JAMA Cardiol 2:1100-1107. https://doi.org/10.1001/jamacardio.2017.2471

Danad I, Szymonifka J, Schulman-Marcus J, Min JK (2016). Static and dynamic assessment of myocardial perfusion by computed tomography. Eur Heart J Cardiovasc Imaging 17:836–844. https://doi.org/10.1093/ehjci/jew044

Danad I, Uusitalo V, Kero T, et al (2014). Quantitative Assessment of Myocardial Perfusion in the Detection of Significant Coronary Artery Disease: Cutoff Values and Diagnostic Accuracy of Quantitative [15O]H2O PET Imaging. J Am Coll Cardiol 64:1464–1475. https://doi.org/10.1016/j.jacc.2014.05.069

D'Antonio A, Assante R, Zampella E, et al (2023). Myocardial blood flow evaluation with dynamic cadmium-zinc-telluride single-photon emission computed tomography: Bright and dark sides. Diagn Interv Imaging 104:323–329. https://doi.org/10.1016/j.diii.2023.02.001

Davies JE, Sen S, Dehbi H-M, et al (2017). Use of the Instantaneous Wave-free Ratio or Fractional Flow Reserve in PCI. N Engl J Med 376:1824–1834. https://doi.org/10.1056/NEJMoa1700445

De Bruyne B, Paulus WJ, Pijls NHJ (1994). Rationale and application of coronary transstenotic pressure gradient measurements. Cathet Cardiovasc Diagn 33:250–261. https://doi.org/10.1002/ccd.1810330312

De Bruyne B, Pijls NHJ, Kalesan B, et al (2012). Fractional Flow Reserve–Guided PCI versus Medical Therapy in Stable Coronary Disease. N Engl J Med 367:991–1001. https://doi.org/10.1056/NEJMoa1205361

Decker JA, O'Doherty J, Schoepf UJ, et al (2023). Stent imaging on a clinical dual-source photon-counting detector CT system—impact of luminal attenuation and sharp kernels on lumen visibility. Eur Radiol 33:2469–2477. https://doi.org/10.1007/s00330-022-09283-4

Del Buono MG, Montone RA, Camilli M, et al (2021). Coronary Microvascular Dysfunction Across the Spectrum of Cardiovascular Diseases. J Am Coll Cardiol 78:1352–1371. https://doi.org/10.1016/j.jacc.2021.07.042

Devineni A, Levine MB, Melaku GD, et al (2022). Diagnostic comparison of automatic and manual TIMI frame-counting-generated quantitative flow ratio (QFR) values. Int J Cardiovasc Imaging 38:1663–1670. https://doi.org/10.1007/s10554-022-02666-0

Dey D, Gaur S, Ovrehus KA, et al (2018). Integrated prediction of lesion-specific ischaemia from quantitative coronary CT angiography using machine learning: a multicentre study. Eur Radiol 28:2655–2664. https://doi.org/10.1007/s00330-017-5223-z

Dey D, Slomka PJ, Leeson P, et al (2019). Artificial Intelligence in Cardiovascular Imaging: JACC State-of-the-Art Review. J Am Coll Cardiol 73:1317–1335. https://doi.org/10.1016/j.jacc.2018.12.054

Diamond GA, Forrester JS (1979). Analysis of Probability as an Aid in the Clinical Diagnosis of Coronary-Artery Disease. N Engl J Med 300:1350–1358. https://doi.org/10.1056/NEJM197906143002402

Diletti R, den Dekker WK, Bennett J, et al (2023). Immediate versus staged complete revascularisation in patients presenting with acute coronary syndrome and multivessel coronary disease (BIOVASC): a prospective, open-label, non-inferiority, randomised trial. The Lancet. https://doi.org/10.1016/S0140-6736(23)00351-3

Ding D, Yang J, Westra J, et al (2019). Accuracy of 3-dimensional and 2-dimensional quantitative coronary angiography for predicting physiological significance of coronary stenosis: a FAVOR II substudy. Cardiovasc Diagn Ther 9:481–491. https://doi.org/10.21037/cdt.2019.09.07

Doucette JW, Corl PD, Payne HM, et al (1992). Validation of a Doppler guide wire for intravascular measurement of coronary artery flow velocity. Circulation 85:1899–1911. https://doi.org/10.1161/01.CIR.85.5.1899

Douglas PS, Hoffmann U, Patel MR, et al (2015). Outcomes of anatomical versus functional testing for coronary artery disease. N Engl J Med 372:1291–1300. https://doi.org/10.1056/NEJMoa1415516

Driessen RS, Danad I, Stuijfzand WJ, et al (2019). Comparison of Coronary Computed Tomography Angiography, Fractional Flow Reserve, and Perfusion Imaging for Ischemia Diagnosis. J Am Coll Cardiol 73:161–173. https://doi.org/10.1016/j.jacc.2018.10.056

Driessen RS, Raijmakers PG, Stuijfzand WJ, Knaapen P (2017). Myocardial perfusion imaging with PET. Int J Cardiovasc Imaging 33:1021–1031. https://doi.org/10.1007/s10554-017-1084-4

Driessen RS, Stuijfzand WJ, Raijmakers PG, et al (2018). Effect of Plaque Burden and Morphology on Myocardial Blood Flow and Fractional Flow Reserve. J Am Coll Cardiol 71:499–509. https://doi.org/10.1016/j.jacc.2017.11.054

Koons E, VanMeter PD, Rajendran K, et al (2022). Improved assessment of coronary artery luminal stenosis with heavy calcifications using high-resolution photon-counting detector CT. Pro SPIE Int Soc Opt Eng 1231:120311A. https:// doi:10.1117/12.2613019

Engstrøm T, Kelbæk H, Helqvist S, et al (2015). Complete revascularisation versus treatment of the culprit lesion only in patients with ST-segment elevation myocardial infarction and multivessel disease (DANAMI-3—PRIMULTI): an open-label, randomised controlled trial. Lancet 386:665–671. https://doi.org/10.1016/S0140-6736(15)60648-1

European Commission (2020). White Paper On Artificial Intelligence - A European approach to excellence and trust. https://commission.europa.eu/publications/white-paper-artificial-intelligence-european-approach-excellence-and-trust_en, accessed Feb 24, 2024.

Fiuza-Luces C, Garatachea N, Berger NA, Lucia A (2013). Exercise is the Real Polypill. Physiology 28:330–358. https://doi.org/10.1152/physiol.00019.2013

Fokkema ML, James SK, Albertsson P, et al (2016). Outcome after percutaneous coronary intervention for different indications: long-term results from the Swedish Coronary Angiography and Angioplasty Registry (SCAAR). EuroIntervention 12:303–311. https://doi.org/10.4244/EIJY15M10_07

Gaemperli O, Maurovich- Horvat P, Nieman K, et al. (2022) EACVI Handbook of Cardiovascular CT. Oxford University Press, ISBN: 9780192884459.

Gaemperli O, Schepis T, Koepfli P, et al (2007). Accuracy of 64-slice CT angiography for the detection of functionally relevant coronary stenoses as assessed with myocardial perfusion SPECT. Eur J Nucl Med Mol Imaging 34:1162–1171. https://doi.org/10.1007/s00259-006-0307-z

Gaemperli O, Schepis T, Valenta I, et al (2008). Functionally relevant coronary artery disease: comparison of 64-section CT angiography with myocardial perfusion SPECT. Radiology 248:414–423. https://doi.org/10.1148/radiol.2482071307

Geleijnse ML, Fioretti PM, Roelandt JRTC (1997). Methodology, Feasibility, Safety and Diagnostic Accuracy of Dobutamine Stress Echocardiography. J Am Coll Cardiol 30:595–606. https://doi.org/10.1016/S0735-1097(97)00206-4

Gershlick AH, Khan JN, Kelly DJ, et al (2015). Randomized trial of complete versus lesion-only revascularization in patients undergoing primary percutaneous coronary intervention for STEMI and multivessel disease: the CvLPRIT trial. J Am Coll Cardiol 65:963–972. https://doi.org/10.1016/j.jacc.2014.12.038

Gimelli A, Achenbach S, Buechel RR, et al (2018). Strategies for radiation dose reduction in nuclear cardiology and cardiac computed tomography imaging: a report from the European Association of Cardiovascular Imaging (EACVI), the Cardiovascular Committee of European Association of Nuclear Medicine (EANM), and the European Society of Cardiovascular Radiology (ESCR). Eur Heart J 39:286–296. https://doi.org/10.1093/eurheartj/ehx582

Glagov S, Weisenberg E, Zarins CK, et al (1987). Compensatory Enlargement of Human Atherosclerotic Coronary Arteries. N Engl J Med 316:1371–1375. https://doi.org/10.1056/NEJM198705283162204

Götberg M, Christiansen EH, Gudmundsdottir IJ, et al (2017). Instantaneous Wave-free Ratio versus Fractional Flow Reserve to Guide PCI. N Engl J Med 376:1813–1823. https://doi.org/10.1056/NEJMoa1616540

Götberg M, Berntorp K, Rylance R, et al (2022). 5-Year Outcomes of PCI Guided by Measurement of Instantaneous Wave-Free Ratio Versus Fractional Flow Reserve. J Am Coll Cardiol 79:965–974. https://doi.org/10.1016/j.jacc.2021.12.030

Gould KL, Kirkeeide RL, Buchi M (1990). Coronary flow reserve as a physiologic measure of stenosis severity. J Am Coll Cardiol 15:459–474. https://doi.org/10.1016/S0735-1097(10)80078-6

Greenwood JP, Herzog BA, Brown JM, et al (2016). Prognostic Value of Cardiovascular Magnetic Resonance and Single-Photon Emission Computed Tomography in Suspected Coronary Heart Disease: Long-Term Follow-up of a Prospective, Diagnostic Accuracy Cohort Study. Ann Intern Med 165:1–9. https://doi.org/10.7326/M15-1801

Griffin WF, Choi AD, Riess JS, et al (2023). AI Evaluation of Stenosis on Coronary CTA, Comparison With Quantitative Coronary Angiography and Fractional Flow Reserve. JACC Cardiovasc Imaging 16:193–205. https://doi.org/10.1016/j.jcmg.2021.10.020

Gueret P, Deux J-F, Bonello L, et al (2013). Diagnostic Performance of Computed Tomography Coronary Angiography (from the Prospective National Multicenter Multivendor EVASCAN Study). Am J Cardiol 111:471–478. https://doi.org/10.1016/j.amjcard.2012.10.029

Gulati M, Levy PD, Mukherjee D, et al (2021). 2021 AHA/ACC/ASE/CHEST/SAEM/SCCT/SCMR Guideline for the Evaluation and Diagnosis of Chest Pain: A Report of the American College of Cardiology/American Heart Association Joint Committee on Clinical Practice Guidelines. Circulation 16:54–122. https://doi.org/10.1161/CIR.0000000000001029

Hachamovitch R, Hayes SW, Friedman JD, et al (2003). Comparison of the short-term survival benefit associated with revascularization compared with medical therapy in patients with no prior coronary artery disease undergoing stress myocardial perfusion single photon emission computed tomography. Circulation 107:2900–2907. https://doi.org/10.1161/01.CIR.0000072790.23090.41

Hachamovitch R, Rozanski A, Shaw LJ, et al (2011). Impact of ischaemia and scar on the therapeutic benefit derived from myocardial revascularization vs. medical therapy among patients undergoing stress-rest myocardial perfusion scintigraphy. Eur Heart J 32:1012–1024. https://doi.org/10.1093/eurheartj/ehq500

Hadamitzky M, Achenbach S, Al-Mallah M, et al (2013). Optimized Prognostic Score for Coronary Computed Tomographic Angiography: Results From the CONFIRM Registry (COronary CT Angiography EvaluatioN For Clinical Outcomes: An InteRnational Multicenter Registry). J Am Coll Cardiol 62:468–476. https://doi.org/10.1016/j.jacc.2013.04.064

Hagar MT, Soschynski M, Saffar R, et al (2023). Accuracy of Ultrahigh-Resolution Photon-counting CT for Detecting Coronary Artery Disease in a High-Risk Population. Radiology 307:e223305. https://doi.org/10.1148/radiol.223305

Hamilton MCK, Charters PFP, Lyen S, et al (2022). Computed tomography-derived fractional flow reserve (FFRCT) has no additional clinical impact over the anatomical Coronary Artery Disease -

Reporting and Data System (CAD-RADS) in real-world elective healthcare of coronary artery disease. Clin Radiol 77:883–890. https://doi.org/10.1016/j.crad.2022.05.031

Hecht HS, Bhatti T (2008). How much calcium is too much calcium for coronary computerized tomographic angiography? J Cardiovasc Comput Tomogr 2:183–187. https://doi.org/10.1016/j.jcct.2008.04.003

Hochman JS, Anthopolos R, Reynolds HR, et al (2023). Survival After Invasive or Conservative Management of Stable Coronary Disease. Circulation 147:8–19. https://doi.org/10.1161/CIRCULATIONAHA.122.062714

Ibanez B, James S, Agewall S, et al (2018). 2017 ESC Guidelines for the management of acute myocardial infarction in patients presenting with ST-segment elevation. Eur Heart J 39:119–177. https://doi.org/10.1093/eurheartj/ehx393

Ihdayhid AR, Norgaard BL, Gaur S, et al (2019). Prognostic Value and Risk Continuum of Noninvasive Fractional Flow Reserve Derived from Coronary CT Angiography. Radiology 292:343–351. https://doi.org/10.1148/radiol.2019182264

Huang J-Y, Huang CK, Yen R-F, et al (2016). Diagnostic Performance of Attenuation-Corrected Myocardial Perfusion Imaging for Coronary Artery Disease: A Systematic Review and Meta-Analysis. J Nucl Med 57:1893. https://doi.org/10.2967/jnumed.115.171462

Johnson NP, Tóth GG, Lai D, et al (2014). Prognostic Value of Fractional Flow Reserve. J Am Coll Cardiol 64:1641–1654. https://doi.org/10.1016/j.jacc.2014.07.973

Juárez-Orozco LE, Tio RA, Alexanderson E, et al (2018). Quantitative myocardial perfusion evaluation with positron emission tomography and the risk of cardiovascular events in patients with coronary artery disease: a systematic review of prognostic studies. Eur Heart J Cardiovasc Imaging 19:1179–1187. https://doi.org/10.1093/ehjci/jex331

Juarez-Orozco LE, Saraste A, Capodanno D, et al (2019). Impact of a decreasing pre-test probability on the performance of diagnostic tests for coronary artery disease. Eur Heart J Cardiovasc Imaging 20:1198–1207. https://doi.org/10.1093/ehjci/jez054

Juarez-Orozco LE, Knol RJJ, Sanchez-Catasus CA, et al (2020). Machine learning in the integration of simple variables for identifying patients with myocardial ischemia. J Nucl Cardiol 27:147–155. https://doi.org/10.1007/s12350-018-1304-x

Kajander S, Joutsiniemi E, Saraste M, et al (2010). Cardiac Positron Emission Tomography/Computed Tomography Imaging Accurately Detects Anatomically and Functionally Significant Coronary Artery Disease. Circulation 122:603–613. https://doi.org/10.1161/CIRCULATIONAHA.109.915009

Kivimäki M, Steptoe A (2018). Effects of stress on the development and progression of cardiovascular disease. Nat Rev Cardiol 15:215–229. https://doi.org/10.1038/nrcardio.2017.189

Klopp EH, Gott VL (1975). A Simple Model of the Hemodynamic Effects of a Proximal Coronary Artery Narrowing. Ann Thorac Surg 19:309–312. https://doi.org/10.1016/S0003-4975(10)64022-2

Knuuti J, Ballo H, Juarez-Orozco LE, et al (2018). The performance of non-invasive tests to rule-in and rule-out significant coronary artery stenosis in patients with stable angina: a meta-analysis focused on post-test disease probability. Eur Heart J 39:3322–3330. https://doi.org/10.1093/eurheartj/ehy267

Knuuti J, Wijns W, Saraste A, et al (2020). 2019 ESC Guidelines for the diagnosis and management of chronic coronary syndromes. Eur Heart J 41:407–477. https://doi.org/10.1093/eurheartj/ehz425

Lauri F, Macaya F, Mejía-Rentería H, et al (2020). Angiography-derived functional assessment of non-culprit coronary stenoses during primary percutaneous coronary intervention for ST-elevation myocardial infarction. EuroIntervention 15:e1594-e1601. https://doi.org/10.4244/EIJ-D-18-01165

Layland J, Oldroyd KG, Curzen N, et al (2015). Fractional flow reserve vs. angiography in guiding management to optimize outcomes in non-ST-segment elevation myocardial infarction: the British Heart Foundation FAMOUS-NSTEMI randomized trial. Eur Heart J 36:100–111. https://doi.org/10.1093/eurheartj/ehu338

Lee J-G, Jun S, Cho Y-W, et al (2017). Deep Learning in Medical Imaging: General Overview. Korean J Radiol 18:570–584. https://doi.org/10.3348/kjr.2017.18.4.570

Lee JM, Kim HK, Park KH, et al (2023). Fractional flow reserve versus angiography-guided strategy in acute myocardial infarction with multivessel disease: a randomized trial. Eur Heart J 44:473–484. https://doi.org/10.1093/eurheartj/ehac763

Leipsic J, Abbara S, Achenbach S, et al (2014). SCCT guidelines for the interpretation and reporting of coronary CT angiography: A report of the Society of Cardiovascular Computed Tomography Guidelines Committee. J Cardiovasc Comput Tomogr 8:342–358. https://doi.org/10.1016/j.jcct.2014.07.003

Leng S, Bruesewitz M, Tao S, et al (2019). Photon-counting Detector CT: System Design and Clinical Applications of an Emerging Technology. RadioGraphics 39:729–743. https://doi.org/10.1148/rg.2019180115

Libby P (2013). Mechanisms of Acute Coronary Syndromes and Their Implications for Therapy. N Engl J Med 368:2004–2013. https://doi.org/10.1056/NEJMra1216063

Libby P, Ridker PM, Maseri A (2002). Inflammation and Atherosclerosis. Circulation 105:1135–1143. https://doi.org/10.1161/hc0902.104353

Libby P, Theroux P (2005). Pathophysiology of Coronary Artery Disease. Circulation 111:3481–3488. https://doi.org/10.1161/CIRCULATIONAHA.105.537878

Liga R, Vontobel J, Rovai D, et al (2016). Multicentre multi-device hybrid imaging study of coronary artery disease: results from the EValuation of INtegrated Cardiac Imaging for the Detection and Characterization of Ischaemic Heart Disease (EVINCI) hybrid imaging population. Eur Heart J Cardiovasc Imaging 17:951–960. https://doi.org/10.1093/ehjci/jew038

Lin A, van Diemen PA, Motwani M, et al (2022). Machine Learning From Quantitative Coronary Computed Tomography Angiography Predicts Fractional Flow Reserve-Defined Ischemia and Impaired Myocardial Blood Flow. Circ Cardiovasc Imaging 15:e014369. https://doi.org/10.1161/CIRCIMAGING.122.014369

Lipinski MJ, McVey CM, Berger JS, et al (2013). Prognostic Value of Stress Cardiac Magnetic Resonance Imaging in Patients With Known or Suspected Coronary Artery Disease: A Systematic Review and Meta-Analysis. J Am Coll Cardiol 62:826–838. https://doi.org/10.1016/j.jacc.2013.03.080

Lipkin I, Telluri A, Kim Y, et al (2022). Coronary CTA With AI-QCT Interpretation: Comparison With Myocardial Perfusion Imaging for Detection of Obstructive Stenosis Using Invasive Angiography as Reference Standard. AJR Am J Roentgenol 219:407–419. https://doi.org/10.2214/AJR.21.27289

Peters MJL, Symmons DPM, McCarey D, et al (2010). EULAR evidence-based recommendations for cardiovascular risk management in patients with rheumatoid arthritis and other forms of inflammatory arthritis. Ann Rheum Dis 69:325. https://doi.org/10.1136/ard.2009.113696

Maaniitty T, Stenström I, Bax JJ, et al (2017). Prognostic Value of Coronary CT Angiography With Selective PET Perfusion Imaging in Coronary Artery Disease. JACC Cardiovasc Imaging 10:1361–1370. https://doi.org/10.1016/j.jcmg.2016.10.025

Maaniitty T, Bär S, Nabeta T, et al (2023). Prognostic Value Of A Novel Artificial Intelligence-based CCTA-derived Ischemia Algorithm In Patients With Suspected Coronary Artery Disease: Comparison Against Hybrid CCTA/PET Perfusion Imaging. J Cardiovasc Comput Tomogr 17:S2. https://doi.org/10.1016/j.jcct.2023.05.010

Magro M, Nauta S, Simsek C, et al (2011). Value of the SYNTAX score in patients treated by primary percutaneous coronary intervention for acute ST-elevation myocardial infarction: The MI SYNTAXscore study. Am Heart J 161:771–781. https://doi.org/10.1016/j.ahj.2011.01.004

Magro M, Räber L, Heg D, et al (2014). The MI SYNTAX score for risk stratification in patients undergoing primary percutaneous coronary intervention for treatment of acute myocardial infarction: A substudy of the COMFORTABLE AMI trial. Int J Cardiol 175:314–322. https://doi.org/10.1016/j.ijcard.2014.05.029

Mannil M, von Spiczak J, Manka R, Alkadhi H (2018). Texture Analysis and Machine Learning for Detecting Myocardial Infarction in Noncontrast Low-Dose Computed Tomography: Unveiling the Invisible. Invest Radiol 53:338-343.

Maron DJ, Hochman JS, Reynolds HR, et al (2020). Initial Invasive or Conservative Strategy for Stable Coronary Disease. N Engl J Med 382:1395–1407. https://doi.org/10.1056/NEJMoa1915922

Mayr A, Binder H, Gefeller O, Schmid M (2014). The Evolution of Boosting Algorithms: From Machine Learning to Statistical Modelling. Methods Inf Med 53:419–427. https://doi.org/10.3414/ME13-01-0122

Medina A, Suárez de Lezo J, Pan M (2006). Una clasificación simple de las lesiones coronarias en bifurcación. Rev Esp Cardiol Engl Ed 59:183. https://doi.org/10.1157/13084649

Mehta SR, McGrath BP (2023). Anatomy vs. physiology: how should we achieve complete revascularization in acute coronary syndromes? Eur Heart J 44:485–487. https://doi.org/10.1093/eurheartj/ehac786

Mehta SR, Wood DA, Storey RF, et al (2019). Complete Revascularization with Multivessel PCI for Myocardial Infarction. N Engl J Med 381:1411–1421. https://doi.org/10.1056/NEJMoa1907775

Meijboom WB, Van Mieghem CAG, van Pelt N, et al (2008). Comprehensive Assessment of Coronary Artery Stenoses. J Am Coll Cardiol 52:636–643. https://doi.org/10.1016/j.jacc.2008.05.024

Metz LD, Beattie M, Hom R, et al (2007). The Prognostic Value of Normal Exercise Myocardial Perfusion Imaging and Exercise Echocardiography: A Meta-Analysis. J Am Coll Cardiol 49:227–237. https://doi.org/10.1016/j.jacc.2006.08.048

Min JK, Dunning A, Lin FY, et al (2011). Age- and Sex-Related Differences in All-Cause Mortality Risk Based on Coronary Computed Tomography Angiography Findings: Results From the International Multicenter CONFIRM (Coronary CT Angiography Evaluation for Clinical Outcomes: An International Multicenter Registry) of 23,854 Patients Without Known Coronary Artery Disease. J Am Coll Cardiol 58:849–860. https://doi.org/10.1016/j.jacc.2011.02.074

Min JK, Taylor CA, Achenbach S, et al (2015). Noninvasive Fractional Flow Reserve Derived From Coronary CT Angiography: Clinical Data and Scientific Principles. JACC Cardiovasc Imaging 8:1209–1222. https://doi.org/10.1016/j.jcmg.2015.08.006

Mittal TK, Hothi SS, Venugopal V, et al (2023). The Use and Efficacy of FFR-CT: Real-World Multicenter Audit of Clinical Data With Cost Analysis. JACC Cardiovasc Imaging. https://doi.org/10.1016/j.jcmg.2023.02.005

Molinaro AM, Simon R, Pfeiffer RM (2005). Prediction error estimation: a comparison of resampling methods. Bioinforma Oxf Engl 21:3301–3307. https://doi.org/10.1093/bioinformatics/bti499

Morris PD, Ryan D, Morton AC, et al (2013). Virtual Fractional Flow Reserve From Coronary Angiography: Modeling the Significance of Coronary Lesions: Results From the VIRTU-1 (VIRTUal Fractional Flow Reserve From Coronary Angiography) Study. JACC Cardiovasc Interv 6:149–157. https://doi.org/10.1016/j.jcin.2012.08.024

Mortensen MB, Dzaye O, Steffensen FH, et al (2020). Impact of Plaque Burden Versus Stenosis on Ischemic Events in Patients With Coronary Atherosclerosis. J Am Coll Cardiol 76:2803–2813. https://doi.org/10.1016/j.jacc.2020.10.021

Moschovitis A, Yamaji K, Taniwaki M, et al (2019). Five-year clinical outcomes and intracoronary imaging findings of the COMFORTABLE AMI trial: randomized comparison of biodegradable polymer-based biolimus-eluting stents with bare-metal stents in patients with acute ST-segment elevation myocardial infarction. Eur Heart J 40:1909-1919. https://doi.org/10.1093/eurheartj/ehz074

Nabeta T, Bär S, Maaniitty T, et al (2023). Incremental value of a CCTA-derived AI-based ischemia algorithm over standard CCTA interpretation for coronary ischemia in patients with suspected coronary artery disease. Eur Heart J 44:ehad655.149. https://doi.org/10.1093/eurheartj/ehad655.149

Nakamura S, Kitagawa K, Goto Y, et al (2020). Prognostic Value of Stress Dynamic Computed Tomography Perfusion With Computed Tomography Delayed Enhancement. JACC Cardiovasc Imaging 13:1721–1734. https://doi.org/10.1016/j.jcmg.2019.12.017

Narula J, Chandrashekhar Y, Ahmadi A, et al (2021). SCCT 2021 Expert Consensus Document on Coronary Computed Tomographic Angiography: A Report of the Society of Cardiovascular

Computed Tomography. J Cardiovasc Comput Tomogr 15:192–217. https://doi.org/10.1016/j.jcct.2020.11.001

National Institute for Health and Care Excellence. HeartFlow FFRCT for estimating fractional flow reserve from coronary CT angiography. February 13, 2017. Updated May 19, 2021. Accessed Jun 15, 2023.

Navarese EP, Lansky AJ, Kereiakes DJ, et al (2021). Cardiac mortality in patients randomised to elective coronary revascularisation plus medical therapy or medical therapy alone: a systematic review and meta-analysis. Eur Heart J 42:4638–4651. https://doi.org/10.1093/eurheartj/ehab246

Neumann F-J, Sousa-Uva M, Ahlsson A, et al (2019). 2018 ESC/EACTS Guidelines on myocardial revascularization. Eur Heart J 40:87–165. https://doi.org/10.1093/eurheartj/ehy394

Nerlekar N, Ha FJ, Cheshire C, et al (2018). Computed Tomographic Coronary Angiography–Derived Plaque Characteristics Predict Major Adverse Cardiovascular Events. Circ Cardiovasc Imaging 11:e006973. https://doi.org/10.1161/CIRCIMAGING.117.006973

Nielsen LH, Bøtker HE, Sørensen HT, et al (2017). Prognostic assessment of stable coronary artery disease as determined by coronary computed tomography angiography: a Danish multicentre cohort study. Eur Heart J 38:413–421. https://doi.org/10.1093/eurheartj/ehw548

Nishina H, Slomka PJ, Abidov A, et al (2006). Combined Supine and Prone Quantitative Myocardial Perfusion SPECT: Method Development and Clinical Validation in Patients with No Known Coronary Artery Disease. J Nucl Med 47:51-58.

Nørgaard BL, Leipsic J, Gaur S, et al (2014). Diagnostic performance of noninvasive fractional flow reserve derived from coronary computed tomography angiography in suspected coronary artery disease: the NXT trial (Analysis of Coronary Blood Flow Using CT Angiography: Next Steps). J Am Coll Cardiol 63:1145–1155. https://doi.org/10.1016/j.jacc.2013.11.043

Nørgaard BL, Terkelsen CJ, Mathiassen ON, et al (2018). Coronary CT Angiographic and Flow Reserve-Guided Management of Patients With Stable Ischemic Heart Disease. J Am Coll Cardiol 72:2123–2134. https://doi.org/10.1016/j.jacc.2018.07.043

Ntalianis A, Sels J-W, Davidavicius G, et al (2010). Fractional flow reserve for the assessment of nonculprit coronary artery stenoses in patients with acute myocardial infarction. JACC Cardiovasc Interv 3:1274–1281. https://doi.org/10.1016/j.jcin.2010.08.025

Nurmohamed NS, Bom MJ, Jukema RA, et al (2023). AI-Guided Quantitative Plaque Staging Predicts Long-Term Cardiovascular Outcomes in Patients at Risk for Atherosclerotic CVD. JACC Cardiovasc Imaging. https://doi.org/10.1016/j.jcmg.2023.05.020

Nurmohamed NS, Danad I, Jukema RA, et al (2024a). Development and validation of a quantitative coronary CT angiography model for diagnosis of vessel-specific coronary ischemia. JACC Cardiovasc Imaging Feb 19:S1936-878X(24)00039-1, [ePub ahead of print], https://doi.org/10.1016/j.jcmg.2024.01.007

Nurmohamed NS, Cole JH, Budoff MJ, et al (2024b). Impact of atherosclerosis imaging-quantitative computed tomography on diagnostic certainty, downstream testing, coronary revascularization, and medical therapy: the CERTAIN study. Eur Heart J Cardiovasc Imaging Jan 25;jeae029, [ePub ahead of print], https://doi.org/10.1093/ehjci/jeae029

Otsuka T, Bär S, Losdat S, et al (2021). Effect of Timing of Staged Percutaneous Coronary Intervention on Clinical Outcomes in Patients With Acute Coronary Syndromes. J Am Heart Assoc 10:e023129. https://doi.org/10.1161/JAHA.121.023129

Park D-W, Clare RM, Schulte PJ, et al (2014). Extent, Location, and Clinical Significance of Non–Infarct-Related Coronary Artery Disease Among Patients With ST-Elevation Myocardial Infarction. JAMA 312:2019. https://doi.org/10.1001/jama.2014.15095

Park S-J, Kang S-J, Ahn J-M, et al (2012). Visual-Functional Mismatch Between Coronary Angiography and Fractional Flow Reserve. JACC Cardiovasc Interv 5:1029–1036. https://doi.org/10.1016/j.jcin.2012.07.007

Patel MR, Nørgaard BL, Fairbairn TA, et al (2020). 1-Year Impact on Medical Practice and Clinical Outcomes of FFRCT: The ADVANCE Registry. JACC Cardiovasc Imaging 13:97–105. https://doi.org/10.1016/j.jcmg.2019.03.003

Patel MR, Peterson ED, Dai D, et al (2010). Low Diagnostic Yield of Elective Coronary Angiography. N Engl J Med 362:886–895. https://doi.org/10.1056/NEJMoa0907272

Pazhenkottil AP, Benz DC, Gräni C, et al (2018). Hybrid SPECT Perfusion Imaging and Coronary CT Angiography: Long-term Prognostic Value for Cardiovascular Outcomes. Radiology 288:694–702. https://doi.org/10.1148/radiol.2018171303

Petraco R, Escaned J, Sen S, et al (2013). Classification performance of instantaneous wave-free ratio (iFR) and fractional flow reserve in a clinical population of intermediate coronary stenoses: results of the ADVISE registry. EuroIntervention 9:91–101. https://doi.org/10.4244/EIJV9I1A14

Picano E (1992). Stress echocardiography. From pathophysiological toy to diagnostic tool. Circulation 85:1604–1612. https://doi.org/10.1161/01.CIR.85.4.1604

Picano E, Molinaro S, Pasanisi E (2008). The diagnostic accuracy of pharmacological stress echocardiography for the assessment of coronary artery disease: a meta-analysis. Cardiovasc Ultrasound 6:30. https://doi.org/10.1186/1476-7120-6-30

Pijls NH, De Bruyne B, Peels K, et al (1996). Measurement of fractional flow reserve to assess the functional severity of coronary-artery stenoses. N Engl J Med 334:1703–1708. https://doi.org/10.1056/NEJM199606273342604

Pijls NH, van Son JA, Kirkeeide RL, et al (1993). Experimental basis of determining maximum coronary, myocardial, and collateral blood flow by pressure measurements for assessing functional stenosis severity before and after percutaneous transluminal coronary angioplasty. Circulation 87:1354–1367. https://doi.org/10.1161/01.CIR.87.4.1354

Pijls NHJ, Fearon WF, Tonino PAL, et al (2010). Fractional Flow Reserve Versus Angiography for Guiding Percutaneous Coronary Intervention in Patients With Multivessel Coronary Artery Disease: 2-Year Follow-Up of the FAME (Fractional Flow Reserve Versus Angiography for Multivessel Evaluation) Study. J Am Coll Cardiol 56:177–184. https://doi.org/10.1016/j.jacc.2010.04.012

Pijls NHJ, Tonino PAL (2011). The crux of maximum hyperemia: the last remaining barrier for routine use of fractional flow reserve. JACC Cardiovasc Interv 4:1093–1095. https://doi.org/10.1016/j.jcin.2011.08.007

Pijls NHJ, Van Gelder B, Van der Voort P, et al (1995). Fractional Flow Reserve. Circulation 92:3183–3193. https://doi.org/10.1161/01.CIR.92.11.3183

Pijls NHJ, Van ‘t Veer M, Oldroyd KG, et al (2012). Instantaneous Wave-Free Ratio or Fractional Flow Reserve Without Hyperemia: Novelty or Nonsense? J Am Coll Cardiol 59:1916–1917. https://doi.org/10.1016/j.jacc.2012.01.049

Piróth Z, Boxma-de Klerk BM, Omerovic E, et al (2020). The Natural History of Nonculprit Lesions in STEMI. JACC Cardiovasc Interv 13:954–961. https://doi.org/10.1016/j.jcin.2020.02.015

Pontone G, Rossi A, Guglielmo M, et al (2022a). Clinical applications of cardiac computed tomography: a consensus paper of the European Association of Cardiovascular Imaging—part I. Eur Heart J Cardiovasc Imaging 23:299–314. https://doi.org/10.1093/ehjci/jeab293

Pontone G, Rossi A, Guglielmo M, et al (2022b). Clinical applications of cardiac computed tomography: a consensus paper of the European Association of Cardiovascular Imaging—part II. Eur Heart J Cardiovasc Imaging 23:e136–e161. https://doi.org/10.1093/ehjci/jeab292

Puymirat E, Cayla G, Simon T, et al (2021). Multivessel PCI Guided by FFR or Angiography for Myocardial Infarction. N Engl J Med 385:297–308. https://doi.org/10.1056/NEJMoa2104650

Räber L, Kelbaek H, Ostoijc M, et al (2012a). Comparison of biolimus eluted from an erodible stent coating with bare metal stents in acute ST-elevation myocardial infarction (COMFORTABLE AMI trial): rationale and design. EuroIntervention 7:1435–1443. https://doi.org/10.4244/EIJV7I12A224

Räber L, Kelbæk H, Ostojic M, et al (2012b). Effect of Biolimus-Eluting Stents With Biodegradable Polymer vs Bare-Metal Stents on Cardiovascular Events Among Patients With Acute Myocardial Infarction: The COMFORTABLE AMI Randomized TrialBiolimus-Eluting Stents vs Bare-Metal Stents. JAMA 308:777–787. https://doi.org/10.1001/jama.2012.10065

Räber L, Kelbæk H, Taniwaki M, et al (2014). Biolimus-Eluting Stents With Biodegradable Polymer Versus Bare-Metal Stents in Acute Myocardial Infarction. Circ Cardiovasc Interv 7:355–364. https://doi.org/10.1161/CIRCINTERVENTIONS.113.001440

Rajiah PS, François CJ, Leiner T (2023). Cardiac MRI: State of the Art. Radiology 307:e223008. https://doi.org/10.1148/radiol.223008

Rajkumar CA, Foley MJ, Ahmed-Jushuf F, et al (2023). A Placebo-Controlled Trial of Percutaneous Coronary Intervention for Stable Angina. N Engl J Med 389:2319-2330. https://doi.org/10.1056/NEJMoa2310610

Rasmussen LD, Schmidt SE, Knuuti J, et al (2023). Exercise electrocardiography for pre-test assessment of the likelihood of coronary artery disease. Heart heartjnl-2023-322970. https://doi.org/10.1136/heartjnl-2023-322970

Rathod KS, Koganti S, Jain AK, et al (2018). Complete Versus Culprit-Only Lesion Intervention in Patients With Acute Coronary Syndromes. J Am Coll Cardiol 72:1989–1999. https://doi.org/10.1016/j.jacc.2018.07.089

Jonas R, Earls JP, Marques H, et al (2021). Relationship of age, atherosclerosis and angiographic stenosis using artificial intelligence. Open Heart 8:e001832. https://doi.org/10.1136/openhrt-2021-001832

Reeves RA, Halpern EJ, Rao VM (2021). Cardiac Imaging Trends from 2010 to 2019 in the Medicare Population. Radiol Cardiothorac Imaging 3:e210156. https://doi.org/10.1148/ryct.2021210156

Reynolds HR, Shaw LJ, Min JK, et al (2021). Outcomes in the ISCHEMIA Trial Based on Coronary Artery Disease and Ischemia Severity. Circulation 144:1024–1038. https://doi.org/10.1161/CIRCULATIONAHA.120.049755

Roffi M, Patrono C, Collet J-P, et al (2016). 2015 ESC Guidelines for the management of acute coronary syndromes in patients presenting without persistent ST-segment elevation: Task Force for the Management of Acute Coronary Syndromes in Patients Presenting without Persistent ST-Segment Elevation of the European Society of Cardiology (ESC). Eur Heart J 37:267–315. https://doi.org/10.1093/eurheartj/ehv320

Russel SJ (2003). Artificial intelligence: a modern approach. Upper Saddle River, New Jersey: Prentice Hall. ISBN:0130803022.

Ryan TJ, Faxon DP, Gunnar RM, et al (1988). Guidelines for percutaneous transluminal coronary angioplasty. A report of the American College of Cardiology/American Heart Association Task Force on Assessment of Diagnostic and Therapeutic Cardiovascular Procedures (Subcommittee on Percutaneous Transluminal Coronary Angioplasty). Circulation 78:486–502. https://doi.org/10.1161/01.CIR.78.2.486

Darby S, McGale P, Peto R, et al (2003). Mortality from cardiovascular disease more than 10 years after radiotherapy for breast cancer: nationwide cohort study of 90 000 Swedish women. BMJ 326:256. https://doi.org/10.1136/bmj.326.7383.256

Sardella G, Lucisano L, Garbo R, et al (2016). Single-Staged Compared With Multi-Staged PCI in Multivessel NSTEMI Patients: The SMILE Trial. J Am Coll Cardiol 67:264–272. https://doi.org/10.1016/j.jacc.2015.10.082

Sciagrà R, Lubberink M, Hyafil F, et al (2021). EANM procedural guidelines for PET/CT quantitative myocardial perfusion imaging. Eur J Nucl Med Mol Imaging 48:1040–1069. https://doi.org/10.1007/s00259-020-05046-9

SCOT-HEART investigators (2015). CT coronary angiography in patients with suspected angina due to coronary heart disease (SCOT-HEART): an open-label, parallel-group, multicentre trial. Lancet 385:2383–2391. https://doi.org/10.1016/S0140-6736(15)60291-4

Sels J-WEM, Tonino PAL, Siebert U, et al (2011). Fractional flow reserve in unstable angina and non-ST-segment elevation myocardial infarction experience from the FAME (Fractional flow reserve versus Angiography for Multivessel Evaluation) study. JACC Cardiovasc Interv 4:1183–1189. https://doi.org/10.1016/j.jcin.2011.08.008

Sen S, Escaned J, Malik IS, et al (2012). Development and validation of a new adenosine-independent index of stenosis severity from coronary wave-intensity analysis: results of the ADVISE (ADenosine Vasodilator Independent Stenosis Evaluation) study. J Am Coll Cardiol 59:1392–1402. https://doi.org/10.1016/j.jacc.2011.11.003

Serruys PW, Kotoku N, Nørgaard BL, et al (2023). Computed tomographic angiography in coronary artery disease. EuroIntervention 18:e1307–e1327. https://doi.org/10.4244/EIJ-D-22-00776

Sicari R, Nihoyannopoulos P, Evangelista A, et al (2009). Stress Echocardiography Expert Consensus Statement—Executive Summary: European Association of Echocardiography (EAE) (a registered branch of the ESC). Eur Heart J 30:278–289. https://doi.org/10.1093/eurheartj/ehn492

Siebert VR, Borgaonkar S, Jia X, et al (2019). Meta-analysis Comparing Multivessel Versus Culprit Coronary Arterial Revascularization for Patients With Non-ST-Segment Elevation Acute Coronary Syndromes. Am J Cardiol 124:1501–1511. https://doi.org/10.1016/j.amjcard.2019.07.071

Slart RHJA, Williams MC, Juarez-Orozco LE, et al (2021). Position paper of the EACVI and EANM on artificial intelligence applications in multimodality cardiovascular imaging using SPECT/CT, PET/CT, and cardiac CT. Eur J Nucl Med Mol Imaging 48:1399–1413. https://doi.org/10.1007/s00259-021-05341-z

Smits PC, Abdel-Wahab M, Neumann F-J, et al (2017). Fractional Flow Reserve–Guided Multivessel Angioplasty in Myocardial Infarction. N Engl J Med 376:1234–1244. https://doi.org/10.1056/NEJMoa1701067

Song Lei, Xu Bo, Tu Shengxian, et al (2022). 2-Year Outcomes of Angiographic Quantitative Flow Ratio-Guided Coronary Interventions. J Am Coll Cardiol 80:2089–2101. https://doi.org/10.1016/j.jacc.2022.09.007

Sorajja P, Gersh BJ, Cox DA, et al (2007). Impact of multivessel disease on reperfusion success and clinical outcomes in patients undergoing primary percutaneous coronary intervention for acute myocardial infarction. Eur Heart J 28:1709–1716. https://doi.org/10.1093/eurheartj/ehm184

Spertus JA, Jones PG, Maron DJ, et al (2020). Health-Status Outcomes with Invasive or Conservative Care in Coronary Disease. N Engl J Med 382:1408–1419. https://doi.org/10.1056/NEJMoa1916370

Spitaleri G, Tebaldi M, Biscaglia S, et al (2018). Quantitative Flow Ratio Identifies Nonculprit Coronary Lesions Requiring Revascularization in Patients With ST-Segment–Elevation Myocardial Infarction and Multivessel Disease. Circ Cardiovasc Interv 11:e006023. https://doi.org/10.1161/CIRCINTERVENTIONS.117.006023

Stähli BE, Varbella F, Linke A, et al (2023). Timing of Complete Revascularization with Multivessel PCI for Myocardial Infarction. N Engl J Med 389:1368-1379. https://doi.org/10.1056/NEJMoa2307823

Stein T, Rau A, Russe MF, et al (2023). Photon-Counting Computed Tomography – Basic Principles, Potenzial Benefits, and Initial Clinical Experience. RöFo - Fortschritte Auf Dem Geb Röntgenstrahlen Bildgeb Verfahr 195:691–698. https://doi.org/10.1055/a-2018-3396

Stenström I, Maaniitty T, Uusitalo V, et al (2017). Frequency and angiographic characteristics of coronary microvascular dysfunction in stable angina: a hybrid imaging study. Eur Heart J Cardiovasc Imaging 18:1206–1213. https://doi.org/10.1093/ehjci/jex193

Stenström I, Maaniitty T, Uusitalo V, et al (2019). Absolute Stress Myocardial Blood Flow After Coronary CT Angiography Guides Referral to Invasive Angiography. JACC Cardiovasc Imaging 12:2266–2267. https://doi.org/10.1016/j.jcmg.2019.08.002

Stone GW, Maehara A, Lansky AJ, et al (2011). A Prospective Natural-History Study of Coronary Atherosclerosis. N Engl J Med 364:226–235. https://doi.org/10.1056/NEJMoa1002358

Stuijfzand WJ, van Rosendael AR, Lin FY, et al (2020). Stress Myocardial Perfusion Imaging vs Coronary Computed Tomographic Angiography for Diagnosis of Invasive Vessel-Specific Coronary Physiology: Predictive Modeling Results From the Computed Tomographic Evaluation of Atherosclerotic Determinants of Myocardial Ischemia (CREDENCE) Trial. JAMA Cardiol 5:1338–1348. https://doi.org/10.1001/jamacardio.2020.3409

Szolovits P (1988). Artificial Intelligence in Medical Diagnosis. Ann Intern Med 108:80. https://doi.org/10.7326/0003-4819-108-1-80

Taylor CA, Fonte TA, Min JK (2013). Computational Fluid Dynamics Applied to Cardiac Computed Tomography for Noninvasive Quantification of Fractional Flow Reserve. J Am Coll Cardiol 61:2233–2241. https://doi.org/10.1016/j.jacc.2012.11.083

Maurovich-Horvat P, Bosserdt M, Kofoed KF, et al (2022). CT or Invasive Coronary Angiography in Stable Chest Pain. N Engl J Med 386:1591–1602. https://doi.org/10.1056/NEJMoa2200963

The SCOT-HEART Investigators (2018). Coronary CT Angiography and 5-Year Risk of Myocardial Infarction. N Engl J Med 379:924–933. https://doi.org/10.1056/NEJMoa1805971

Thomsen C, Abdulla J (2016). Characteristics of high-risk coronary plaques identified by computed tomographic angiography and associated prognosis: a systematic review and meta-analysis. Eur Heart J Cardiovasc Imaging 17:120–129. https://doi.org/10.1093/ehjci/jev325

Thygesen K, Alpert JS, Jaffe AS, et al (2019). Fourth universal definition of myocardial infarction (2018). Eur Heart J 40:237–269. https://doi.org/10.1093/eurheartj/ehy462

Timmis A, Vardas P, Townsend N, et al (2022). European Society of Cardiology: cardiovascular disease statistics 2021. Eur Heart J 43:716–799. https://doi.org/10.1093/eurheartj/ehab892

Tonino PAL, De Bruyne B, Pijls NHJ, et al (2009). Fractional Flow Reserve versus Angiography for Guiding Percutaneous Coronary Intervention. N Engl J Med 360:213–224. https://doi.org/10.1056/NEJMoa0807611

Tonino PAL, Fearon WF, De Bruyne B, et al (2010). Angiographic versus functional severity of coronary artery stenoses in the FAME study fractional flow reserve versus angiography in multivessel evaluation. J Am Coll Cardiol 55:2816–2821. https://doi.org/10.1016/j.jacc.2009.11.096

Tu S, Barbato E, Köszegi Z, et al (2014). Fractional Flow Reserve Calculation From 3-Dimensional Quantitative Coronary Angiography and TIMI Frame Count. JACC Cardiovasc Interv 7:768–777. https://doi.org/10.1016/j.jcin.2014.03.004

Tu S, Westra J, Yang J, et al (2016). Diagnostic Accuracy of Fast Computational Approaches to Derive Fractional Flow Reserve From Diagnostic Coronary Angiography: The International Multicenter FAVOR Pilot Study. JACC Cardiovasc Interv 9:2024–2035. https://doi.org/10.1016/j.jcin.2016.07.013

Ueki Y, Kuwahara K (2023). Periprocedural myocardial infarction in patients undergoing percutaneous coronary intervention. J Cardiol 81:364–372. https://doi.org/10.1016/j.jjcc.2022.11.005

Valdiviezo C, Ambrose M, Mehra V, et al (2010). Quantitative and qualitative analysis and interpretation of CT perfusion imaging. J Nucl Cardiol 17:1091–1100. https://doi.org/10.1007/s12350-010-9291-6

van Assen M, De Cecco CN, Eid M, et al (2019). Prognostic value of CT myocardial perfusion imaging and CT-derived fractional flow reserve for major adverse cardiac events in patients with coronary artery disease. J Cardiovasc Comput Tomogr 13:26–33. https://doi.org/10.1016/j.jcct.2019.02.005

van Assen M, Muscogiuri G, Caruso D, et al (2020). Artificial intelligence in cardiac radiology. Radiol Med 125:1186–1199. https://doi.org/10.1007/s11547-020-01277-w

van der Hoeven NW, Janssens GN, de Waard GA, et al (2019). Temporal Changes in Coronary Hyperemic and Resting Hemodynamic Indices in Nonculprit Vessels of Patients With ST-Segment Elevation Myocardial Infarction. JAMA Cardiol 4:736–744. https://doi.org/10.1001/jamacardio.2019.2138

van Nunen LX, Zimmermann FM, Tonino PAL, et al (2015). Fractional flow reserve versus angiography for guidance of PCI in patients with multivessel coronary artery disease (FAME): 5-year follow-up of a randomised controlled trial. Lancet 386:1853–1860. https://doi.org/10.1016/S0140-6736(15)00057-4

Veltman CE, de Wit-van der Veen BJ, de Roos A, et al (2013). Myocardial Perfusion Imaging: The Role of SPECT, PET and CMR. In: Marzullo P, Mariani G (eds) From Basic Cardiac Imaging to Image Fusion: Core Competencies Versus Technological Progress. Springer Milan, Milano, pp 29–49. DOI:10.1007/978-88-470-2760-2_3

Murthy VL, Bateman TM, Beanlands RS, et al (2018) Clinical Quantification of Myocardial Blood Flow Using PET: Joint Position Paper of the SNMMI Cardiovascular Council and the ASNC. J Nucl Med 59:273. https://doi.org/10.2967/jnumed.117.201368

Virmani R, Burke AP, Farb A, Kolodgie FD (2006). Pathology of the Vulnerable Plaque. Detect Vulnerable Plaques 47:C13–C18. https://doi.org/10.1016/j.jacc.2005.10.065

Vranckx P, Cutlip DE, Mehran R, et al (2010). Myocardial infarction adjudication in contemporary all-comer stent trials: balancing sensitivity and specificity. Addendum to the historical MI definitions used in stent studies. EuroIntervention 5:871–874. https://doi.org/10.4244/eijv5i7a146

Wald DS, Morris JK, Wald NJ, et al (2013). Randomized Trial of Preventive Angioplasty in Myocardial Infarction. N Engl J Med 369:1115–1123. https://doi.org/10.1056/NEJMoa1305520

Wang L, Travieso A, van der Hoeven N, et al (2023). Improved Nonculprit Stenosis Assessment in Patients With ST-Segment Elevation Myocardial Infarction Using Quantitative Flow Ratio. JACC Cardiovasc Interv 16:1828-1830. https://doi.org/10.1016/j.jcin.2023.04.045

Westra J, Sejr-Hansen M, Koltowski L, et al (2022). Reproducibility of quantitative flow ratio: the QREP study. EuroIntervention 17:1252–1259. https://doi.org/10.4244/EIJ-D-21-00425

Westra J, Andersen BK, Campo G, et al (2018). Diagnostic Performance of In-Procedure Angiography-Derived Quantitative Flow Reserve Compared to Pressure-Derived Fractional Flow Reserve: The FAVOR II Europe-Japan Study. J Am Heart Assoc 7:e009603. https://doi.org/10.1161/JAHA.118.009603

Williams M, Moss AJ, Dweck M, et al (2019). Coronary Artery Plaque Characteristics Associated With Adverse Outcomes in the SCOT-HEART Study. J Am Coll Cardiol 73:291–301. https://doi.org/10.1016/j.jacc.2018.10.066

Wood DA, Cairns JA, Wang J, et al (2019). Timing of Staged Nonculprit Artery Revascularization in Patients With ST-Segment Elevation Myocardial Infarction. J Am Coll Cardiol 74:2713–2723. https://doi.org/10.1016/j.jacc.2019.09.051

Levine GN, Bates ER, Blankenship JC, et al (2011). 2011 ACCF/AHA/SCAI Guideline for Percutaneous Coronary Intervention: A Report of the American College of Cardiology Foundation/American Heart Association Task Force on Practice Guidelines and the Society for Cardiovascular Angiography and Interventions. Circulation 124:e574-e651. https://doi.org/10.1161/CIR.0b013e31823ba622

Xaplanteris P, Fournier S, Pijls NHJ, et al (2018). Five-Year Outcomes with PCI Guided by Fractional Flow Reserve. N Engl J Med 379:250–259. https://doi.org/10.1056/NEJMoa1803538

Xu B, Tu S, Qiao S, et al (2017). Diagnostic Accuracy of Angiography-Based Quantitative Flow Ratio Measurements for Online Assessment of Coronary Stenosis. J Am Coll Cardiol 70:3077–3087. https://doi.org/10.1016/j.jacc.2017.10.035

Xu B, Tu S, Song L, et al (2021). Angiographic quantitative flow ratio-guided coronary intervention (FAVOR III China): a multicentre, randomised, sham-controlled trial. Lancet 398:2149–2159. https://doi.org/10.1016/S0140-6736(21)02248-0

Yang S, Koo B-K, Narula J (2022). Interactions Between Morphological Plaque Characteristics and Coronary Physiology: From Pathophysiological Basis to Clinical Implications. JACC Cardiovasc Imaging 15:1139–1151. https://doi.org/10.1016/j.jcmg.2021.10.009

Zeleznik R, Foldyna B, Eslami P, et al (2021). Deep convolutional neural networks to predict cardiovascular risk from computed tomography. Nat Commun 12:715. https://doi.org/10.1038/s41467-021-20966-2

Zhuang B, Wang S, Zhao S, Lu M (2020). Computed tomography angiography-derived fractional flow reserve (CT-FFR) for the detection of myocardial ischemia with invasive fractional flow reserve

as reference: systematic review and meta-analysis. Eur Radiol 30:712–725. https://doi.org/10.1007/s00330-019-06470-8

Zimmermann FM, Ferrara A, Johnson NP, et al (2015). Deferral vs. performance of percutaneous coronary intervention of functionally non-significant coronary stenosis: 15-year follow-up of the DEFER trial. Eur Heart J 36:3182–3188. https://doi.org/10.1093/eurheartj/ehv452

Zimmermann FM, Omerovic E, Fournier S, et al (2019). Fractional flow reserve-guided percutaneous coronary intervention vs. medical therapy for patients with stable coronary lesions: meta-analysis of individual patient data. Eur Heart J 40:180–186. https://doi.org/10.1093/eurheartj/ehy812

Ziubryte G, Jarusevicius G (2021). Fractional flow reserve, quantitative flow ratio, and instantaneous wave-free ratio: a comparison of the procedure-related dose of ionising radiation. Adv Interv Cardiol 17:33–38. https://doi.org/10.5114/aic.2021.104765

TURUN
YLIOPISTO
UNIVERSITY
OF TURKU

Painosalama, Turku, Finland 2024

ISBN 978-951-29-9709-1 (PRINT)
ISBN 978-951-29-9710-7 (PDF)
ISSN 0355-9483 (Print)
ISSN 2343-3213 (Online)